Analysis of alpha-synuclein amyloid fibrils and their effects on the cellular proteome

Megan Victoria Pickard

Submitted in accordance with the requirements for the degree of

Master of Science by Research

The University of Leeds

School of Biology

February 2021

The candidate confirms that the work submitted is her own and that appropriate credit has been given where reference has been made to the work of others.

Acknowledgements

I would like to thank Dr Eric Hewitt for his supervision and support throughout this project. Thank you to Michael Davies for producing the fibrils used during this project and to Dr Kate Heesom and her team at the University of Bristol Proteomics Facility for conducting proteomic analysis.

Abstract

Misfolded α-synuclein aggregates into amyloid fibrils. These fibrils are the principal component of Lewy Bodies, intracellular inclusions that are one of the pathological hallmarks of Parkinson's disease. Despite the accumulation of α-synuclein fibrils being a marker for disease, their contribution to Lewy Body pathology and disease progression is not well understood. Exogenous α-synuclein fibrils are able to seed the formation of Lewy Bodies by promoting the aggregation of endogenous α-synuclein. Using proteomics, this project aimed to determine how the presence of α-synuclein fibrils affected the cellular proteome in the early stages of Lewy Body formation using SH-SY5Y cells that overexpress GFP-α-synuclein as a model. Tandem mass tagging quantitative proteomics identified 11 proteins with significantly altered levels resulting from exposure of the SH-SY5Y GFP-α-synuclein cell line to α-synuclein fibrils for 1 and 5 days. Among these proteins were members of the collagen and microtubule-associated protein families, they have roles in a plethora of cellular processes including signalling, structural maintenance and intracellular organisation. Alterations to their function could cause cellular dysfunction, which could contribute to the pathogenic conditions seen in Lewy Body formation and Parkinson's disease. This highlights the importance of proteomics in further understanding the contribution that α-synuclein has in the pathology and progression of Parkinson's disease and other related diseases.

Table of Contents

1. List of Figures

2. List of Tables

3. Abbreviations

AD	Alzheimer's disease
ALP	Autophagy-lysosomal pathway
ALS	Amyotrophic lateral sclerosis
APP	Amyloid precursor protein
ATP	Adenosine Triphosphate
BAC	Bacterial artificial chromosome
CBE	Conduritol B epoxide
CCDC9B	Coiled-coil domain-containing protein 9B
CID	Collision induced dissociation
COL1A1	Collagen α-1(I) chain
COL1A2	Collagen α-2(I) chain
COL2A1	Collagen α-1(II) chain
COL4A2	Collagen α-2(IV) chain
CMA	Chaperone-mediated autophagy
CNS	Central nervous system
cryoEM	Cryogenic electron microscopy
CSNK2A1	Casein Kinase 2 Alpha 1
DLB	Dementia with Lewy Bodies
DMV	Dorsal motor nucleus of the vagal nerve
ER	Endoplasmic reticulum
ESCs	Embryonic stem cells
ESI	Electrospray ionisation
GBA	Glucosidase beta acid
GC	Glucosylceramide
GCase	Glucocerebrosidase
GCIs	Glial cytoplasmic inclusion
GD	Gaucher's disease
GI	Gastro-intestinal
GO	Gene Ontology
GRP78/BIP	Glucose regulated protein 78
HGF	Hepatocyte growth factor
IMM	Inner mitochondrial membrane
iPSCs	Induced pluripotent stem cells
LDH	Lactate Dehydrogenase
LAMP-2A	Lysosomal-associated membrane protein type 2A
LBs	Lewy Bodies
LC3	Microtubule associated protein 1A/1B-light chain 3
LNs	Lewy Neurite
LSDs	Lysosomal storage disorders
MAO-B	Monoamine oxidase-B
MAN2A1	Alpha-mannosidase 2
MAPs	Microtubule associated proteins
MAP4	Microtubule associated protein 4
MARK1	Microtubule affinity-regulating kinase 1
MEF2D	Myocyte enhancer factor 2

miRNA	microRNA
MS	Mass spectrometry
MS/MS	Tandem mass spectrometry
MSA	Multiple system atrophy
MTT	3-(4,5-Dimethylthiazol-2-yl)-2,5-Diphenyltetrazolium Bromide
MVBs	Multivesicular bodies
m/z	Mass-to-charge ratio
NAC	Non-amyloid component
NHS	N-Hydroxysuccinimide
OMM	Outer mitochondrial membrane
PD	Parkinson's Disease
PNS	Peripheral nervous system
PP2A	Protein phosphatase 2
RTF1	RNA Polymerase-Associated Protein RTF1 Homolog
SCI	Spinal cord injury
SIK3	Non-specific serine/threonine protein kinase
SILAC	Stable isotope labelling by amino acids in cell culture
SN	Substantia nigra pars compacta
SNCA	α-synuclein
SPARC	Secreted Protein Acidic And Cysteine Rich
TARDBP	TARD DNA binding protein
TMT	Tandem mass tagging
TOM	Translocase of outer mitochondrial
TTYH3	Protein tweety homolog 3
UPR	Unfolded protein response
UPS	Ubiquitin proteasome system
vWF	von Willebrand factor
WT	Wild-type
XP32	Skin-specific protein 32

4. Introduction

4.1. Background

Parkinson's disease (PD) is the second most common neurological disorder after Alzheimer's disease (AD), affecting over ten million people worldwide [1]. This age-related degenerative disease affects both the central and peripheral nervous systems and is characterised by the loss of dopaminergic neurons in the substantia nigra pars compacta (SN), the region of the brain responsible for coordination of body movement [2]. Gradual loss of dopaminergic neurons in this region results in the decline of motor skills, cognitive function and other processes with clinical symptoms including bradykinesia, tremor, anxiety and sometimes dementia [3]. In combination with the loss of dopaminergic neurons, reduced levels of dopamine is responsible for most of the clinical symptoms exhibited by patients with PD. The current treatments available for PD only provide symptomatic release. The first of these is levodopa, when administered it is absorbed by neurons and converted into dopamine [4]. Dopamine agonists can also be administered as a substitute for dopamine [5]. The final treatment is Monoamine oxidase-B (MAO-B) inhibitors. MAO-B inhibitors prevent the activity of the enzyme MAO-B which acts to break down dopamine, this in turn results in an increase in dopamine levels [5]. As these treatments only provide symptomatic release, they do not inhibit the progression of the disease and as a result, become less effective over time with the progressive loss of dopaminergic neurons.

The main histopathological hallmark of PD, after the loss of dopaminergic neurons, is the presence of the proteinaceous cytoplasmic inclusions known as Lewy Bodies (LBs) found in the cytoplasm and Lewy Neurites (LNs) found in the neurites of neurons surviving in the SN region. These are proteinaceous cytoplasmic inclusions which mainly contain aggregates of the protein α-synuclein [2, 6], (Fig. 1).

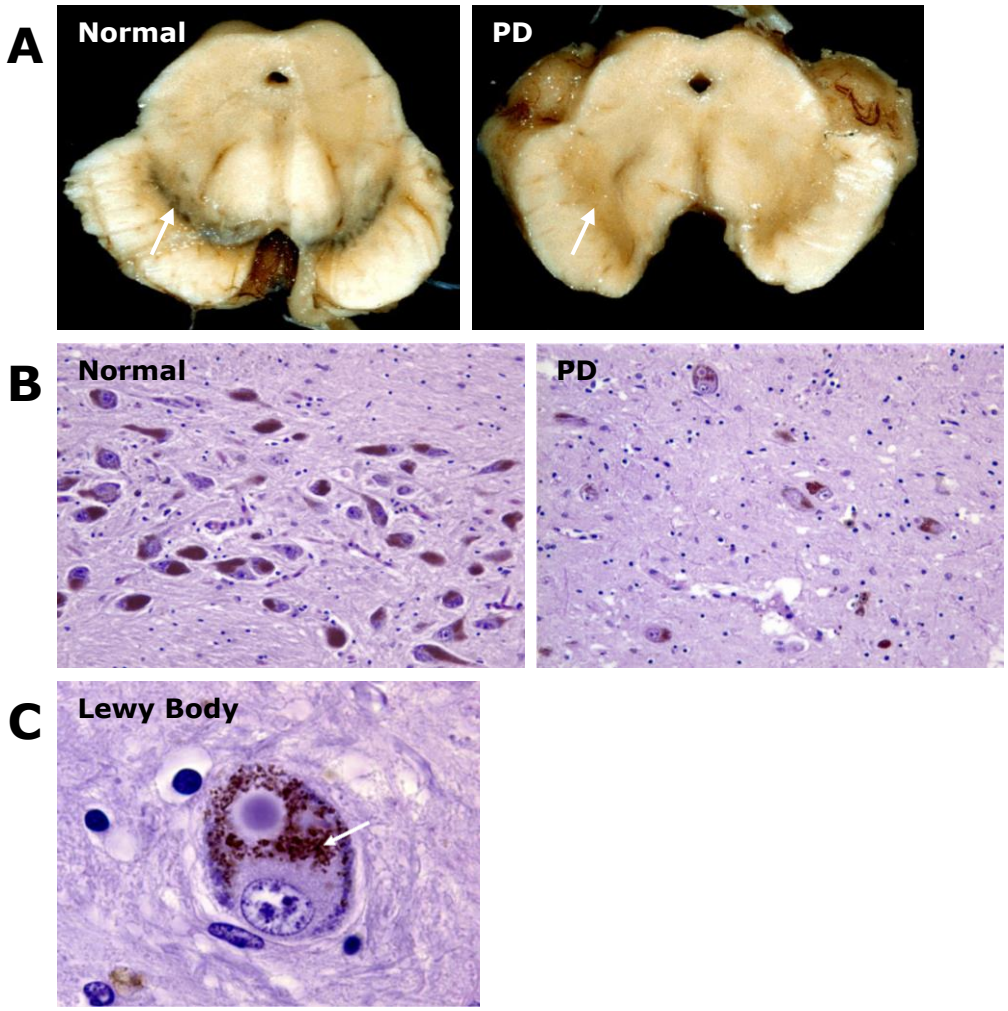

FIGURE 1. **Substantia nigra from normal and Parkinson's disease brains.** A) Dopaminergic neurons are lost in the substantia nigra during PD. This is shown by the arrows in the normal and PD images which indicate a lack of pigmentation. B) Magnified images of substantia nigra tissue clearly show the loss of pigmented neurons during PD. C) Magnified image of a Lewy Body in the substantia nigra present in PD. The arrow indicates the presence of aggregated α-synuclein. (Figure taken from [6]).

LBs were first discovered over 100 years ago with the presence of α-synuclein first reported 23 years ago [7, 8]. Since their discovery, the presence of filaments in LBs has been one of the most consistent observations. Despite the filaments initially thought to be neurofilaments, the discovery of α-synuclein in LBs shifted interest from understanding the complexity of LBs to understanding the role of α-synuclein in LB formation [9].

Since the discovery of α-synuclein in LBs, the major change in approaches used to study LBs and Lewy pathology was the development of a wider range of antibodies against α-synuclein and other proteins present in LBs. These antibodies have allowed for increased profiling of LB composition, greater appreciation of Lewy pathologies and observation of the distribution of proteins in LBs [10].

4.1.1. Synucleinopathies

Although LBs are the second major histopathological hallmark of PD, LBs and pathological α-synuclein aggregates are present in several diseases collectively termed synucleinopathies. Different clinical and pathological phenotypes are seen between synucleinopathies, even though they are caused by aggregation of the same protein. In PD and dementia with Lewy bodies (DLB), α-synuclein aggregates in neuronal cells forming LBs, whereas in multiple system atrophy (MSA), α-synuclein aggregates in oligodendrocytes forming glial cytoplasmic inclusions (GCIs). All three of these synucleinopathies are rarely familial and in the case of MSA, mutations in α-synuclein have not been observed [11].

The occurrence of GCIs in oligodendrocytes and not neurons highlights the role that the intracellular environment plays in generating different strains of α-synuclein aggregates [12]. These differences suggest that different strains are responsible for the distinct pathology between synucleinopathies [13]. Expression of α-synuclein in oligodendrocytes reproduces the MSA phenotype, however, α-synuclein is not expressed by oligodendrocytes under physiological conditions and is not upregulated during MSA [14]. Regardless of the source, α-synuclein accumulates in MSA, suggesting a process distinct from Lewy pathology.

DLB more closely resembles PD in terms of LB pathology, however, DLB predominantly presents dementia whereas, PD presents motor symptoms [15]. Different seeding kinetics of α-synuclein in patients with DLB were observed when compared to PD. It was shown that in DLB-seeded reactions the generation of a proteinase K-resistant fibrillary α-synuclein occurred, whereas in PD, wild-type (WT) α-synuclein was not converted by seeds. The differences in kinetics and the products produced between DLB and PD indicate an existence of α-synuclein strains [16].

α-synuclein also deposits in other neurodegenerative disorders. Lewy pathology is observed in 60% of AD cases but it is mostly restricted to the amygdala compared to PD or DLB [17].

4.2. The SNCA gene

In the 1990s, mutations in the *SNCA* gene were discovered to be associated with early-onset familial forms of PD [18]. The *SNCA* gene encodes the protein α-synuclein and is located on chromosome 4q22.1. Mutations in SNCA are responsible for both familial and a small percentage of sporadic forms of the disease with seven dominant mutations linked to familial PD; A53T, A53E, A53V, A30P, E46K, G51D and H50Q [13, 19]. Of the three missense mutations discovered, the first one identified, A53T, appears to be the

most frequent with it seen in a total of 12 families. The other two missense mutations, A30P and E46K have each been identified in one family each [18]. Penetrance of the missense mutations appears high with the A53T mutation suggested to be around 85% [19]. It is believed that the missense *SNCA* mutations cause PD through a toxic gain of function and presence of α-synuclein aggregates within LBs may be an attempt to remove damaged α-synuclein [20].

While all these single amino acid mutations lead to early onset of the disease, they have different effects on α-synuclein aggregation rate. G51D, A30P and A53E slow the rate of fibril formation while E46K, H50Q and A53T lead to an increase in fibril formation rate [19]. The dominant mutations also affect the association of α-synuclein with phospholipid membranes. G51D, A30P and A53E result in reduced phospholipid binding while E46K and A53T have been shown to increase phospholipid binding [19].

Due to the presence of α-synuclein aggregates within LBs and the range of effects the seven mutations cause, extensive work has been conducted to elucidate the role of α-synuclein in PD, beginning with understanding the structure of the protein.

4.3. Structure of α-synuclein

α-synuclein is comprised of 140 amino acids and is expressed at high levels in the brain, predominantly localised to the pre-synapse of neurons where it is believed to be involved in several processes [20]. The soluble form of α-synuclein is natively unstructured but it adopts a partial α-helix upon binding to membranes [21]. The protein contains three major regions: an amphipathic N-terminal region (1-60), a non-amyloid component (NAC) (61-95) and a C-terminal region (96-140). The N-terminal region has seven highly conserved 11 amino-acid repeat sequences forming an amphipathic α-helix which enables the protein to bind with membranes [21]. The NAC region is a hydrophobic region which is amyloidogenic and responsible for protein aggregation [22]. The C-terminal region is polar and contains majority of the protein's post-translational modification sites [23], it also mediates interactions with other proteins and ligands [24], (Fig. 2).

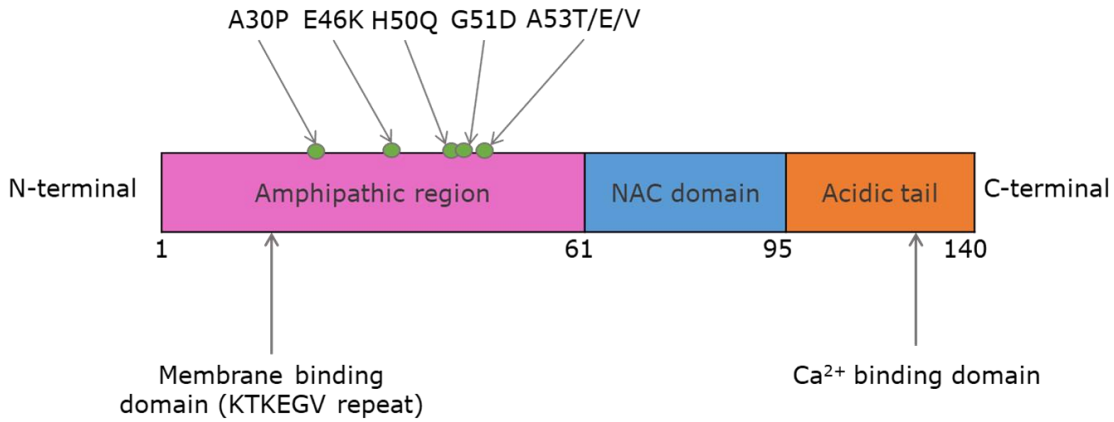

FIGURE 2. **Structure of the α-synuclein protein**. The N-terminal domain (pink) is composed of KTKEGV repeats. Missense mutations associated with familial PD have been found in this region. The central non-amyloid component (NAC) domain (blue) is responsible for α-synuclein aggregation. The C-terminal domain (orange) is the acidic tail containing the calcium binding site.

4.4. Physiological role of α-synuclein

α-synuclein is widely expressed by neural populations within both the central and peripheral nervous systems, predominantly located at nerve terminals [25]. Under physiological conditions, monomeric α-synuclein is natively unfolded. In the absence of a transmembrane domain or a lipid anchor, it is unclear how α-synuclein localises to the nerve terminal, however, this is proposed to be dependent on its amphipathic N-terminus. The N-terminus contains seven 11 residue repeats which have been suggested to adopt an α-helix conformation, essential for binding to curved membranes [26]. Binding to the phospholipid headgroups of the membrane requires basic residues such as lysine found on opposite sides of the helix (Fig. 3).

Although the interaction between α-synuclein and the lipid membrane is weak, α-synuclein is known to be highly localised at the synapses where it interacts with synaptic vesicles, likely via the aforementioned α-helix conformation [26].

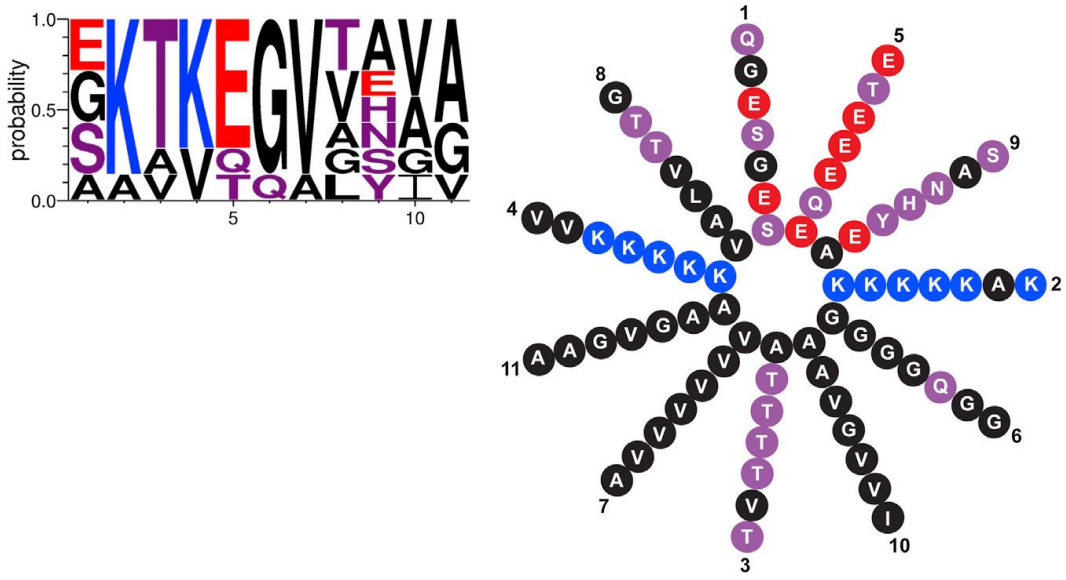

FIGURE 3. **The proposed α-helical formation of the N-terminus of α-synuclein upon membrane binding**. The N-terminus of α-synuclein contains seven 11 residue repeats. The consensus sequence of repeats is given on the left. The height of the single letter amino acid code indicates the probability of finding that residue in the repeats. The helical wheel is given on the right. The numbers around the wheel represent the position of a residue within a repeat, while the distance from the centre represents which of the seven repeats the residues are located in. Blue indicates basic, red acidic, purple polar uncharged and black non-polar residues. (Figure taken from [26]).

The release of neurotransmitters at nerve terminals is a highly regulated process and relies upon the formation of the SNARE complex. The SNARE complex is formed of four α-helices, one from each synaptobrevin-II, syntaxin-1A and two from SNAP-25 [27]. Syntaxin-1A is located on the vesicle membrane while synaptobrevin-II and SNAP-25 are located on the plasma membrane [28]. Vesicle fusion during presynaptic exocytosis is coupled to the Ca^{2+} receptor synaptotagmin. Ca^{2+} binding to synaptotagmin allows for formation of the SNARE complex at the plasma membrane and subsequent release of neurotransmitters into the synaptic cleft [29]. α-synuclein has been shown to promote assembly of the SNARE complex by binding to synaptobrevin-II via its C-terminus [30, 31]. This function of α-synuclein is important with increased synaptic activity and ageing, therefore maintenance of the SNARE complex is essential. Aggregation of α-synuclein has been suggested to impair the function of the SNARE complex. Aggregated forms of α-synuclein could bind to multiple synaptobrevin-II preventing its interaction with the other members of the SNARE complex, resulting in a reduction of neurotransmitter release [31], (Fig. 4). Loss of α-synuclein function, for example, by sequestration of α-synuclein in LBs would have a similar effect; resulting in a loss of neuronal function and possible contributions to synucleinopathies [30].

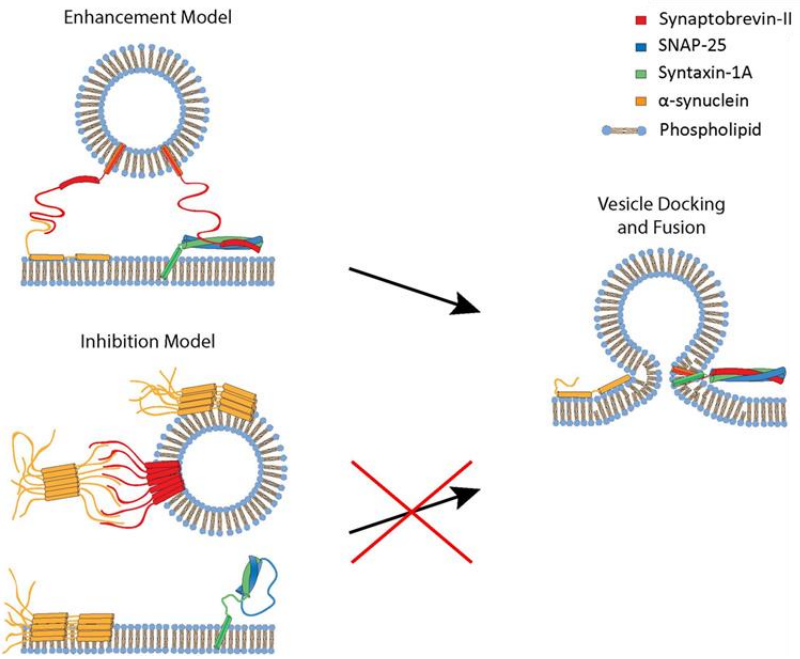

FIGURE 4. **Proposed mechanistic model for enhancement and inhibition of SNARE-dependent vesicle fusion by α-synuclein.** In the enhancement model, monomeric α-synuclein acts as a cross-bridge to facilitate vesicle docking to the phospholipid bilayer. The inhibition model involves aggregated α-synuclein interacting and clustering with several synaptobrevin-II, thus preventing synaptobrevin-II from engaging in SNARE complex formation and vesicle fusion (Figure taken from [31]).

α-synuclein might also act as a fatty acid binding protein, promoting polyunsaturated fatty acid uptake into cells, via clathrin-dependent endocytosis [32]. This was supported by analysis of α-synuclein knockout mice which presented a reduction in brain cardiolipin [33]. Changes in fatty acid uptake and metabolism also supported the role of α-synuclein as a fatty acid binding protein. The uptake of palmitic acid in the brain of α-synuclein gene-ablated mice decreased as well as its incorporation into the brain acyl-CoA pool [34, 35]. Although uptake of docosahexaenoic acid was not affected in the same model, incorporation into the brain acyl-CoA pool was elevated 1.5-fold [34, 35]. This showed that α-synuclein has effects on the uptake and metabolism of fatty acids.

It has been reported that α-synuclein interacts with a number of proteins that may regulate its activity. Tubulin appears to interact with aggregated α-synuclein, resulting in microtubule dysfunction. Overexpression of α-synuclein in SH-SY5Y cells led to disruption of the microtubules network and trafficking, this was associated with mislocalisation of tubulin to α-synuclein aggregates in degenerating neurites [36].

Recently, the small GTPase Rab3a has been suggested to regulate the membrane association of α-synuclein in a GTP-dependent manner [37]. Rab3a is involved in the docking of synaptic vesicles to the membrane during neurotransmitter release suggesting a relationship between this process and the involvement of α-synuclein in the synaptic-vesicle cycle, the extent of which is unclear at present.

4.4.1. Amyloid fibril formation and structure

In LBs, α-synuclein is present in the form of amyloid fibrils. The aggregation of α-synuclein into amyloid fibrils consists of three phases. First is the lag phase, this is the rate-limiting step where oligomers form an aggregation-competent nucleus [38]. Second is the elongation phase where the nucleus is converted into protofilaments that aggregate into fibrils. Within the protofilaments, α-synuclein is organised into a cross-β structure whereby β-strands are arranged into β-sheets perpendicular to the fibril axis [39]. The cross-β structure is a common characteristic among amyloids. The final stage of aggregation is the stationary phase at which point the majority of the soluble α-synuclein has been converted into fibrils [38].

Recently, atomic resolution structures of α-synuclein have been elucidated using solid state NMR [40] and cryogenic electron microscopy (cryoEM) on reconstituted α-synuclein fibrils [41, 42]. The deduced Greek-key conformation showed that each α-synuclein subunit in the fibril adopts a β-sheet conformation with hydrogen bonding between adjacent α-synuclein subunits. The β-sheet rich core is located between residues 42-102 comprising of a hydrophobic region that forms right-angled spirals and is largely comprised of Ala/Val residues [41, 42]. The outer surface of the fibril is mostly hydrophilic [41, 42], (Fig. 5A). The 3D map of α-synuclein fibrils shows two protofilaments interacting with each other via two β-sheets from each protofilament forming hydrophobic zipper geometry, resulting in the two polymorphs; the rod conformation (polymorph 1a) and the twisted conformation (polymorph 1b), [41, 42] .

The rod fibrils are 10nm wide composing of two adjacent protofilaments that form a hydrophobic zipper with a potential salt bridge between E57 and H50 of the adjacent subunits [19]. The twister fibrils share the kernel structure that comprises the dimeric protofilament but differs in the interface configuration. The helical pitch of the twister structure is 460 Å compared to 920 Å for the rods (Fig. 5B). Unlike the Greek-key fold and pre-NAC interface (residues 47-56) seen in the rod fibrils, the subunits of the twister fibrils form a bent β-arch with a NAC core interface (residues 68-78), [19], (Fig. 5C).

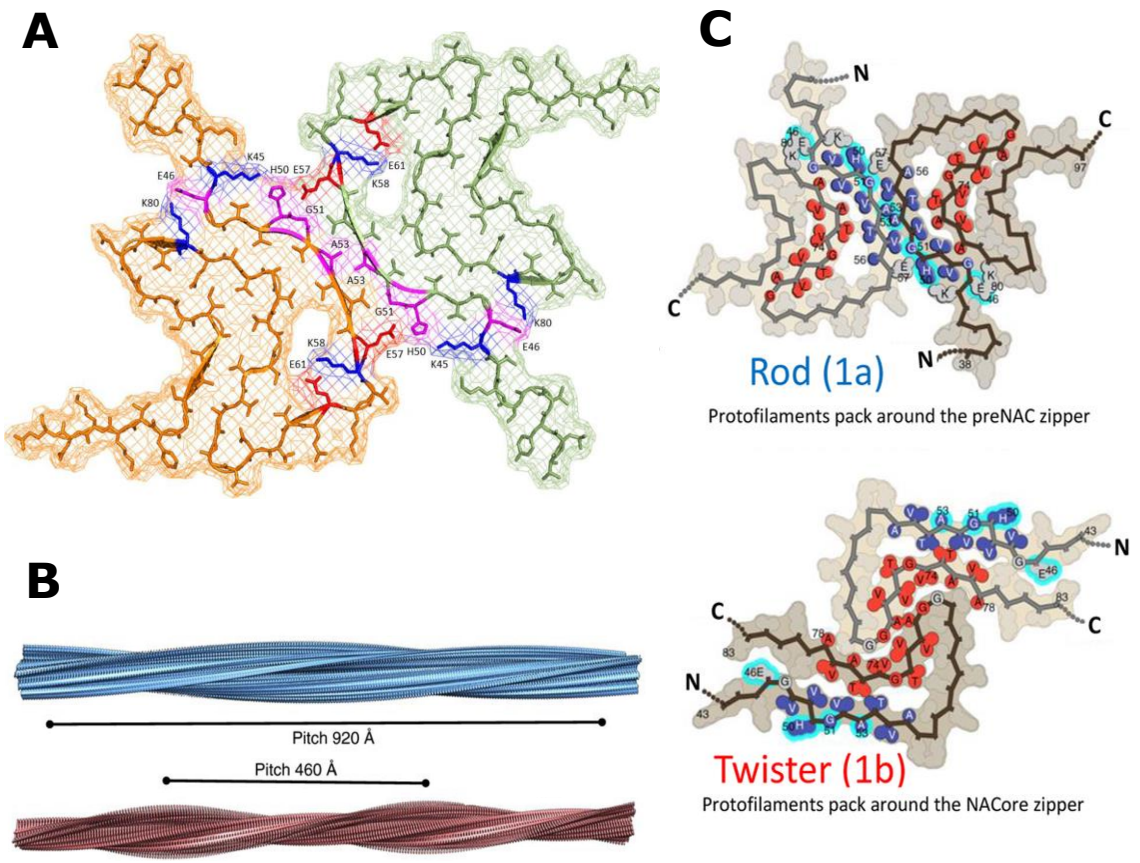

FIGURE 5. **The structure of an α-synuclein fibril**. A) Structure of a single layer within an α-synuclein fibril displaying formation of the Greek-key topology. The early onset mutations are highlighted in pink as well as the three electrostatic interactions which are perturbed in early onset PD. B) 3D model of the rod (top) and twister (bottom) fibril polymorphs, annotated with their helical pitches. C) The interface of the rod fibril is composed of residues within the preNAC region (blue, residues 47-56) in which most early-onset PD mutations are located (cyan). The twister fibril interface is composed of residues within the NAC core region (red, residues 68-78), (Figure taken from [19]).

It is known that familial mutations of PD affect the aggregation of oligomers during the lag phase, which is the rate-limiting step of fibril formation, these mutations also alter fibrillation kinetics [38]. Sahay et al. (2015) investigated the effects of familial PD-mutations A53T, E46K and A30P to alter the long-range intramolecular interactions, structural compactness and conformational equilibrium of α-synuclein [43]. Although the overall secondary structure was the same for these mutant proteins, aggregation studies showed that A30P had slower fibril formation compared to WT α-synuclein while E46K and A53T had a faster fibril formation rate. Despite the differences in fibril formation, all three mutants had an increased propensity to form oligomers [43]. In WT α-synuclein there is a salt bridge between E46 and K80 side chains, which is compromised in the E46K mutant. Electrostatic repulsion destabilised the Greek-key conformation leading to increased oligomerisation compared to WT α-synuclein [44]. The three mutants decreased solvent exposure and altered the rigidity of the C-terminus. All three mutations increased rigidity in the monomeric form but only A53T and E46K fibrils had higher

rigidity compared to WT. This indicated that the mutations differentially affected conformational changes in the NAC, N- and C- terminal regions during α-synuclein aggregation [43].

Li et al. (2018) investigated the effect that several familial mutations located in the pre-NAC region (E46K, H50Q, G51D, A53E, A53T and A53V), had on the rod and twister polymorphs. They proposed that these mutations would disfavour the fibril core of the rod structure but not the twister, due to the mutations being contained in the interface of the rod fibrils and not twister fibrils. These mutations were therefore likely to result in a decrease of the rod polymorph. It was suggested that changes in the type of fibril polymorphs present may alter their activity, for example, their capability to bind to membranes and as such, underlie the differences in phenotype presented by patients with familial PD, concluding that α-synuclein fibril polymorphs may contribute to the pathogenicity of α-synucleinopathies [42].

Two additional polymorphic structures of α-synuclein have been solved by cryo-EM, named polymorph 2a and 2b [45]. Like the rod (polymorph 1a) and twister polymorph (polymorph 1b), these are composed of two protofilaments, 10nm in diameter but they display different arrangements. In the absence of a steric zipper, salt bridges are observed between K45-E57 (polymorph 2a) and K45-E46 (polymorph 2b). Unlike the familial mutations in polymorphs 1a/b which are within a steric zipper structure, for the polymorphs 2a/b they are contained in a hydrophobic cleft [45], (Fig. 6).

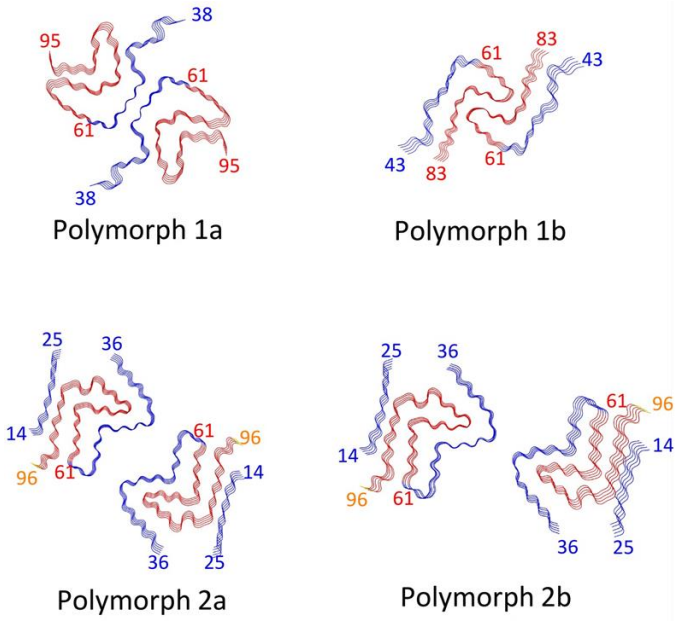

FIGURE 6. **Schematic representations of the four currently characterised α-synuclein polymorphs.** Type 1 polymorphs have steric zipper geometry while the type 2 polymorphs are characterised by a hydrophobic cleft stabilised by intermolecular salt bridges and additional interactions between the NAC region and N-terminus, The N-terminus is shown in blue, NAC region in red and the C-terminus in yellow. It should be noted that not all residues are visible in these structures (Figure taken from [45]).

It has been largely accepted that the native state of α-synuclein changes under pathological conditions, whereby, it misfolds into a partially folded soluble oligomeric state that later forms insoluble fibrils [46]. Once taken up by cells it is unknown how pathological α-synuclein species initiate recruitment of intracellular α-synuclein. The prevailing hypothesis is that internalized α-synuclein escapes from the endocytic pathway allowing it to contact the intracellular pool of monomeric α-synuclein [47]. It has been shown that upon treating primary neurons with preformed fibrils, a small amount within the cells co-localises with endogenous α-synuclein, suggesting that direct conversion and recruitment of monomeric α-synuclein may be enough to initiate α-synuclein pathology [48].

Several studies have suggested that α-synuclein fibrils are not the only species responsible for the pathogenic events seen in synucleinopathies, in fact, it has been proposed that oligomers of α-synuclein may contribute. Work in primary rat neurons showed the formation of two types of oligomers which form during α-synuclein aggregation [49]. Oligomers formed during the early stages of aggregation were shown to be non-toxic but they can later convert into stable protein kinase resistant oligomers which are toxic. Further to this, incubation of primary neurons with fibrils in the absence of monomer release resulted in the release of soluble oligomeric species which resembled the toxic oligomers formed during aggregation [49].

Upon injection of α-synuclein oligomer variants into the rat SN, a decrease in dopaminergic neurons was observed most prominently for E35K and E57K α-synuclein [50]. These two variants have a decreased tendency to form fibrils and were therefore considered as oligomer-promoting variants. Upon addition of the E57K variant to an immortalized human cell line, high-toxicity was induced. An increase in Ca^{2+} influx and a decrease in cell viability, indicative of membrane and cellular dysfunction was observed [50]. Overall, this work indicates a role of α-synuclein oligomers in the pathogenic events of PD.

4.5. Pathological role of α-synuclein

The spread of α-synuclein pathology through different regions of the brain occurs over time. First proposed by Braak et al. (2003), initial appearance of α-synuclein aggregation occurred in the dorsal motor nucleus of the vagal nerve (DMV) and olfactory bulb before progressing further to other brain regions [51], (Fig. 7).

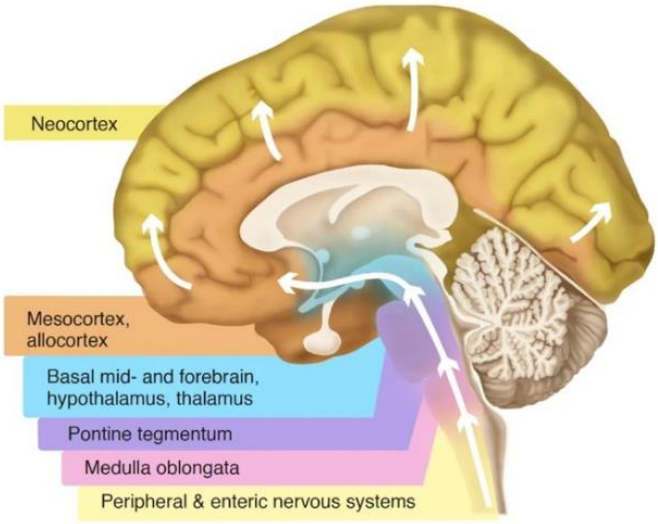

FIGURE 7. **Schematic summarising the staging of Lewy pathology according to the Braak model**. The disease process commences in the lower brainstem in the dorsal motor nucleus of the vagus nerve (DMV), as well as anterior olfactory structures. The disease then ascends rostrally from the DMV through susceptible regions of the medulla, pontine tegmentum, midbrain, and basal forebrain, eventually reaching the cerebral cortex. (Figure taken from [53]).

However, the stages initially proposed to describe the progression only fit half of all α-synucleinopathy cases [52]. Later, a future study evaluated a number of α-synucleinopathies and suggested a revised staging system which saw an initial stage 1 where the olfactory bulb and DMV was affected followed by a divergence into stage 2a (brainstem predominant) or stage 2b (limbic predominant). The two pathways then converge into stage 3 where both brainstem and limbic areas were affected. At this point, the motor manifestations of PD generally appear. During stage 4, α-synuclein deposits are seen in the temporal cortex and in the neocortex by stage 5, likely contributing to the cognitive defects observed in advanced PD [53, 54].

With the appearance of α-synuclein inclusions in the olfactory bulb and DMV prior to the onset of clinical symptoms in PD, the ‘body-first’ hypothesis was proposed [51]. This hypothesis suggested that the pathology may occur at peripheral sites before travelling to the central nervous system inducing the disorder that is recognised as PD. The connection between gastro-intestinal (GI) dysfunction and PD is well established, with constipation being one of the non-motor symptoms of the disease, this supports the ‘body-first’ hypothesis [52]. Recent work in a bacterial artificial chromosome (BAC) rat model supported the ‘body-first’ hypothesis, providing the first animal model to show evidence of α-synuclein propagation to the heart and bi-directional propagation from the duodenum to brainstem to stomach. This also provided an explanation for the cardiac denervation which can occur in the prodromal phase of PD [55].

The spread of α-synuclein aggregates between individual neurons is said to occur in a ‘prion-like’ manner. α-synuclein aggregates generated in one neuron are transferred to

a neighbouring neuron via the synapse, acting as a template for misfolding of α-synuclein in the recipient neurons [53, 54, 56], (Fig. 8).

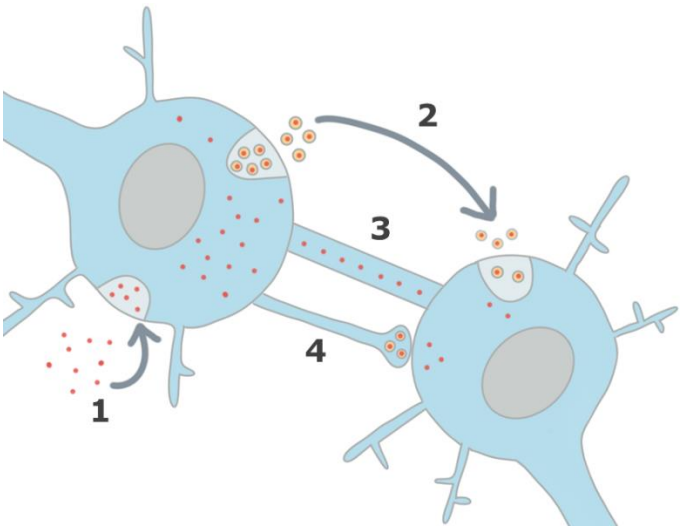

FIGURE 8. **Schematic of the 'prion-like' spread of α-synuclein aggregates.** Seeding-potent aggregates spreading from cell to cell. They enter the cell after binding to their receptor (1). After internalization, aggregates spread over the cell and transmit to second order neurons via exosomes (2) tunnelling nanotubes (3) or the synapse (4).

Unlike prions, pathological α-synuclein shows no evidence of being infectious to other organisms therefore, the transmission is said to be 'prion-like' as it is transmissible between cells in a host not between hosts as is the case for prion diseases [57]. The prion-like propagation of α-synuclein was first suggested when neural transplants injected into the striatum of PD patients more than 10 years prior to death were shown to contain LBs at autopsy [58, 59]. The same effect was seen in animal models. Through transplantation of cortical neuronal stem cells into the hippocampus of mice overexpressing human α-synuclein, it was shown that the human α-synuclein could transfer to the transplanted cells [60].

It was also important to show that α-synuclein could induce prion-like propagation in the absence of diseased material. Truncated mouse α-synuclein, lacking the C-terminus, was injected into the brains of WT mice and shown to cause time-dependent protein spreading and aggregation [61]. Although occurring at a slower rate, the same capacity to inflict synucleinopathy occurred for human α-synuclein aggregates [62]. It has been shown that recombinant α-synuclein fibrils can enter neurons by endocytosis and seed the formation of aggregates composed entirely of endogenous α-synuclein resembling early LB pathology [63]. This was demonstrated by intracerebral injection of α-synuclein fibrils into WT mouse brains. α-synuclein pathology was induced, the spread of which depended on the injection sites and seeding capabilities of the fibrils [64].

4.5.1. Release of α-synuclein aggregates

For the spread of α-synuclein to occur from one cell to the next, α-synuclein must be released. Release of monomeric α-synuclein appears to be a regulated event with very little α-synuclein detected in media and cerebrospinal fluid [65]. Cell culture studies have found that stress on the proteostasis machinery can result in α-synuclein release. While this may benefit the cell initially, this may be the primary mechanism that leads to the transmission of pathological α-synuclein [52].

The co-chaperone DNAJC5 plays a role in secretion of aggregated α-synuclein via the process of misfolding-associated protein secretion [66]. Experiments in immortalised cells saw aggregates being shuttled from the cytosol to the cell surface in a DNAJC5-dependent manner. The aggregates were then endocytosed by other cells and degraded in the lysosome [66].

α-synuclein release has been shown to involve exosomes usually targeted for degradation by the lysosomes [67]. Exosomes are the luminal membranes of multivesicular bodies (MVBs). MVBs form through invagination of endosomal membranes, trapping cytosolic proteins such as α-synuclein in the process. With α-synuclein degradation occurring via the lysosomes, it is plausible that α-synuclein on the pathway to the lysosomes could be susceptible to release in this manner. This release appears to occur with calcium-dependent regulation which may be relevant for the spread of α-synuclein pathogenesis along synaptically connected pathways [68].

Furthermore, the use of quantitative fluorescence microscopy has shown that once lysosomes become overloaded with α-synuclein aggregates, fibrils can be transferred from one cell to another inside lysosomal vesicles via tunnelling nanotubes [69].

4.6. Cellular impact of α-synuclein aggregation

4.6.1. Lysosomes

Lysosomal integrity is impaired with age and elevated release of internalised α-synuclein from damaged lysosomes has been proposed as one of the mechanisms by which age could lead to pathogenic α-synuclein accumulation [70]. Lysosomes are single-membrane organelles that aid in the maintenance of cellular metabolism [71], degrading and recycling a variety of molecules and organelles into their constituent components [72]. Failure of lysosomes leads to the accumulation of dysfunctional proteins and organelles. There are several routes for macromolecules to reach the lysosome. Material from outside the cell is taken up by clathrin-mediated endocytosis, these vesicles then fuse to endosomes which mature into late endosomes fusing with the lysosomes for degradation of their contents [73].

Endosomal/lysosomal function has been shown to act as a barrier to the induction of α-synuclein pathology. However, when compromised it may lower the threshold for pathology transmission. It was suggested that exogenous α-synuclein fibrils may disrupt this function leading to aggregation within the cytoplasm [74].

The inability of lysosomes to digest and degrade molecules leads to lysosomal storage disorders (LSDs). Individually each type of LSD is rare but collectively their rate of incidence is about 1 in 7000 live births which is relatively high [75]. The central nervous system (CNS) and peripheral nervous system (PNS) are particularly vulnerable to storage deficits due to their high content of sphingolipids and ceramide. Intact functioning of lysosomes is crucial for neurons as they do not replicate in adult life and have a large degree of oxidative metabolism [76].

Lysosomal impairment and its role in PD is supported by genetic associations between PD and Gaucher's disease (GD), the most common LSD. GD results from a homozygous mutation in the glucosidase beta acid (*GBA*) gene, encoding the lysosomal hydrolase glucocerebrosidase (GCase), [77]. GCase converts glucosylceramide (GC) into glucose and ceramide, failure of this process leads to impairment of lysosomes and an accumulation of lipids [78]. Although GD is an autosomal recessive disorder, the inheritance of parkinsonism associated with rare *GBA* mutations does not follow Mendelian genetics, increasing the risk of PD in a heterozygous state [79]. Due to this, both gain-of function and loss-of function theories have been proposed [78]. As most mutant alleles result in misfolded GCase, this supports a gain of function role for these mutations. Abnormal conformations could contribute to increased α-synuclein aggregation resulting in the development of parkinsonism, on the other hand, it could lead to lysosomal dysfunction. Parkinsonism could also occur because of loss of function of GCase. The misfolded protein could be degraded leading to enzyme deficiency and substrate accumulation [80].

Accumulation of GC, resulting from a reduction in GCase activity, may promote α-synuclein aggregation through the disruption of its levels within the lysosomes. In support of this, when human dopaminergic neurons were treated with the GCase inhibitor conduritol B epoxide (CBE), GCase activity was reduced and α-synuclein levels were increased [81]. Moreover, high concentrations of GC resulted in increased formation of α-synuclein fibrils in both human induced pluripotent stem cells (iPSCs) cells and primary neurons [82]. Knockdown of *GBA1* causes down regulation of autophagy by inactivation of protein phosphatase 2 (PP2A) in both SK-N-SH neuroblastoma cells and primary rat cortical neurons. The inhibition of the autophagic pathway in turn resulted in increased accumulation of α-synuclein [83]. Disruption of the lysosome reformation process in SH-SY5Y cells was also associated with increased α-synuclein levels [84].

As well as reduced GCase activity leading to an increase in α-synuclein, increased levels of α-synuclein have been shown to decrease GCase activity. This may occur by α-synuclein promoting the impairment of GCase trafficking. In support of this, in primary cortical neurons, the level of GCase retained in the ER can be reduced by lowering α-synuclein levels and conversely, overexpression of α-synuclein can cause accumulation of GCase in the ER [82]. Upon interaction with α-synuclein, GCase moves from its usual position at the membrane with its active site positioned further from the lipid bilayer. The activity of GCase is dependent on its interaction with membrane phospholipids therefore this interaction my also explain the reduction in GCase activity [85]. As reduced GCase activity can increase α-synuclein levels these mechanisms may be part of a positive feedback loop whereby an increase in α-synuclein reduces GCase activity resulting in a continued increase of α-synuclein.

4.6.2. Autophagy

The major pathways for disposal of α-synuclein in the cells are macroautophagy, chaperone-mediated autophagy (CMA) and proteasomal degradation. Macroautophagy describes the engulfment of cytoplasm by phagophores which expand into autophagosomes, mature autophagosomes are then targeted by the lysosomes for degradation [86]. CMA involves direct translocation of unfolded proteins across the lysosome membrane. Chaperone proteins mediate this process by binding to cytosolic substrates which enter the lysosome through interaction with receptors on the lysosomal membrane [87].

In its native form α-synuclein is degraded by CMA [88]. α-synuclein contains a KFERQ CMA recognition motif. This pentapeptide motif is recognised by the chaperone protein Hsc70 allowing the two to bind. At the lysosomal membrane α-synuclein then binds to the lysosomal-associated membrane protein type 2A (LAMP-2A). With the aid of the Hsc70, this receptor transports α-synuclein into the lysosome for degradation. Decreased levels of LAMP-2A and Hsc70 have been associated with α-synuclein aggregation in the early stages of PD [89].

Impairment of the autophagy-lysosomal pathway (ALP) was shown in PD brain samples. The microtubules-associated protein 1A/1B-light chain 3 (LC3), an autophagosomal marker, was present within LBs of PD brains with up to 80% nigral LB being positive for LC3 [90]. Impairment of macroautophagy can lead to an increase in α-synuclein secretion by several pathways. Knockdown of the macro autophagy component Atg5 led to an increase in exosomal α-synuclein aggregates [91]. Also, extracellular vesicles containing α-synuclein are released by neurons under stress. The vesicles are then

taken up by other neurons and trafficked through axons [92]. These results suggest that vesicular transport may be one of the ways in which synucleinopathies spread [47].

Autophagic defects were observed upon silencing of LAMP-2A in the dopaminergic cells of a rat model. Accumulation of autophagic vacuoles were surrounded by α-synuclein puncta positive for ubiquitin [93]. The expression of microRNA (miRNA) targeting LAMP-2A in SH-SY5Y cells led to α-synuclein accumulation after defects in CMA [94]. These miRNAs, miR224 and miR373, are upregulated in the SN of PD patients suggesting that CMA-mediated α-synuclein clearance defects in pathological conditions could contribute to their accumulation.

While CMA acts to regulate the level of α-synuclein and its aggregation within the cytoplasm, α-synuclein can in turn disrupt CMA, altering the turnover of other CMA-dependent proteins. The different mutant forms of α-synuclein vary in the way they affect its ability to be degraded, therefore having different levels of toxicity. In cell culture the A53T and A30P mutants bind strongly to LAMP-2A compared to WT but cannot be internalised by the lysosome, they act as receptor inhibitors preventing the binding of other CMA targets [95]. This results in a compensatory toxic gain-of-function activation of the macroautophagy process to counteract the CMA blockade [96]. These data suggest that α-synuclein is a substrate for macroautophagy and CMA with their impairment contributing to the accumulation and aggregation of α-synuclein in synucleinopathies [97], (Fig. 9).

With the relationship of α-synuclein and the ALP in the accumulation and aggregation of α-synuclein being well established, the role of α-synuclein in the disruption of the ALP is known to contribute to α-synuclein pathology through numerous cellular alterations [97]. Overexpression of WT α-synuclein resulted in inhibition of autophagy through impairment of autophagosome formation. This was suggested to involve a decrease in α-synuclein induced Rab1 activity, which disrupts the localisation of the Atg9 protein involved in autophagosome formation [98]. When α-synuclein transfers from cell to cell, autophagic impairment was observed in the recipient cell with accumulation of deficient lysosomes that had become enlarged, increasing pathology [99].

In PC12 cells, overexpression of mutated A53T α-synuclein decreased autophagic activity. When A53T α-synuclein lacking the CMA recognition motif was then expressed, it did not alter autophagic activity. This was due to upregulation of macro autophagy, compensating for the deficit of CMA, however, this resulted in detrimental conditions which contributed to cell death [100]. The disruption of CMA by A53T α-synuclein also caused abnormal accumulation of the myocyte enhancer factor 2 (MEF2D) in the cytosol. This prevented it from binding to DNA and therefore its role in gene regulation of cellular functions, including cellular dyshomeostasis were inhibited [101].

In combination these data highlight how α-synuclein disrupts the ALP machinery, contributing to cellular dyshomeostasis and neuronal death as well as exacerbating the pathological synucleinopathy by a dual-loop effect (Fig. 9).

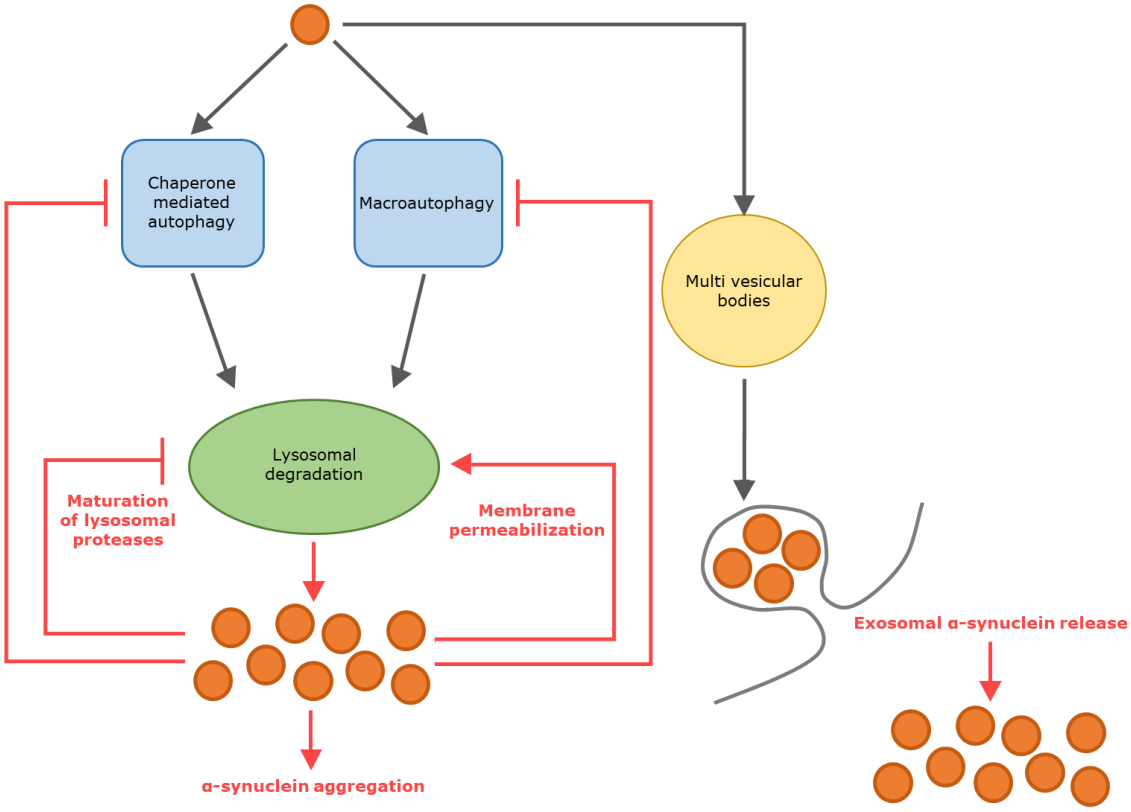

FIGURE 9. **Dual-loop between autophagy lysosomal pathway and α-synuclein**. In physiological conditions α-synuclein is degraded by chaperone mediated autophagy and macroautophagy, with low exosomal release of α-synuclein. In pathological conditions, the clearance of α-synuclein is decreased due to impairment of autophagy. The exosomal pathway is increased to compensate for the loss of autophagy mechanisms resulting in increased release and cell-to-cell propagation of the protein. Reciprocally, accumulated α-synuclein induces cell toxicity by autophagy impairment forcing the cell into a cycle of dyshomeostasis (Figure adapted from [97]).

4.6.3. Mitochondria

Mitochondria have been closely linked to the pathogenesis of PD with a reduction of complex I activity seen in post mortem brain samples of PD patients [102]. This reduction is also seen in transgenic mice overexpressing WT α-synuclein or A53T α-synuclein [103]. Both normal and abnormal α-synuclein have been shown to interact with mitochondria and this binding appears enriched in PD brain samples [104]. The translocation of α-synuclein into the inner mitochondrial membrane structures is not fully understood, but Tom40 a component of the Translocase of outer mitochondrial (TOM) complex is believed to be involved [104]. Evidence of this was shown by decreased levels of Tom40 in the brains of PD patients [105]. Interactions with translocases of the inner membrane, TIM16 and 44 have also been seen with aggregated α-synuclein

favouring TIM44 [106]. These interactions allow for the possibility that α-synuclein can be translocated into the mitochondrial matrix.

DJ-1 is a multi-functional protein with its predominant role in the protection of cells against oxidative stress [107]. Mutations in the *PARK7* gene, encoding DJ-1, account for 0.4% of early onset PD cases, occurring in an autosomal recessive manner [108]. DJ-1 activity is regulated by oxidative modification of its C106 residue. Upon exposure to growth factors and oxidation of C106, DJ-1 translocates to the nucleus playing a role in antioxidant gene regulation [109]. In cells undergoing oxidative stress DJ-1 is localised to the outer mitochondrial membrane (OMM), to maintain a healthy mitochondrial environment [110]. With its role in mitochondrial homeostasis and early onset of PD, the potential relationship between α-synuclein and DJ-1 is of interest. Jin et al. (2007) analysed proteins associated with α-synuclein and/or DJ-1 using stable isotope labelling by amino acids in cell culture (SILAC). This was conducted in dopaminergic mouse embryonic stem cells (ESCs) exposed to rotenone. Rotenone is an inhibitor of the electron transport chain used in cellular models of PD [111]. Although Jin et al. (2007) did not observe a direct interaction between α-synuclein and DJ-1, they shared 114 protein interaction partners with the relative abundance of those proteins altered significantly after rotenone treatment [111]. This work reported five novel proteins that associate with both α-synuclein and DJ-1 including mortalin.

Mortalin is a mitochondrial stress protein which is a part of the mitochondrial import complex. As part of this complex, mortalin acts as a molecular chaperone for the import of nuclear-encoded protein into the mitochondria via the inner mitochondrial membrane (IMM) translocases [112]. Mortalin has a functional role in mitochondrial homeostasis and as such there is interest in its potential involvement in PD development via pathways involving mitochondria, the proteasome and oxidative stress [113].

Overexpression of α-synuclein has been found to fragment mitochondria in neurons preceding deterioration of mitochondrial function [114]. This process occurred through promotion of fission requiring a direct interaction of α-synuclein with mitochondrial membranes, allowing it to remodel them [26].

α-synuclein was also shown to dysregulate mitophagy. In cortical neurons transfected with mutant A53T α-synuclein, the level of healthy mitochondria colocalising with autophagosomes was increased. This was associated with decreased ATP levels resulting in bioenergetic deficits in the neurons. In this context, the role of Parkin, which is to mark mitochondria for degradation by the lysosome, became altered [115].

4.6.4. Endoplasmic reticulum

The Endoplasmic reticulum (ER) is involved in a variety of functions including lipid biosynthesis, protein folding and sorting, and calcium storage. The unfolded protein response (UPR) is a stress response that originates from the ER when there is an increase of unfolded protein in its lumen. The chaperone glucose regulated protein 78 (GRP78/BIP) binds to the luminal domain of stress sensors in the ER and dissociates upon binding to unfolded proteins which results in the initiation of stress signals [46]. α-synuclein has been shown to directly interact with GRP78/BIP [106] and the stress sensors [116]. The expression of GRP78/BIP decreases with age, however, in PD patients an increase occurs in brain tissue affected by α-synuclein pathology [117]. This suggests that accumulation of misfolded α-synuclein in the ER can act as a trigger of the UPR in synucleinopathies.

4.6.5. Microtubules

MAPT, which encodes the microtubule associated protein tau, has been investigated as a candidate gene in PD due to the shared neuropathological characteristics between a number of neurodegenerative diseases. Brain tissue from AD, tauopathies and PD all show aggregation of intraneuronal hyperphosphorylated Tau [118]. *MAPT* is located on chromosome 17 in an interval that is characterised by a large inversion with two haplotypes, H1 and H2. In Caucasian populations H1 has been identified as a genetic risk factor for PD [119].

Tau pathology in PD is often accompanied with α-synuclein pathology [120]. α-synuclein fibrils bind to tau through an ionic interaction and inhibit tau from aiding microtubule assembly. Although this interaction may not be crucial for the formation of LBs or PD pathogenesis, it has been shown that when incubated together they synergistically promote fibrilization [121]. α-synuclein fibrils may interact with other microtubule associated proteins (MAPs) as they have similar microtubule binding domains to tau. Levels of MAPs may be reduced in neurons resulting in disruption of the microtubule network and subsequent neuronal death. Microtubules play a major role in transport of mitochondria, vesicles and organelles. Therefore, disruption of their functions in axons may cause axonal impairment followed by neurodegeneration [122].

4.7. Proteomics and the study of disease mechanisms in PD

4.7.1. Principles of proteomics

With increasing knowledge of the genetics of PD, the mechanisms of disease pathology and progression can be determined, one way this can be achieved is with proteomics. While the genome is more or less constant, the proteome of an organism differs between cell types as well as with time. Proteomics is a powerful approach to confirm the presence and quantity of proteins. Commonly, proteins may be detected using immunoassays or mass spectrometry (MS), however approaches have evolved over the past two decades, with the number of proteins that can be analysed in a single sample increasing from hundreds two decades ago to thousands today [123].

Before MS analysis, proteins are subjected to tryptic digestion, producing peptides. The peptides are then ionized, the most common method used is electrospray ionisation (ESI). The ESI process involves transferring ions from solutions to gaseous phase. Under high voltage, the sample solution, containing sample peptides and solvent typically in water, is released from a capillary needle in the form of liquid droplets [124]. The charged droplets are accelerated towards a counter charge electrode, passing through heated gas [125]. The solvent in the droplets progressively evaporates further concentrating the charge [126]. The resulting ions are separated according to their mass-to-charge ratio (m/z). This is typically done by subjecting them to a magnetic field, ions with different mass-to-charge ratios are deflected to a different degree. The ions are detected and the results are displayed as a spectra of signal intensity of detected ions. Proteins in the sample are then identified by comparison of known masses or characteristic fragmentation patterns with the identified masses [127].

Tandem mass spectrometry (MS/MS) analyses samples using two or more mass analysers coupled together. After the sample has been ionised, the first spectrometer separates the ions by their m/z. Ions with particular m/z ratios are then split into smaller fragment ions. Collision induced dissociation (CID) is the most common method of fragmentation. In the presence of inert gases, ions collide with each other causing them to form smaller defined masses based on their amino acid sequence [126]. Fragmented ions are separated further by a second spectrometer, their spectra are then used to predict protein sequences through database comparison [128], (Fig. 10).

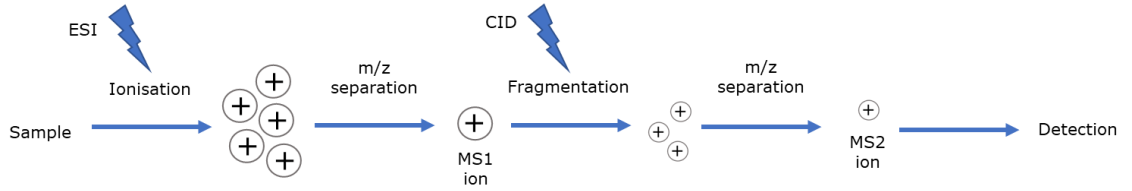

FIGURE 10. **Schematic showing the stages of tandem mass spectrometry**. The sample is ionized, most commonly through by electrospray ionisation (ESI), this produces a mixture of ions. Ions of a specific mass to charge ratio (m/z) are selected (MS1). Selected ions are fragmented usually through collision induced dissociation (CID). The resulting fragment ions are separated again (MS2). The spectrum of the separated fragment ions is then generated.

Database matching of MS/MS data is possible because the peptide ions fragment preferentially at certain points along the backbone [129]. However, fragmentation is not a clean process and the spectrum will often show peaks from side chains and internal fragments, which is why database searches comparing peptides to candidate peptide sequences is essential. When comparing the MS/MS to the candidate sequences, the pool may be limited meaning that the best match is accepted as the correct sequence. For example, if there is no sequence from one half of a peptide in the database but the other half is present and the molecular mass matches, this is accepted as the correct sequence [129].

Initial approaches for database searches of MS/MS data involved selection of sequence tags. These consisted of choosing a short sequence of residues that when combined with the fragment ion mass values that enclose the sequence, peptide mass and the specificity of the enzyme used to produce the initial peptides, inferred the peptide's protein of origin [130]. Due to the expertise required for the selection of appropriate tags, this technique has been superseded by direct searches of the MS/MS peak list [129]. The method of comparing experimental MS/MS spectra against that predicted from candidate peptide sequences had led to the creation of a variety of programs both local and online for performing searches of uninterpreted MS/MS data. All search engines support searching of protein databases with some supporting the search of DNA sequences [129].

While proteomic analysis can be used to qualitatively identify thousands of proteins in biological samples, there is also a need to quantitate them. Global protein dynamics can be studied on a cellular and tissue level using quantitative proteomics which is critical for understanding protein kinetics and the mechanisms of biological processes.

MS/MS is the basis of several quantitative proteomic methods such as tandem mass tagging (TMT). TMT is a quantitative proteomic approach which allows several samples to be analysed at once. Peptides are labelled with isobaric tags that consist of a mass reporter, a mass normalizer and an amine reactive group (Fig. 11A). Each tag has the same overall structure and mass but vary in the distribution of heavy isotopes within the

mass reporter region which is identified during the second round of MS [131], (Fig. 11B). These differences mean that when the mass reporter is cleaved during the second round of MS they can be identified in order of mass [132].

TMT allows digested peptides from multiple samples to be labelled with as many as ten tag variants [131]. After proteins have been denatured and digested, they are labelled with TMT. The differentially labelled samples are then combined and subjected to MS/MS as outlined above in Figure 10. TMT not only allows for identification of the peptides present in the samples but also their relative abundance through comparison of the peptides relative peak size [131].

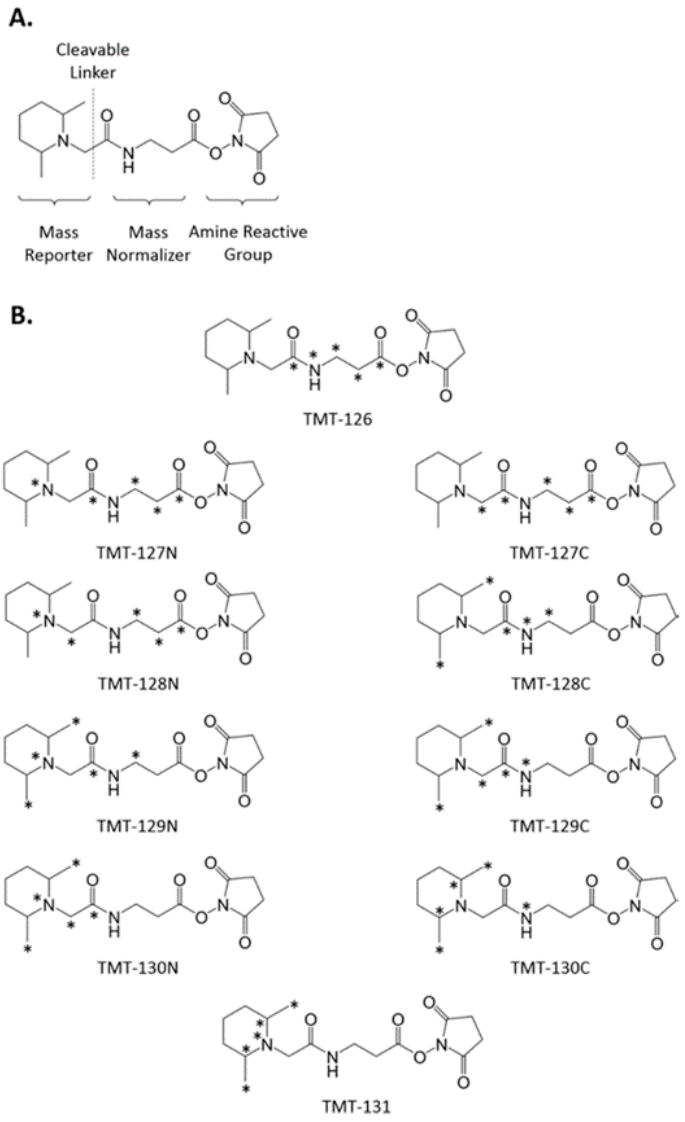

FIGURE 11. **Structure of TMT reagents.** A) TMT reagent consisting of a mass reporter, mass normalizer and amine reactive group. B) 10plex TMT. Heavy labelled C12 and N13 are indicated by asterisks (Figure taken from [131]).

Another quantitative method is stable isotope labelling by amino acids in cell culture (SILAC). SILAC involves labelling protein samples by growing cells in media containing

heavy and light forms of an amino acid. Cell lysates are mixed, from which the proteins are extracted and digested. The samples are then analysed by MS [123, 133], (Fig. 12). The difference in isotope mass allows for the signals of each cell type to be identified and compared. This method is useful for detecting relatively small changes in protein levels or post-translational modifications as the labelling is introduced early in the workflow and is therefore retained throughout the processing steps [126].

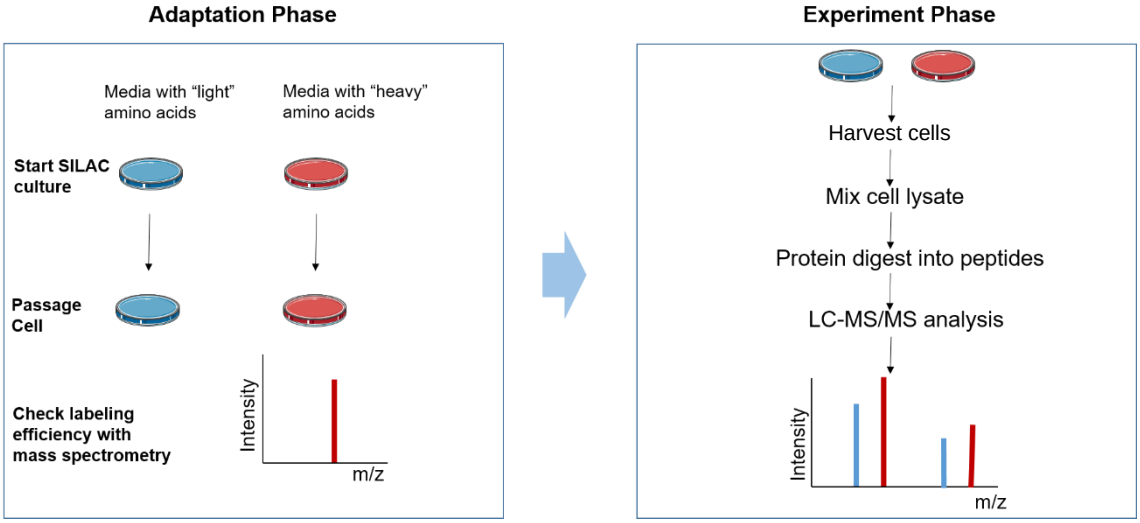

FIGURE 12. **The principle of SILAC.** During the adaptation phase, cells are grown in light and heavy SILAC medium until heavy amino acids are fully incorporated into the growing cells. During the experimental phase, the two cell populations are subjected to different treatments according to the research aim. The cell populations are mixed and the proteins are digested into peptides. Samples are then analysed with LC-MS/MS to identify and quantify the ratio of heavy to light peptides. (Figure taken from [133]).

4.7.2. Proteomic analysis of Interactions with α-synuclein

Proteomics is useful for elucidating the role of α-synuclein in PD and other synucleinopathies. This is largely due to the ability to map thousands of interactions or changes in protein levels within a single sample. As more information is gathered, it will become clearer as to how the role of α-synuclein changes under pathogenic conditions and the implications it has on the progression of PD and other synucleinopathies.

α-synuclein has been suggested to play a role in synaptic homeostasis. Identifying its interaction partners will provide insight into its function under physiological and pathological conditions. Under pathological conditions where α-synuclein is present in LBs, it is mostly phosphorylated at Ser-129, occurring in both familial and sporadic Lewy body diseases, such as PD [134]. The extent of α-synuclein phosphorylation and its aggregation in LBs as steps in disease pathogenesis is still controversial. Pulldown assays were utilised to analyse the protein-protein interactions of phosphorylated and non-phosphorylated α-synuclein. The use of targeted functional proteomics such as pulldown assays provides a broad and unbiased look at protein networks and how they

may change as the result of post-translational modifications. This simple approach allowed for observation of globular cell interactions of α-synuclein [134]. Protein pulldown assays showed that non-phosphorylated α-synuclein protein complexes were enriched for mitochondrial proteins whereas, the proteins pulled down by phosphorylated α-synuclein were of cytoskeletal and vesicular trafficking origin [134]. Alongside α-synuclein, LBs have been shown to contain a variety of proteins including cytoskeletal proteins, MAP1B and tau [111]. As phosphorylated α-synuclein was shown to interact with cytoskeletal elements, their presence in LBs suggests that the production of LBs likely results in-part from these interactions [134].

Mitochondria are the most studied organelle for understanding the pathology of PD due to the autosomal recessive mutations observed in the genes encoding the proteins PINK1, DJ-1 and Parkin which are involved in mitochondrial quality control [135]. Death of dopaminergic neurons resulting from induction of oxidative stress and apoptotic pathways involving mitochondria provides evidence of their contribution to the pathology of PD, the extent of which needs to be determined [136]. MS/MS was used to quantitate any changes in protein expression upon overexpression of α-synuclein in transgenic mice. Overexpression of α-synuclein led to the downregulation of mitochondrial complex I and IV but upregulation of complex III of the electron transport chain. With α-synuclein overexpression causing mitochondrial dysfunction it was suggested that α-synuclein could down regulate complex I and IV and that the upregulation of complex III was a compensatory measure by the cell [137]. Further work will need to determine whether this effect is also observed in human PD pathology, if so, it could provide a greater understanding of the role α-synuclein plays in mitochondrial dysfunction.

Despite clinical benefits of supplementing dopamine levels in PD patients, it has been suspected that dopamine may contribute to PD pathogenesis [138]. Proteomics was used to investigate the interplay between α-synuclein and dopamine in the SH-SY5Y human neuroblastoma cell line [139]. Proteins involved in protein synthesis were less abundant after dopamine treatment suggesting reduced expression under cellular stress conditions [139]. Changes in mitochondrial protein expression were also observed, including the disappearance of VDAC2 upon treatment with dopamine. VDAC2 is a porin of the outer-mitochondrial membrane which regulates mitochondrial calcium homeostasis and mitochondrial-dependent cell death, two major factors in PD [140]. An enriched network model was produced to deduce whether proteins differentially expressed were involved in the same network. This procedure suggested potential involvement of the NF-κB pathway and apoptosis regulation, later shown experimentally by α-synuclein's ability to reduce the activation of NF-κB [139].

When dopamine is not degraded or packaged into synaptic vesicles it becomes oxidised, generating quinones and reactive oxygen species. Extensive evidence has indicated that oxidised dopamine inhibits the aggregation of α-synuclein [141]. Consistent with this, elevation of dopamine levels in SH-SY5Y cells expressing A53T α-synuclein resulted in a reduction of aggregates and an increase in soluble oligomers [141]. Mor et al. (2017) tested the effects *in vivo*, examining α-synuclein in the SN of A53T mice. In the A53T control mice which had been injected with an empty vector, inclusion pathology was absent in the SN, there was no alteration in the levels of insoluble α-synuclein rather they presented a reduction in α-synuclein monomers and an increase in oligomers of different conformations. These findings suggested that the toxicity of dopamine-induced oligomers is not dependent on seeding [142]. Concurrent with this, expression of WT and A53T α-synuclein in dopaminergic neurons in *C. elegans* has been shown to cause neuronal dysfunction and death with increased cytosolic dopamine accumulation [143]. These studies indicate a relationship between dopamine and α-synuclein in the induction of neuronal cell death.

As shown by the presence of GCIs in MSA, aggregated α-synuclein does not just affect neurons in synucleinopathies. In fact, aggregated α-synuclein has been shown to activate microglia which play a major role in neuroinflammation [144]. Liu et al. (2007) aimed to elucidate the mechanism by which aggregated α-synuclein enters microglia using SILAC on primary cultured microglia. They identified 46 microglial membrane proteins whose relative abundance was altered after α-synuclein treatment. Of these proteins, clathrin and calnexin were further evaluated. For the first time they were able to show that microglial endocytosis of aggregated α-synuclein may involve the classic clathrin-mediated endocytic pathway due to the co-localisation of clathrin and aggregated α-synuclein within the microglia [144].

4.7.3. LBs

LBs themselves are valuable samples for proteomic investigations, with these inclusions being a histopathological hallmark of PD and other synucleinopathies. As mentioned previously, there are several proteins present in LBs aside from α-synuclein, which may or may not be relevant to PD progression. Henderson and colleagues performed proteomic analysis on insoluble proteins in a primary neuron model of α-synuclein pathology to identify proteins involved in early LB formation [145]. This approach involved the use of liquid chromatography-MS/MS. As this study aimed to identify a number of proteins, MS/MS was essential for their identification [145]. Several novel proteins were identified in LBs including the microtubule affinity-regulating kinase 1 (MARK1), [145]. MARKs were originally identified as kinases which phosphorylated tau resulting in a

decrease of tau binding to microtubules and their subsequent destabilisation or alteration of microtubule-dependent transport [146]. Moreover, MARKs have been implicated in PD pathways. MARK2 was shown to activate a cleaved form of PINK1, while MARK1 has been identified as a direct substrate of LRRK2, mutations of which are implicated in PD. These findings suggest that MARKs may play a role in the pathogenesis of PD, the extent of which will be determined in future studies [145].

Although the presence of LBs is the pathological hallmark of PD, models commonly used to study the disease have not exhibited the biochemical complexity of LBs in post-mortem brains of PD patients, instead, reproducing specific aspects or stages of LB pathology formation [147]. As these models have not shown the transition from α-synuclein fibrils to LB inclusions, the different stages of LB pathology formation remain to be elucidated. Recent work by Mahul-Mellier et al. (2020) aimed to address this using a cellular seeding-based mouse model. When culturing neurons for proteomic analysis, they extended the seeding process of α-synuclein preformed fibrils from 14 to 21 days, allowing for the formation of LB-like inclusions [147].

Using probes that target different types of lipids they were able to detect several classes of lipids present in their seeding model which are *bona fide* components of LB inclusions derived from post-mortem PD brains, demonstrating that their model recapitulates processes in LB formation. Mahul-Mellier et al. (2020) used proteomics to compare their model to LBs from human brain tissue, with a quarter of the proteins identified in their inclusion data at day 14 and 21 being described previously as components of LBs [148]. In their model, the formation of α-synuclein fibrils occurred as early as days 4-7 with no effect on neuronal viability up to day 14, suggesting that α-synuclein fibrillization is not sufficient to trigger neuron death. As LBs began to form between days 14 and 21, cell function became impaired leading to the conclusion that it is the formation of LBs rather than α-synuclein fibril formation that is the major factor in α-synuclein toxicity [147]. Proteomics was crucial in this study as it allowed for observation of changes in the global cell proteome both in cellular models and patient samples.

4.8. Project Aim

4.8.1. Aim

Although it is known that exogenous α-synuclein fibrils can be taken up by cells and induce aggregation of endogenous α-synuclein intro intracellular inclusions, there is little known about the initial cellular response to uptake. It is also unclear at present as to the events between uptake and initial inclusion formation. Proteomics has provided novel information on PD and other amyloid diseases as well as providing an unbiased

approach for observing changes in protein levels in a cell in response to external factors. Proteomics is therefore a useful method for understanding cellular response upon exposure to α-synuclein fibrils. It can be utilised to detect the presence of α-synuclein in samples such as whole cell lysates, as well as identification of α-synuclein interaction partners. This kind of data is crucial for understanding the effects of α-synuclein aggregation. With the transmission of α-synuclein aggregates known to occur in several ways, identification of pathways associated with α-synuclein can elucidate how such aggregates are implicated in cellular dysfunction and ultimately neuronal death.

This project aims to examine the response of cells upon initial exposure to extracellular α-synuclein fibrils and after the fibrils have seeded endogenous inclusions. Proteomics will be used to study the cellular response by identifying changes in the cellular proteome.

4.8.2. Objectives

1. Establish and characterise a cellular model to study the effect of exogenous α-synuclein fibrils on cells.
2. Analyse the effect that exposure to exogenous α-synuclein has on the cellular proteome.
3. Use bioinformatics tools to analyse the changes in the cellular proteome and determine the functional consequences for the cells.

5. Results

5.1. Characterisation of an experimental model for the study of the effects of exogenous α-synuclein fibrils on cells

In this project the effect of α-synuclein fibrils on the proteome of the neuroblastoma cell line SH-SY5Y GFP-α-synuclein was observed. This cell line was chosen as it overexpresses α-synuclein and it can act as a model for LB formation, with exogenous fibrils promoting α-synuclein aggregation into intracellular inclusions [149]. However, it was necessary that the cellular model was characterized prior to proteomic analysis to observe the effects that α-synuclein fibrils had on GFP-α-synuclein cells. This involved determining the toxicity of α-synuclein fibrils on the cells, observing the internalisation of the fibrils and their ability to seed GFP-α-synuclein aggregation.

5.1.1. Characterisation of the effect of α-synuclein fibrils on SH-SY5Y GFP-α-synuclein cell viability

The SH-SY5Y GFP-α-synuclein cell line used for this project was derived from the neuroblastoma SH-SY5Y cell line which had been stably transfected with GFP-α-synuclein [150, 151]. The GFP-α-synuclein fusion is 49 kDa in size, it has GFP at the N-terminus, a short linker region followed by the full-length wild type α-synuclein sequence at the C-terminus (Fig. 13). The GFP-α-synuclein can be visualised by confocal microscopy, appearing green when imaged. As the fusion protein was overexpressed in the SH-SY5Y GFP-α-synuclein cell line, it was easy to visualise during microscopy. Furthermore, with the ability of SH-SY5Y GFP-α-synuclein cells to be seeded, forming cytoplasmic inclusions upon incubation with α-synuclein fibrils, this cell line can serve as a model of LB formation.

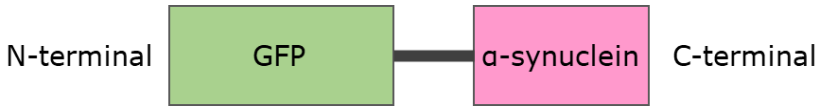

MVSKGAELFTGIVPILIELNGDVNGHKFSVSGEGEGDATYGKLTLKFICTTGKLPV
PWPTLVTTLSYGVQCFSRYPDHMKQHDFFKSAMPEGYIQERTIFFEDDGNYKSR
AEVKFEGDTLVNRIELTGTDFKEDGNILGNKMEYNYNAHNVYIMTDKAKNGIKVN
FKIRHNIEDGSVQLADHYQQNTPIGDGPVLLPDNHYLSTQSALSKDPNEKRDHMI
YFGFVTAAAITHGMDELYKSGLRSRAQASNSMDVFMKGLSKAKEGVVAAAEKTK
QGVAEAAGKTKEGVLYVGSKTKEGVVHGVATVAEKTKEQVTNVGGAVVTGVTA
VAQKTVEGAGSIAAATGFVKKDQLGKNEEGAPQEGILEDMPVDPDNEAYEMPSE
EGYQDYEPEA

FIGURE 13. **Schematic of the GFP-α-synuclein protein.** The fusion protein is 49 kDa in size. The GFP region (green) is connected to the α-synuclein region (pink) via a short linker region (black). The predicted protein sequence is given underneath (Sequence provided by the Hewitt research group).

5.1.2. Production of Alexa Fluor 594-labelled α-synuclein fibrils

α-synuclein fibrils used in this project were labelled with a fluorescent dye to enable them to be visualised using fluorescence microscopy. Labelled fibrils for use in this project were produced and provided by Michael Davies of the Hewitt research group. Briefly, monomeric α-synuclein was labelled with Alexa Fluor 594 on lysine residues by N-Hydroxysuccinimide (NHS) chemistry, and unreacted label removed by size exclusion chromatography. Labelled and unlabelled monomeric α-synuclein were incubated for 3 days and constantly agitated to produce fibrils (Fig. 14).

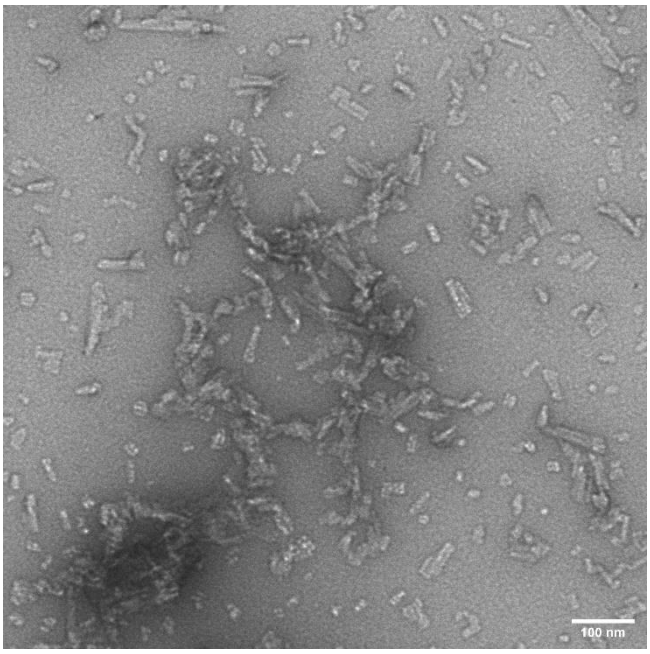

FIGURE 14. **EM image of sonicated Alexa Fluor 594-labelled α-synuclein fibrils.** Fibrils were produced by incubation of 500 μM monomeric α-synuclein with 5% Alexa Fluor 594-labelled monomer for 3 days at 42°C and constantly agitated at 1500 rpm. Image produced by Michael Davies of the Hewitt research group. Scale bar = 100 nm.

5.1.3. Analysis of the impact of α-synuclein fibrils on cell viability

In initial experiments the response of the SH-SY5Y GFP-α-synuclein cells to incubation with α-synuclein fibrils, was characterised by determining if the fibrils were toxic to these cells. Three different assays were used, each measuring an aspect of cellular function and in combination they could infer whether the addition of fibrils affected cell viability.

5.1.3.1. Analysis of the effect of α-synuclein fibrils on cellular Adenosine Triphosphate (ATP) levels

ATP is present in metabolically active cells and is therefore a marker for cell viability. The ATPlite assay system is based on the production of light caused by the reaction of ATP with added luciferase and D-luciferin [152], (Fig. 15). The light that is emitted is directly proportional to the ATP concentration of the cells within samples; reduced levels of ATP would therefore be indicative of increased cellular stress or death.

$$\text{ATP} + \text{D-Luciferin} + O_2 \xrightarrow[Mg^2]{\text{Luciferase}} \text{Oxyluciferin} + \text{AMP} + PP_i + CO_2 + \text{Light}$$

FIGURE 15. **Schematic of the reaction during the ATP assay.** This assay uses firefly luciferase to convert ATP and luciferin to oxyluciferin and light. The amount of light emitted in this reaction is directly proportional to the concentration of ATP present (Figure adapted from [152]).

SH-SY5Y GFP-α-synuclein cells were incubated for 24 hr in the presence or absence of Alexa Fluor 594-labelled α-synuclein fibrils or PBS buffer prior to the ATP assay. Immediately before the assay, control cells were lysed with detergent containing buffer, causing cell death and subsequent reduction in the level of ATP. These cells served as a background reading against which the sample cells were compared. Once the assay was complete the luminescence of each sample was measured.

There was no luminescence observed in the lysis control cells, however, upon comparison there was luminescence which did not differ significantly between cells incubated with fibrils and cells incubated with the PBS buffer control. This demonstrated that there was no reduction in ATP levels when fibrils were added to the cells (Fig. 16), (Table 1).

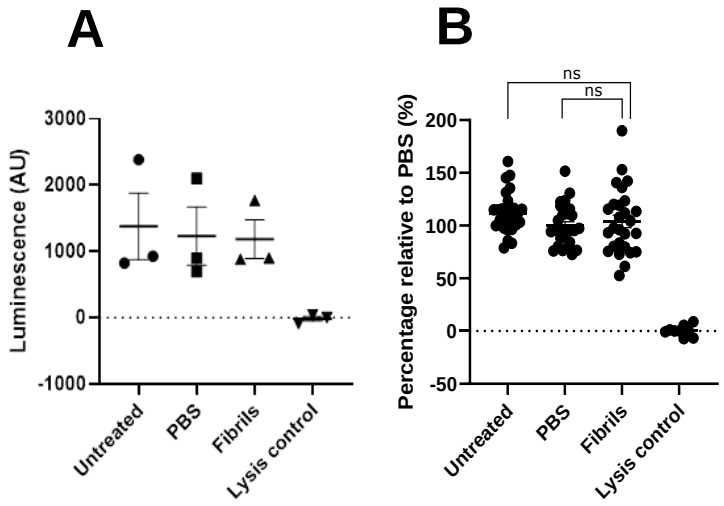

FIGURE 16. **ATP assay conducted on SH-SY5Y GFP-α-synuclein cells after 24 hr incubation with Alexa Fluor 594-labelled α-synuclein fibrils.** Cells were incubated with 1 µM Alexa Fluor 594-labelled α-synuclein fibrils (final concentration monomer equivalent) in PBS, equivalent volume of PBS or untreated for 24 hr. Lysis control samples were treated with 20 µL lysis buffer prior to assays. A: Luminescence measured after ATP assay. AU, arbitrary units. B: ATP assay normalised to cells incubated with PBS. Results are expressed as mean ± 1 S.E.M, n=3. Welch's ANOVA and Dunnett's T3 multiple comparison tests were used for analysis of the data set (ns, not significant). The assay was conducted in triplicate each with nine replicates.

TABLE 1. **Dunnett's T3 multiple comparisons test of ATP assay on SH-SY5Y GFP-α-synuclein cells incubated with α-synuclein fibrils for 24 hr.**

	Mean Difference	Adjusted *p*-value
Untreated vs PBS	11.73	0.1661
Untreated vs Fibrils	7.848	0.8374
Untreated vs Lysis control	111.7	<0.0001
PBS vs Fibrils	-3.883	0.9940
PBS vs Lysis control	99.94	<0.0001
Fibrils vs Lysis control	103.8	<0.0001

5.1.3.2. Analysis of the effect α-synuclein fibrils has on the cellular release of Lactate Dehydrogenase (LDH)

LDH is a soluble cytosolic enzyme and damage to the plasma membrane results in the release of LDH into the cell media. For example, during the initial stages of apoptosis, the cytoskeleton breaks up resulting in membrane blebbing, this leads to damage of the plasma membrane through which cytosolic contents are released [153]. The release of LDH can be used to determine the level of membrane damage in cells and thus infer whether there is any reduction in cell viability. The amount of LDH released into the media can be quantified by the following reaction. LDH catalyses the conversion of lactate to pyruvate via NAD+ reduction to NADH. In the assay, diaphorase then uses NADH to reduce INT to a red formazan product that can be measured at 490nm [154], (Fig. 17). The level of formazan produced is directly proportional to the amount of LDH released into the medium.

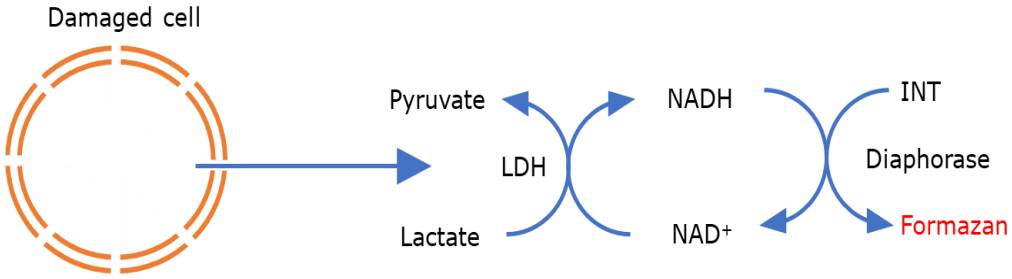

FIGURE 17. **Schematic of the enzymatic reaction during the LDH assay.** LDH catalyses the conversion of lactate to pyruvate which is concomitant with the reduction of NAD+ to NADH. Diaphorase utilises NADH to reduce INT to a red formazan product allowing for colorimetric quantification (Figure adapted from [154]).

SH-SY5Y GFP-α-synuclein cells were incubated for 24 hr in the presence or absence of Alexa Fluor 594-labelled α-synuclein fibrils or PBS buffer prior to the LDH assay. Immediately before the assay, positive control cells were lysed with detergent containing buffer. This permeabilised the plasma membrane allowing these cells to serve as a background reading for LDH release into the medium.

The level of LDH released into the medium did not differ significantly between cells treated with PBS or fibrils. This demonstrated that the fibrils did not cause any significant damage to the plasma membrane (Fig. 18), (Table 2).

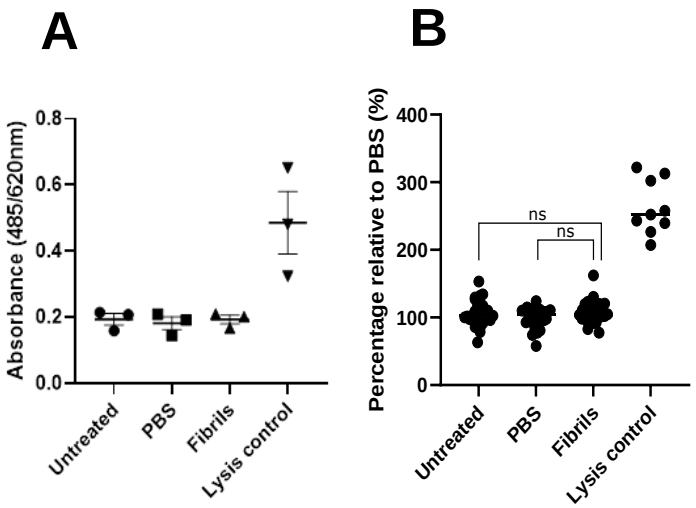

FIGURE 18. **LDH assay conducted on SH-SY5Y GFP-α-synuclein cells after 24 hr incubation with Alexa Fluor 594 labelled α-synuclein fibrils.** Cells were incubated with 1 μM Alexa Fluor 594 labelled α-synuclein fibrils (final concentration monomer equivalent) in PBS, equivalent volume of PBS or untreated for 24 hr. LDH positive control samples were treated with 20 μL LDH lysis buffer prior to assays. A: Absorbance measured at 485/620 nm after LDH assay. B: LDH assay normalised to PBS. Results are expressed as mean ± 1 S.E.M, n=3. Kruskal-Wallis and Dunn's multiple comparisons tests were used for analysis of the data set (ns, not significant). The assay was conducted in triplicate each with nine replicates.

TABLE 2. **Dunn's multiple comparisons test of LDH assay on SH-SY5Y GFP-α-synuclein cells incubated with α-synuclein fibrils for 24 hr.**

	Mean Rank Difference	Adjusted *p*-value
Untreated vs PBS	6.944	>0.9999
Untreated vs Fibrils	0.500	>0.9999
Untreated vs Lysis control	-42.52	0.0001
PBS vs Fibrils	-6.444	>0.9999
PBS vs Lysis control	-49.46	<0.0001
Fibrils vs Lysis control	-43.02	0.0001

5.1.3.3. Analysis of the effect α-synuclein fibrils has on the cellular reduction of 3-(4,5-Dimethylthiazol-2-yl)-2,5-Diphenyltetrazolium Bromide (MTT)

The MTT assay is a colorimetric assay for assessing cell metabolic activity. MTT is reduced to insoluble purple formazan via NADPH dependent oxidoreductase enzymes. The level of formazan produced is directly proportional to the amount of MTT reduced and can indicate cellular viability [155], (Fig. 19).

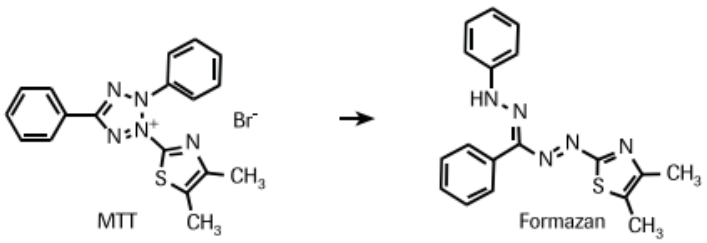

FIGURE 19. **Schematic of the reaction during the MTT assay.** MTT is reduced to insoluble purple formazan (Figure taken from [155]).

SH-SY5Y GFP-α-synuclein cells were incubated for 24 hr in the presence or absence of Alexa Fluor 594-labelled α-synuclein fibrils or PBS buffer prior to the MTT assay. Immediately before the assay, control cells were lysed. This caused cell death, providing a background level of MTT reduction against which the cells incubated with PBS and fibrils could be compared.

There was a small, but not statistically significant, decrease in the reduction of MTT for cells incubated with fibrils when compared to cells incubated with PBS samples. These data support the outcome of the other assays, whereby addition of fibrils is not cytotoxic to SH-SY5Y GFP-α-synuclein cells (Fig. 20), (Table 3).

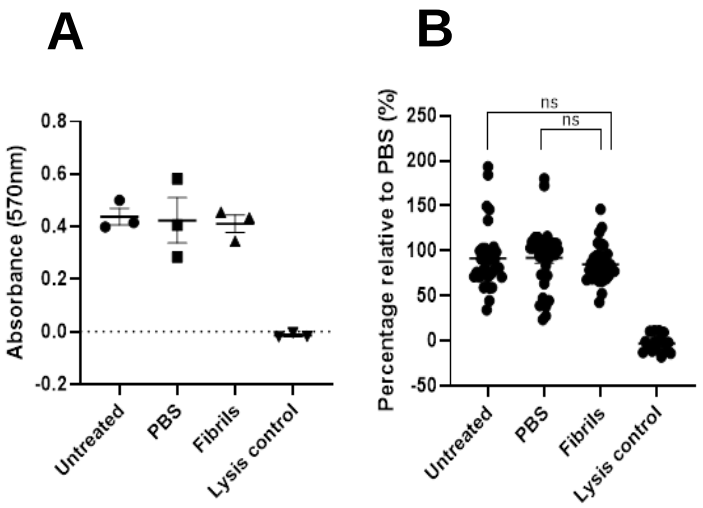

FIGURE 20. **MTT assay conducted on SH-SY5Y GFP-α-synuclein cells after 24 hr incubation with Alexa Fluor 594 labelled α-synuclein fibrils.** Cells were incubated with 1 μM Alexa Fluor 594 labelled α-synuclein fibrils (final concentration monomer equivalent) in PBS, equivalent volume of PBS or untreated for 24 hr. Lysis control samples were treated with 20 μL lysis buffer prior to assays. A: Absorbance measured at 570 nm after MTT assay. B: MTT assay normalised to PBS. Results are expressed as mean ± 1 S.E.M, n=3. Kruskal-Wallis and Dunn's multiple comparisons tests were used for analysis of the data set (ns, not significant). The assay was conducted in triplicate each with nine replicates.

TABLE 3. **Dunn's multiple comparisons test of MTT assay on SH-SY5Y GFP-α-synuclein cells incubated with α-synuclein fibrils for 24 hr.**

	Mean Rank Difference	Adjusted *p*-value
Untreated vs PBS	-10.04	>0.9999
Untreated vs Fibrils	3.271	>0.9999
Untreated vs Lysis control	58.74	<0.0001
PBS vs Fibrils	13.31	0.6913
PBS vs Lysis control	68.79	<0.0001
Fibrils vs Lysis control	55.47	<0.0001

5.1.4. Analysis of fibril uptake and localisation in SH-SY5Y GFP-α-synuclein cells

As the incubation of SH-SY5Y GFP-α-synuclein cells with fibrils did not result in cell death, the interaction of fibrils with the cells was investigated next.

To analyse the interaction of α-synuclein fibrils with the SH-SY5Y GFP-α-synuclein cell line confocal microscopy was used, in order to observe the uptake and subsequent localisation of the fibrils. Upon endocytosis, fibrils are trafficked to the lysosomes. This has been shown previously in the SH-SY5Y cell line whereby after 24 hr exposure to Alexa Fluor 647-labelled α-synuclein fibrils, co-localisation of the fibrils with the lysosomal marker LAMP-1 was observed [156].

SH-SY5Y GFP-α-synuclein cells were incubated for 24 hr in the presence or absence of Alexa Fluor 594-labelled α-synuclein fibrils. After the incubation, LysoTracker Deep Red was used to identify lysosomes. Lysotracker probes are freely permeant to the cell membrane with a high selectivity for acidic organelles such as the lysosomes [157]. LysoTracker Deep Red was used during imaging as it allowed for multiplex imaging with GFP and Alexa Fluor 594 [157].

Live cell confocal microscopy demonstrated that Alexa Fluor 594-labelled α-synuclein fibrils exhibited a punctate distribution with a degree of co-localisation with the LysoTracker after 24 hr incubation. It can therefore be inferred that a proportion of the fibrils were internalised and sorted to lysosomes (Fig. 21). The same confocal imaging analysis was then applied to a 5-day incubation, after which co-localisation of Alexa Fluor 594-labelled α-synuclein fibrils with lysosomes was still present (Fig. 22). These results are consistent with other studies in which fibrils were shown to be internalised and localised with lysosomes [147, 156].

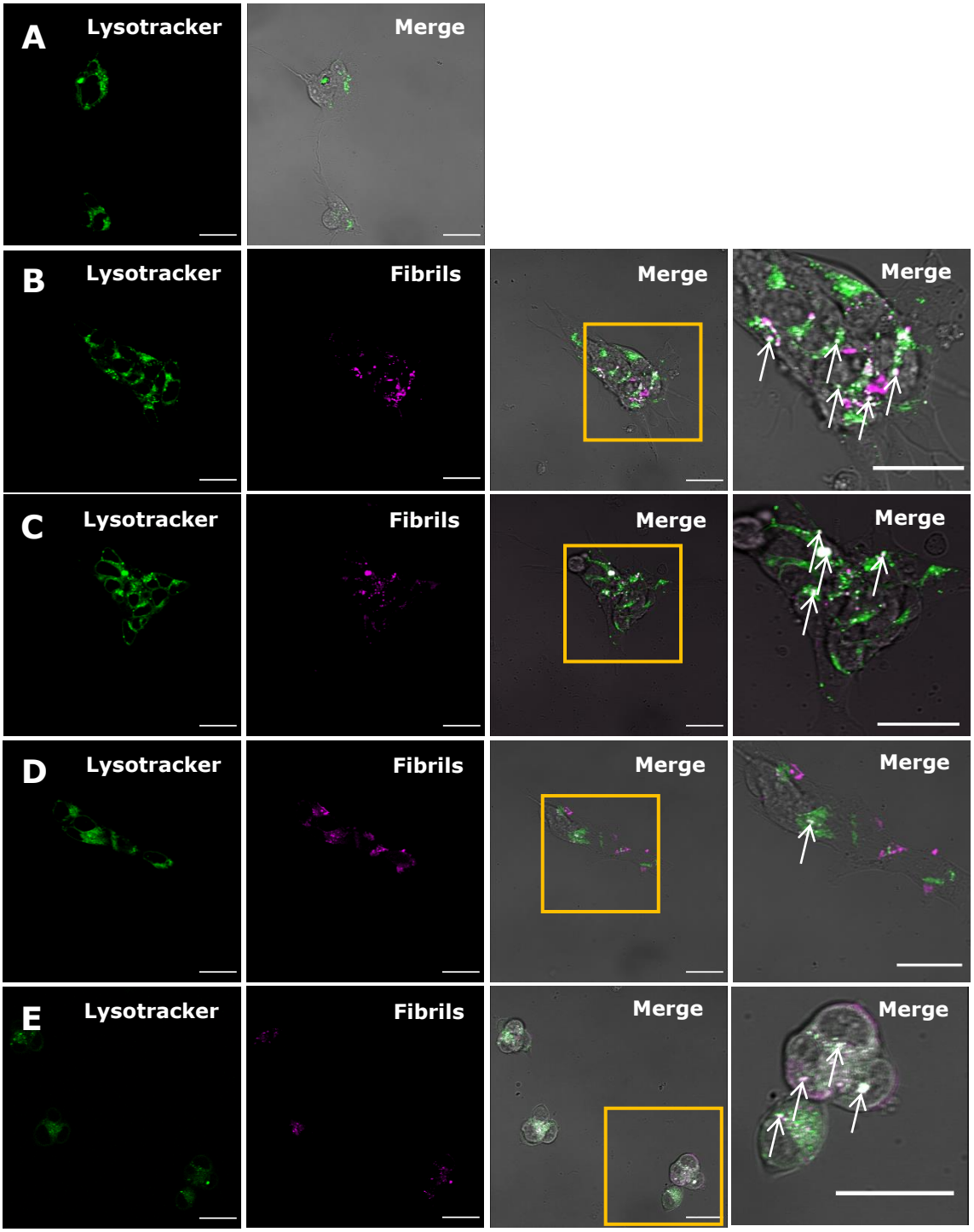

FIGURE 21. **Live cell confocal microscopy of α-synuclein fibrils incubated with SH-SY5Y GFP-α-synuclein cells for 24 hr.** GFP-α-synuclein SH-SY5Y cells were incubated for 24 hr in the presence or absence of 1 μM Alexa Fluor 594-labelled α-synuclein fibrils (monomer equivalent concentration), or 10 μL PBS buffer. A: PBS buffer. B-E: Alexa Fluor 594-labelled α-synuclein fibrils, Cells were imaged in media containing Hoechst and deep red Lysotracker. Lysotracker is presented in green and fibrils are presented in magenta. In the merged images, white arrows indicate co-localisation of fibrils with Lysotracker, yellow boxes highlight the origin of the zoomed in merge images. Images are presented with false colouring. Images were taken at 40X magnification. Scale bars = 25μm.

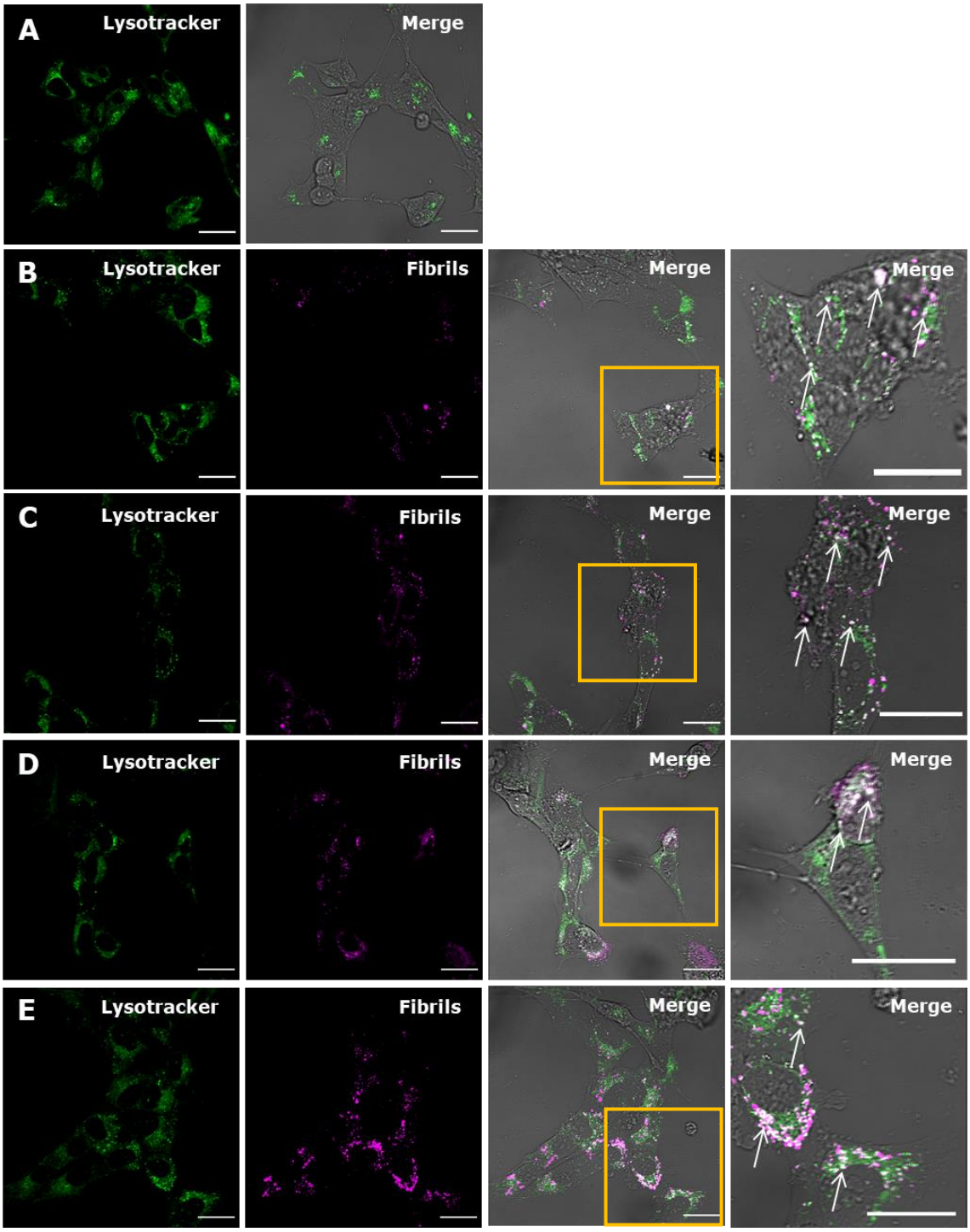

FIGURE 22. **Live cell confocal microscopy of α-synuclein fibrils incubated with SH-SY5Y GFP-α-synuclein cells for 5 days.** GFP-α-synuclein SH-SY5Y cells were incubated for 5 days in the presence or absence of 1 μM Alexa Fluor 594-labelled α-synuclein fibrils (monomer equivalent concentration), or 10 μL PBS buffer. A: PBS buffer. B-E: Alexa Fluor 594-labelled α-synuclein fibrils, Cells were imaged in media containing Hoechst and deep red Lysotracker. Lysotracker is presented in green and fibrils are presented in magenta. In the merged images, white arrows indicate co-localisation of fibrils with Lysotracker, yellow boxes highlight the origin of the zoomed in merge images. Images are presented with false colouring. Images were taken at 40X magnification. Scale bars = 25 μm.

5.1.5. Analysis of the seeding of intracellular GFP-α-synuclein by exogenous fibrils in SH-SY5Y GFP-α-synuclein cells

With the presence of α-synuclein fibrils in LBs, there has been much research on elucidating the mechanism for the formation of inclusions. α-synuclein fibrils have been suggested to have prion-like properties, whereby α-synuclein aggregates generated in one cell are transferred to neighbouring neurons via the synapse, acting as a template for misfolding of α-synuclein in the recipient neurons [53, 54, 56]. As shown herein, after internalisation, α-synuclein is trafficked to the lysosomes via the endocytic pathway. However, the prevailing hypothesis for fibril formation suggests that some α-synuclein escapes the endocytic pathway into the cytosol, where it can interact with intracellular monomeric α-synuclein [47]. Through this interaction it is believed that pathogenic α-synuclein can cause intracellular α-synuclein monomers to form insoluble fibrils [48].

It has previously been shown that seeding of α-synuclein can occur as early as 5-days *in vitro* through incubation of cells with α-synuclein fibrils. Preformed fibrils were shown to be endocytosed by primary neurons and induced recruitment of endogenously expressed α-synuclein into insoluble aggregates after 5-days incubation [147].

The final stage of characterising the cellular model involved demonstrating that exposure of SH-SY5Y GFP-α-synuclein cells for 5 days to exogenous fibrils can seed the aggregation of cytosolic α-synuclein, thus recapitulating previous observations in mouse primary neuronal cultures [147, 149]. The goal was to demonstrate the formation of insoluble GFP-α-synuclein inclusions within the cells as shown previously [147, 149]. In this seeding assay only a small percentage of GFP-α-synuclein formed insoluble inclusions. To visualise these inclusions, soluble GFP-α-synuclein was removed by permeabilising the cells with saponin detergent before fixation. After 5-days incubation in the absence of fibrils, no inclusions were observed. However, upon exposure to α-synuclein fibrils, detergent insoluble GFP-α-synuclein puncta were observed, consistent with the formation of intracellular inclusions (Fig. 23). This demonstrates that the cell model can recapitulate seeding of α-synuclein aggregation by exogenous fibrils and as such, it can be used as a model system for the cellular effects of α-synuclein fibrils on the proteome [147, 149].

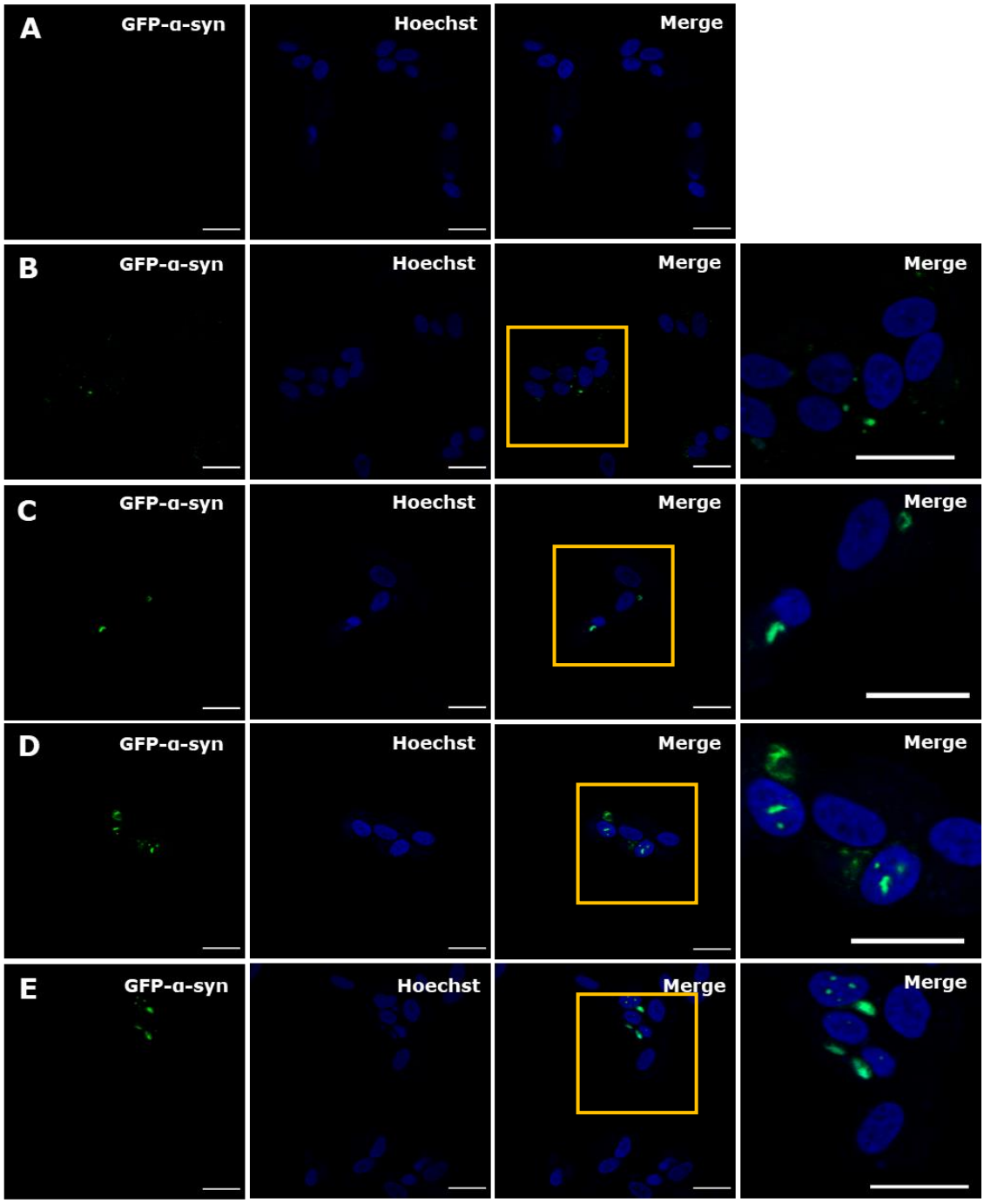

FIGURE 23. **Insoluble inclusions of α-synuclein are present after a 5-day seeding assay with α-synuclein fibrils.** SH-SY5Y GFP-α-synuclein cells were incubated for 5 days in the presence of 1 µM Alexa Fluor 594-labelled α-synuclein fibrils (monomer equivalent concentration), or 10 µL PBS buffer. A: PBS buffer. B-E: Alexa Fluor 594-labelled α-synuclein fibrils. Cells were permeabilised with saponin to remove soluble GFP-α-synuclein prior to fixation followed by staining with Hoechst in PBS buffer. GFP-α-synuclein inclusions (green), nuclei (blue), yellow boxes highlight the origin of the zoomed in merge images. Images are presented with false colouring. Images were taken at 40X magnification. Scale bars = 25 µm.

Having demonstrated experimentally that α-synuclein inclusions can form in the SH-SY5Y GFP-α-synuclein cells, combined with the cell line's overexpression of GFP-α-synuclein, they are ideal for use in proteomic analysis of protein changes resulting from the formation of α-synuclein inclusions.

5.2. Sample preparation for proteomic analysis

Having demonstrated that the experimental model, SH-SY5Y GFP-α-synuclein cells, can take up exogenous α-synuclein fibrils and that these can then seed α-synuclein aggregation, it can therefore be used as a model to study cellular effects of α-synuclein fibril uptake and the cellular effects of α-synuclein aggregation in the cytosol. To study this, proteomic analysis of the SH-SY5Y GFP-α-synuclein cells was conducted to observe whether the expression of proteins was altered in response to these events.

Having established the lack of toxicity α-synuclein fibrils have on the cell-system, whole cell lysate samples were prepared for proteomic analysis. SH-SY5Y GFP-α-synuclein cells were plated in triplicate with three independent experimental repeats for each timepoint: 0, 1 and 5-days incubation with Alexa Fluor 594-labelled α-synuclein fibrils. Cells were cultured for a total of 6 days. After 24 hrs, fibrils were added to the 5-day dishes, then to the 1-day dishes after another 4 days. This allowed for collection on the same day and comparison of cells at the same stage of growth, subjected to different lengths of fibril incubation. Cell lysates were produced from the SH-SY5Y GFP-α-synuclein cells and a bicinchoninic acid (BCA) assay was used to determine the protein concentration of each sample, this ensured equal amounts of protein in each sample sent for proteomic analysis.

Samples of cell lysates containing at least 2 mg/mL of protein were selected for further analysis as they contained sufficient protein for TMT-MS analysis. The presence of protein within each sample was confirmed by separating samples on an acrylamide gel (Fig. 24). With protein presence confirmed, 50 µg of each sample was sent to the University of Bristol Proteomics Facility for TMT-MS analysis.

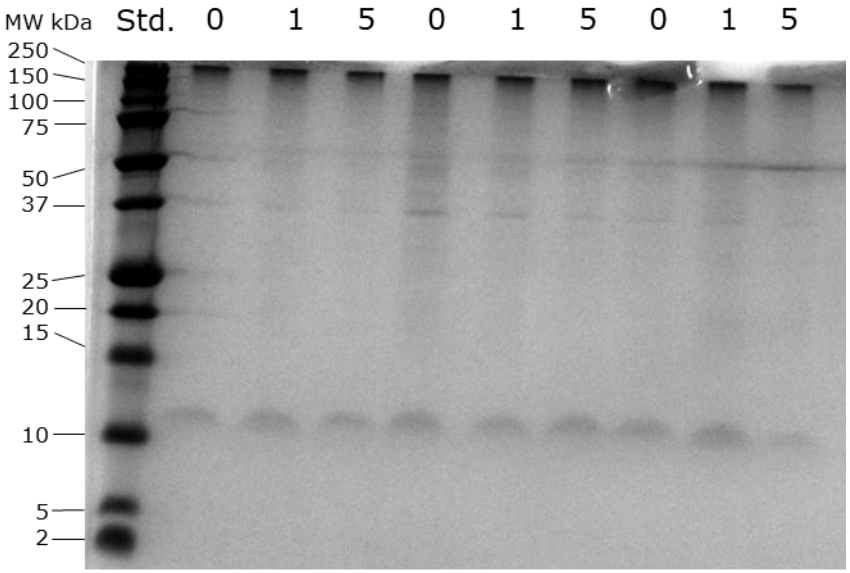

FIGURE 24. **Confirmation of protein present in whole cell lysate samples.** Samples were produced from lysed SH-SY5Y GFP-α-synuclein cells after incubation with 1 μM Alexa Fluor 594-labelled α-synuclein fibrils (monomer equivalent concentration) for 0, 1 or 5 days. Proteins were separated on a tris-tricine gel (30% (w/v) acrylamide), with each lane containing 0.5 mg/mL of protein, followed by overnight staining with PageBlue Protein Staining Solution (Thermo Scientific). The molecular weight of the protein standards (Std.) is given on the left.

5.3. Proteomics reveals quantitative changes in proteins from whole cell lysates incubated with α-synuclein fibrils

TMT-MS identified a total of 7263 proteins present in the whole cell lysate samples. After excluding contaminants and proteins presenting less than two unique peptides, this was reduced to 5802 proteins. Comparison of these proteins to a previously published proteome of the SH-SY5Y cell line revealed a coverage of 50.03% with the whole cell lysate proteins matching 2619 of the 5235 proteins of the SH-SY5Y cell line [158]. 3183 proteins from the whole cell lysates were absent in the previously published proteome.

Proteins from this set of 5802 proteins were selected if they had a fold change of at least 1.5 up or down for either 1 or 5-day incubation with α-synuclein fibrils when compared to 0 days. There were 124 proteins with an increase and seven with a decrease after either 1 or 5-day incubation with α-synuclein fibrils. Paired t-tests were used to determine which of these peptides presented significant fold changes. There was a total of 11 proteins that had a significant fold change after 1-day or 5-day incubation (Table 4). Of these proteins, α-synuclein and collagen α-1(II) chain (COL2A1) were significantly increased after 1-day and 5-day incubation, whereas, microtubule-associated protein 4 (MAP4) was significantly decreased after both timepoints. The increase of α-synuclein was consistent with the addition of α-synuclein fibrils to the cells, thus acting as an internal control for the ability of the proteomics methodology to detect changes in protein level.

TABLE 4. **Proteins that present a significant fold change after SH-SY5Y GFP-α-synuclein cells were incubated with Alexa Fluor 594-labelled α-synuclein fibrils.**

		Day 1		Day 5	
Protein	**Gene Name**	**Fold Change**	***p*-value**	**Fold Change**	***p*-value**
α-synuclein	NACP	1.872	0.0180	3.306	0.0031
Collagen α-1(II) chain	COL2A1	1.518	0.0020	1.661	0.0279
Collagen α-1(I) chain	COL1A1	6.062	0.0297	---	---
Collagen α-2(I) chain	COL1A2	2.847	0.0373	---	---
Microtubule-associated protein 4	MAP4	0.617	0.0123	0.578	0.0110
RNA polymerase-associated protein RTF1 homolog	RTF1	0.543	0.0017	---	---
Non-specific serine/threonine protein kinase	SIK3	---	---	1.917	0.0244
Skin-specific protein 32	XP32	---	---	2.628	0.0296
Protein tweety homolog 3	TTYH3	---	---	1.861	0.0463
Alpha-mannosidase 2	MAN2A1	---	---	1.557	0.0157
Coiled-coil domain-containing protein 9B	CCDC9B	---	---	1.551	0.0081

PANTHER 16.0 was used to conduct gene ontology (GO) enrichment analysis for the 11 proteins that presented significant fold changes after incubation with Alexa Fluor 594-labelled α-synuclein fibrils [159]. GO hierarchically classifies genes into terms to describe the complexity of biological systems. The terms are grouped into three categories: biological process, molecular function and cellular component providing an indication as to how each of the terms relates to one another [160, 161]. GO enrichment analysis finds which GO terms are over-represented for the set of genes being analysed in comparison to a reference list of the organism's whole genome. For this project, the GO enrichment analysis applied the Fisher's exact test to the genes of the 11 significant proteins against the *H. sapiens* genome (Table 5), [159]. The GO enrichment analysis was also used to identify reactome pathways that the list of genes belonged to (Table 6 and 7), [162].

The only enriched biological process was collagen fibril organisation for collagen α-1(I) chain (COL1A1), collagen α-2(I) chain (COL1A2) and COL2A1, with several cellular components related to collagen fibrils and trimerization. The cellular components: supramolecular fibre and supramolecular polymer were enriched for the three collagen proteins as well as α-synuclein (SNCA) and MAP4.

Several pathways were enriched for the proteins with significant fold change after incubation with α-synuclein fibrils. The first of these was integrin interactions for COL1A1, COL1A2 and COL2A1. The collagen proteins associate in trimers which then form fibres localised in the extracellular matrix, it is there where they interact with integrin proteins [162]. MET activation of PTK2 signalling was enriched for COL1A1,

COL1A2 and COL2A1. This occurs during hepatocyte growth factor-induced cell motility. Phosphorylated MET interacts with a complex of collagen fibres and integrin which allows MET to activate the focal adhesion kinase PTK2 [163].

Platelet aggregation and GP1b-IX-V signalling were enriched for COL1A1 and COL1A2. During platelet aggregation the type I collagen fibres that consist of COL1A1 and COL1A2 fibrils form a complex with von Willebrand factor (vWF) which then binds to the GP1b-IX-V receptor on the cell surface following injury [164].

With the enrichment of terms and pathways involving COL1A1, COL1A2 and COL2A1 and their significant fold change after incubation with α-synuclein, it is possible that their activity is altered in response to fibril exposure.

TABLE 5. **Gene Ontology (GO) enrichment analysis for proteins with significant fold change after SH-SY5Y GFP-α-synuclein cells were incubated for 1-day and 5-days with Alexa Fluor 594-labelled α-synuclein fibrils.** (Generated using [159]).

Category	GO ID	Description	Genes	Fold enrichment	*p*-value	FDR
Biological process	GO:0030199	collagen fibril organization	COL1A1 COL1A2 COL2A1	> 100	2.61E-06	4.15E-02
Molecular function	GO:0048407	platelet-derived growth factor binding	COL1A1 COL1A2 COL2A1	> 100	4.11E-08	1.96E-04
Molecular function	GO:0030020	extracellular matrix structural constituent conferring tensile strength	COL1A1 COL1A2 COL2A1	> 100	1.48E-06	3.54E-03
Cellular component	GO:0005584	collagen type I trimer	COL1A1 COL1A2	> 100	1.55E-06	7.79E-04
Cellular component	GO:0005583	fibrillar collagen trimer	COL1A1 COL1A2 COL2A1	> 100	5.13E-08	1.03E-04
Cellular component	GO:0098643	banded collagen fibril	COL1A1 COL1A2 COL2A1	> 100	5.13E-08	5.15E-05
Cellular component	GO:0099512	supramolecular fibre	COL1A1 COL1A2 COL2A1 SNCA MAP4	9.28	1.03E-04	3.44E-02
Cellular component	GO:0099081	supramolecular polymer	COL1A1 COL1A2 COL2A1 SNCA MAP4	9.20	1.07E-04	3.06E-02
Cellular component	GO:0098644	complex of collagen trimers	COL1A1 COL1A2 COL2A1	> 100	2.28E-07	1.52E-04
Cellular component	GO:0005581	collagen trimer	COL2A1	62.41	1.43E-05	5.74E-03

TABLE 6. **Pathways that were enriched for proteins with significant fold change after SH-SY5Y GFP-α-synuclein cells were incubated for 1-day and 5-days with Alexa Fluor 594-labelled α-synuclein fibrils.** Indentations indicate hierarchal relations. (Generated using [159]).

Pathway	Reactome ID	Genes	Fold enrichment	*p*-value	FDR
GP1b-IX-V activation signalling	R-HSA-430116	COL1A1 COL1A2	> 100	2.01E-05	3.83E-03
Anchoring fibril formation	R-HSA-2214320	COL1A1 COL1A2	> 100	3.51E-05	6.16E-03
Assembly of collagen fibrils and other multimeric structures	R-HSA-2022090	COL1A1 COL1A2 COL2A1	93.61	4.42E-06	2.02E-03
Collagen formation	R-HSA-1474290	COL1A1 COL1A2 COL2A1	63.11	1.38E-05	2.88E-03
Platelet Adhesion to exposed collagen	R-HSA-75892	COL1A1 COL1A2	> 100	3.51E-05	5.72E-03
Crosslinking of collagen fibrils	R-HSA-2243919	COL1A1 COL1A2	> 100	4.90E-05	7.46E-03
Scavenging by Class A Receptors	R-HSA-3000480	COL1A1 COL1A2	> 100	5.41E-05	7.27E-03
MET activates PTK2 signalling	R-HSA-8874081	COL1A1 COL1A2 COL2A1	> 100	6.12E-07	1.40E-03
MET promotes cell motility	R-HSA-8875878	COL1A1 COL1A2 COL2A1	> 100	1.38E-06	1.58E-03
Signalling by MET	R-HSA-6806834	COL1A1 COL1A2 COL2A1	73.91	8.75E-06	2.22E-03
Syndecan interactions	R-HSA-3000170	COL1A1 COL1A2	> 100	1.04E-04	1.32E-02
Non-integrin membrane-ECM interactions	R-HSA-3000171	COL1A1 COL1A2 COL2A1	95.20	4.21E-06	2.40E-03

TABLE 7. **Pathways that were enriched for proteins with significant fold change after SH-SY5Y GFP-α-synuclein cells were incubated for 1-day and 5-days with Alexa Fluor 594-labelled α-synuclein fibrils.** Indentations indicate hierarchal relations. (Continued from TABLE 6. Generated using [159]).

Pathway	Reactome ID	Genes	Fold enrichment	*p*-value	FDR
Collagen chain trimerization	R-HSA-8948216	COL1A1 COL1A2 COL2A1	> 100	1.81E-06	1.38E-03
Collagen biosynthesis and modifying enzymes	R-HSA-1650814	COL1A1 COL1A2 COL2A1	83.83	6.07E-06	1.98E-03
GPVI-mediated activation cascade	R-HSA-114604	COL1A1 COL1A2	> 100	1.71E-04	1.95E-02
Platelet Aggregation (Plug Formation)	R-HSA-76009	COL1A1 COL1A2	98.54	2.00E-04	2.17E-02
Collagen degradation	R-HSA-1442490	COL1A1 COL1A2 COL2A1	87.76	5.32E-06	2.03E-03
Degradation of the extracellular matrix	R-HSA-1474228	COL1A1 COL1A2 COL2A1	40.12	5.18E-05	7.40E-03
ECM proteoglycans	R-HSA-3000178	COL1A1 COL1A2 COL2A1	73.91	8.75E-06	2.50E-03
Integrin cell surface interactions	R-HSA-216083	COL1A1 COL1A2 COL2A1	66.87	1.17E-05	2.67E-03
Immunoregulatory interactions between a Lymphoid and a non-Lymphoid cell	R-HSA-198933	COL1A1 COL1A2 COL2A1	28.23	1.45E-04	1.74E-02

STRING analysis was used to observe interactions between the 11 proteins whose levels were significantly altered in the SH-SY5Y GFP-α-synuclein cells upon exposure to Alexa Fluor 594-labelled α-synuclein fibrils. STRING is a database of known and predicted protein-protein interactions including both physical and functional associations. It includes computational predictions, knowledge transfer between organisms and information collected in other databases. Protein-protein interactions are given scores which indicate the confidence of an association as opposed to the strength or specificity of the interaction [165]. STRING analysis did not present any direct association between α-synuclein (SNCA) and the other 10 proteins with significantly altered levels [165], (Fig. 25). There is a cluster consisting of: COL2A1, COL1A2 and COL1A1. This was to be expected given their presence in the enriched pathways (Table 6 and 7).

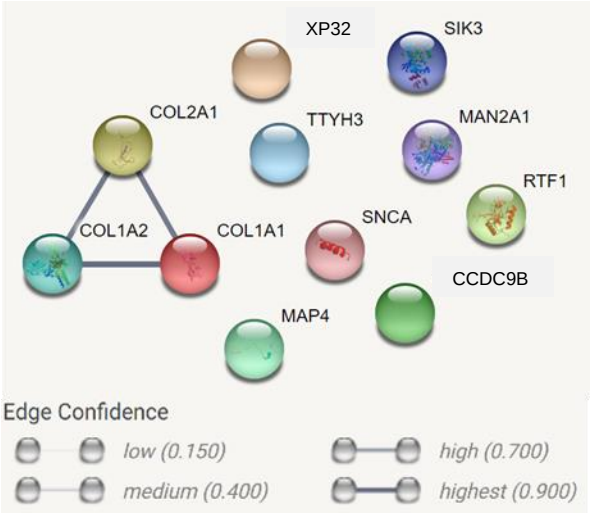

FIGURE 25. **STRING protein association network for the proteins with significant fold change after SH-SY5Y GFP-α-synuclein cells were incubated with α-synuclein fibrils for 1 and 5 days.** Number of nodes: 11, number of edges: 3 (vs 1 expected edges), PPI enrichment *p*-value 0.0157. Confidence score threshold was set at 0.4 (medium). Saturation of edges represents the confidence for a predicted association between proteins (Figure generated using [165]).

To explore the relationship between α-synuclein and the 10 other proteins with significantly altered levels, the STRING analysis was expanded to include proteins from the database that are associated either physically or functionally with the list of 11 proteins whose levels altered significantly upon cell exposure to α-synuclein fibrils. The search was expanded to include proteins from the database to explore if there were any indirect associations of α-synuclein and the 10 other proteins with significantly altered levels via proteins from the database. Upon expanding the analysis, both COL1A2 and α-synuclein (SNCA) have associations with amyloid precursor protein (APP). However, the indirect association of COL1A2 and α-synuclein is predicted to be more likely via APP then Secreted Protein Acidic And Cysteine Rich (SPARC), rather than APP directly, as indicated in the figure by the intensity of the edges [165], (Fig. 26). α-synuclein is also

indirectly associated with RNA Polymerase-Associated Protein RTF1 Homolog (RTF1) through Casein Kinase 2 Alpha 1 (CSNK2A1) [165], (Fig. 26).

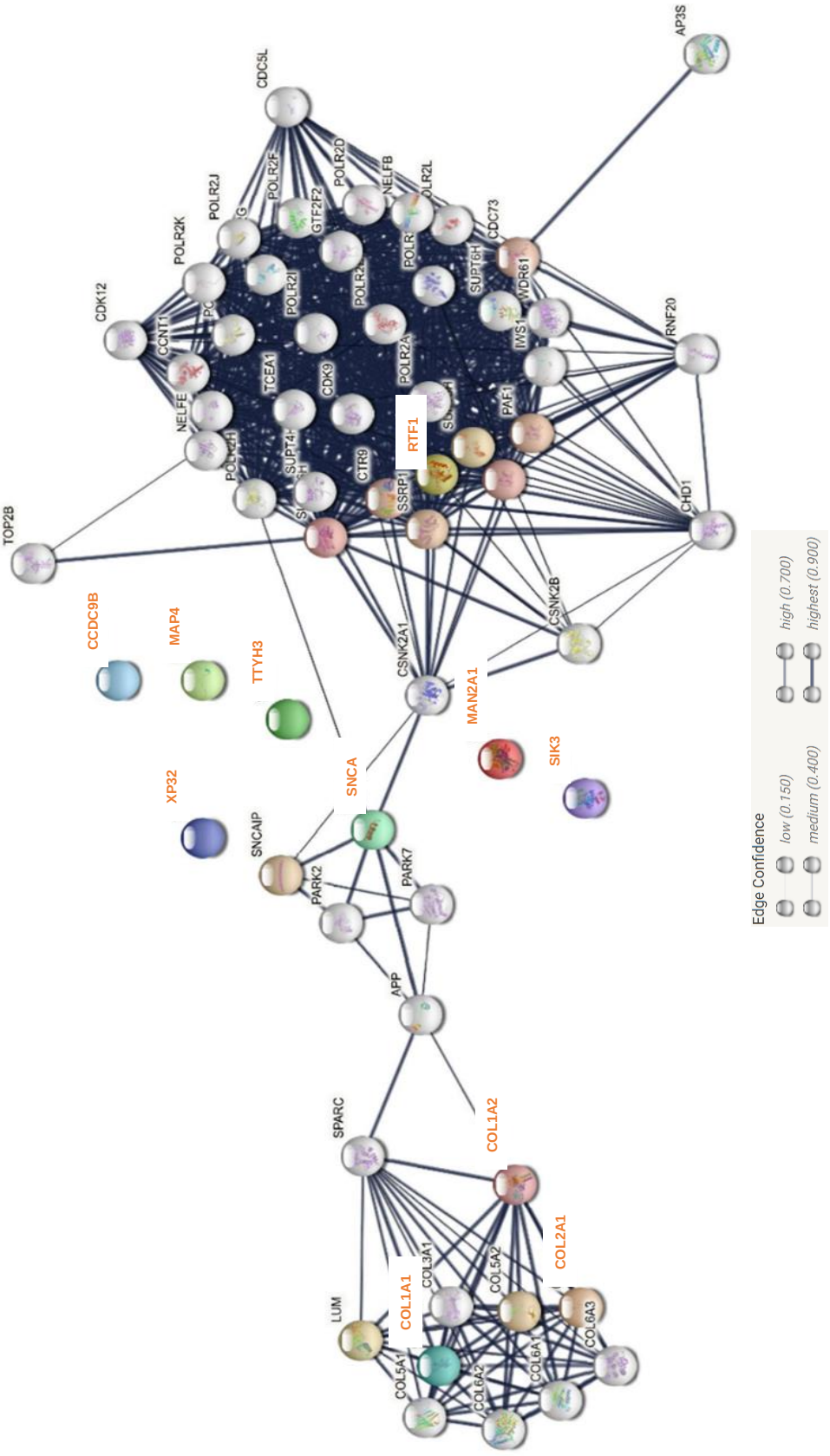

FIGURE 26. **Extended STRING network showing associations of database proteins with those presenting significant fold change after SH-SY5Y GFP-α-synuclein cells were incubated with α-synuclein fibrils for 1 and 5 days**. Number of nodes: 61, number of edges:634 (vs 140 expected edges), PPI enrichment *p*-value < 1.0e-16. Proteins with significantly altered levels after exposure to α-synuclein fibrils are given in orange. Confidence score threshold was set at 0.4 (medium). Saturation of edges represents the confidence for a predicted association. between proteins (Figure generated using [165]).

The 11 proteins whose levels were significantly altered in the SH-SY5Y GFP-α-synuclein cells upon exposure to Alexa Fluor 594-labelled α-synuclein fibrils were compared to lists from previous publications that focussed on α-synuclein interactions, α-synuclein fibril uptake, PD models and LBs in a variety of different model systems and sample types (Table 8). Of the 11 proteins with significant fold change after incubation with α-synuclein fibrils, five of them had not been identified in the examined proteomic studies, they were: COL2A1, RTF1, skin-specific protein 32 (XP32), alpha-mannosidase 2 (MAN2A1) and coiled-coil domain-containing protein 9B (CCDC9B).

COL1A1 and COL1A2 were present in cortical LB inclusions from post-mortem human brain samples [166]. MAP4 was identified in pulldown experiments of α-synuclein interaction partners. The pulldown focussed on identifying partners of phosphorylated and non-phosphorylated α-synuclein. MAP4 was identified regardless of the phosphorylation state of α-synuclein [134]. Mahul-Mellier et al. (2020) incubated neurons with α-synuclein preformed fibrils in a LB formation model. Non-specific serine/threonine protein kinase (SIK3) and protein tweety homolog 3 (TTYH3) increased after 14 and 21 days respectively [147].

TABLE 8. **Presence of the proteins with significant fold change after incubation with α-synuclein fibrils in lists of significant proteins given by previous proteomic publications.** First author, cell type and method of study are given for each publication.

Publication	Protein (gene name)										
	SNCA (NACP)	COL2A1	COL1A1	COL1A2	MAP4	RTF1	SIK3	XP32	TTYH3	MAN2A1	CCDC9B
Alberio et al. (2010), [139] Overexpression of α-synuclein in SH-SY5Y human cells	X										
McFarland et al. (2008), [134] Peptide pulldown for α-synuclein interaction partners in mouse neurons	X				X						
Leverenz et al. (2007), [166] Extraction of cortical LB inclusions from post mortem human brain	X		X	X							
Henderson et al. (2017), [145] Incubation of mouse neurons with α-synuclein preformed fibrils	X										
Zhang et al. (2013), [137] Overexpression of α-synuclein in a transgenic mouse model											
Mahul-Mellier et al. (2020), [147] Production of a LB model in primary mouse neurons	X						X		X		

6. Discussion

In this project, proteomics was used to study the effects of α-synuclein fibrils on the cellular proteome. It revealed that exposure of SH-SY5Y GFP-α-synuclein cells to α-synuclein fibrils resulted in the altered expression of a number of cellular proteins.

6.1. Proteins identified by proteomic analysis

Several of the proteins that presented significant fold changes after incubation of SH-SY5Y GFP-α-synuclein cells with Alexa Fluor 594-labelled α-synuclein fibrils have been identified in previous publications that utilised proteomics to study α-synuclein interactions, α-synuclein fibril uptake, PD models and LB formation (Table 8). Collagen α-1(I) chain (COL1A1) and collagen α-2(I) chain (COL1A2) were identified by Leverenz et al. (2007) in LBs extracted from neurons in the temporal cortex of dementia with LB (DLB) human brain samples [166]. However, homologs of COL1A1 and COL1A2 were not identified in the LB formation model developed by Mahul-Mellier et al. (2020) which involved incubating primary hippocampal mouse neurons with preformed α-synuclein fibrils [147]. With a significant increase of COL1A1 and COL1A2 seen in this project after 1-day incubation of SH-SY5Y GFP-α-synuclein cells with α-synuclein-fibrils and not after 5-days, it could be a transient response to the initial exposure. Therefore, it would be interesting to observe the levels of COL1A1 and COL1A2 with additional time points during the first 5 days, as well as observing their expression over the extended timepoints used by Mahul-Mellier et al. (2020), [147].

COL1A1 and COL1A2 form type 1 collagen fibrils. They are involved in the activation of PTK2 via the receptor tyrosine kinase MET. When complexed with integrins α2βI or α3β1, the type 1 collagen fibrils interact with active MET which in turn activates PTK2 [167], (Fig. 27).

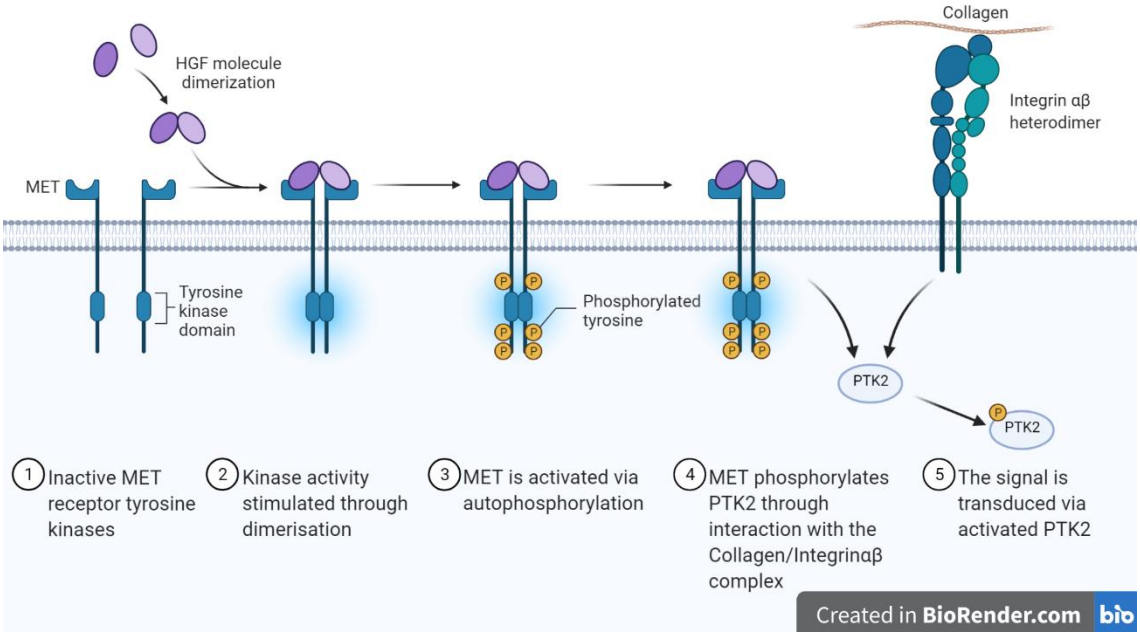

FIGURE 27. **Signal transduction via MET, a receptor tyrosine kinase.** When MET interacts with the dimerised signalling molecule Hepatocyte Growth Factor (HGF), it allows MET to dimerise via its tyrosine kinase domain. MET autophosphorylates and becomes activated. By interacting with the collagen/integrinαβ complex, MET phosphorylates PTK2. Phosphorylation of PTK2 activates it, allowing the signal to be transduced inside the cell. Created with BioRender.com.

Lee et al. (2020) showed that PTK2 plays a role in neurotoxicity [168]. TAR DNA binding protein (TARDBP) proteinopathies occur in several neurodegenerative diseases including amyotrophic lateral sclerosis (ALS) and Alzheimer's disease (AD) [169, 170]. These proteinopathies cause impairment of the ubiquitin proteasome system (UPS) resulting in an accumulation of ubiquitinated proteins and a reduction in proteosome activity in neurons. Inhibition of PTK2 is reported to suppress the neurotoxicity induced by UPS impairment, allowing for alternative clearance of poly-ubiquitinated proteins via the autophagy-lysosomal pathway (ALP) with the aid of sequestosome 1 [168].

It would be interesting to investigate whether the initial increase in COL1A1 and COL1A2 observed in this project contributes to the neurotoxic role of PTK2 highlighted by Lee et al. (2020), [168]. As the activation of PTK2 by MET promotes cell motility [171], perhaps the initial increase in COL1A1 and COL1A2 is a way of bringing cells into proximity of each other to aid fibril transmission. This could be investigated using live cell tracking coupled with fluorescent labelling of the type 1 collagen fibrils and α-synuclein fibrils.

In this project, collagen α-1(II) chain (COL2A1) increased significantly after both 1 and 5-days incubation with α-synuclein fibrils and was not identified in the previous proteomic studies focussed on α-synuclein interactions, α-synuclein fibril uptake, PD models and LB formation (Table 8). Type II collagen is an essential component of the

cartilage extracellular matrix, maintaining the structure of connective tissues. It is important in bone formation, growth and joint function as well as playing roles in development and function of the eye and inner ear [172]. Type II collagen is implicated in a variety of disorders that present skeletal dysplasia, short stature as well as hearing and vision impairment [173]. Despite being significantly increased in this project, COL2A1 is not implicated in neurodegenerative disease and it has not been found as an interaction partner of α-synuclein.

Changes in *COL4A2* expression, which encodes collagen α-2(IV) chain (COL4A2), have also been observed in A30P α-synuclein transgenic mice [174]. *COL4A2* was upregulated in both transgenic mice and dopaminergic neurons expressing A30P α-synuclein [174]. COL4A2 is a major component of the basement membranes, an extracellular matrix structure that supports and influences cell signalling. Surprisingly, Paiva et al. (2018) found that α-synuclein did not bind to the DNA sequence of the COL4A2 gene, but it did bind to the promoter region for *COL11A1* which was also highly upregulated in the A30P α-synuclein transgenic mice [174]. This suggests a potential role of α-synuclein in regulating expression of collagen-related genes and it could provide an explanation for the significant increases in COL1A1, COL1A2 and COL2A1 seen in this project.

The induction of astrogliosis and glial scar formation are often present in central nervous system (CNS) injuries, especially spinal cord injury (SCI). Genome-wide expression analysis found that several genes encoding extracellular matrix proteins were elevated 14 days post-injury, with those encoding COL1A1 and COL1A2 being highly expressed [175]. The upregulation of collagen type I in the injured extracellular matrix environment is believed to contribute to astrogliosis and astrocytic scar formation. This was suggested to occur through signalling pathways involving integrins and N-cadherin [175]. Prevention of collagen type I signalling has been shown to potentially promote axonal regrowth and enhance functional recovery, reducing astrocytic scar formation [176]. If inhibition of collagen type I signalling promotes neuronal functionality, in combination with the presence of collagen type I in LBs and the ability of α-synuclein to alter collagen gene transcription, this points towards collagen proteins, especially type I, having a potential role in α-synuclein pathology.

Microtubule-associated protein 4 (MAP4) was significantly decreased after GFP-α-synuclein cells were incubated with α-synuclein fibrils for 1 and 5 days. MAP4 was also associated with monomeric α-synuclein in pulldown experiments of α-synuclein interaction partners, regardless of α-synuclein's phosphorylation state [134]. Microtubules are a major component of the cytoskeleton that are assembled from α/β

tubulin heterodimers. They play roles in a plethora of cellular processes including cell division, motility, development and intracellular organisation [177]. Distinct arrays of microtubules are responsible for their varying functions and the formation of such structures requires interaction with the microtubule-associated proteins (MAPs), [177]. MAPs are abundantly expressed in the nervous system; some have overlapping roles while others have opposing activities to organise the microtubule cytoskeletal architecture [178].

MAP4 is part of the MAP2/Tau family of MAP proteins which also includes tau and MAP2 [179]. The MAP2/Tau family plays roles in intracellular traffic control. Tau is important in the transport of synaptic vesicles and organelles with its overexpression shown to impede their transport [180]. MAP2 controls cargo sorting in differentiated neurons, distinguishing KIF1 and KIF5 dependent cargoes [181]. MAP4 has been shown to activate kinesin 2-driven transport in both *Xenopus* melanocytes and *in vitro* motility assays as well as inhibiting dynein motility [182, 183]. The MAP2/Tau family can also regulate microtubule dynamics through the control of microtubule-severing enzymes. MAP4 was shown to inhibit katanin-mediated microtubule severing, with tau, MAP2 and MAP4 all serving to protect microtubules against severing when katanin was overexpressed in mammalian cells [184, 185].

Due to their involvement in a wide range of cellular processes, MAP proteins are implicated in a number of diseases. For example, mice lacking tau display age-onset neurodegeneration resulting in Parkinsonism and dementia [186]. In a cellular model of Prion disease, *MAP2* was shown to be downregulated, which corresponded with low levels of tubulin [187]. MAP1B-deficient neurons exhibit presynaptic structural deficiencies and altered physiology, and mice with *MAP1A* gene mutations display Purkinje-cell degeneration [188, 189]. In all these cases it is not the pathological accumulation of the MAPs that is responsible for the disease but rather it is the deficiency that leads to the pathology. This highlights their importance in cellular homeostasis and that alterations in their interactions with microtubules is sufficient to induce pathological events that lead to neuronal disorders [177].

With the level of MAP4 being significantly decreased in this project after 1 and 5-days incubation with α-synuclein fibrils, it will be interesting to determine how the reduction in MAP4 affects intracellular transport. As kinesin 2-driven transport is activated by MAP4 [182, 183], the decrease in MAP4 levels could disrupt this transport causing accumulation of kinesin 2 cargo. Accumulation of cargo could then result in cell signalling being compromised and targeting of the cargo for clearance for example, by the UPS. If MAP4 levels could not be restored by the cells, or if other MAP proteins could not compensate for its decrease, this could lead to cellular dysfunction and cell

death. To determine whether the decrease in MAP4 does affect kinesin 2-driven transport, kinesin 2 and its cargo could be subjected to immunofluorescent staining in SH-SY5Y GFP-α-synuclein cells exposed to α-synuclein fibrils. This would provide a simple method for observing any disruption to kinesin 2 trafficking and any subsequent accumulation of cargo, as mislocalised cargo would be easily identifiable. Kinesin-2 activity could be monitored using immunofluorescent staining coupled with live cell imaging whereby the time taken to load and deposit cargo could be monitored. If this was implicated, then immunofluorescent staining could also be used to determine whether kinesin 2 becomes targeted for degradation through observation of its localisation with certain organelles over time. These studies could also be applied to longer time points than those used in this project to determine the long-term implications of decreased MAP4 levels.

Both Protein tweety homolog 3 (TTYH3) and non-specific serine/threonine protein kinase (SIK3) increased in SH-SY5Y GFP-α-synuclein cells after incubation with α-synuclein fibrils for 5-days. TTYH3 and SIK3 also increased in the LB formation model by Mahul-Mellier et al. (2020) after incubation of primary hippocampal mouse neurons with α-synuclein preformed fibrils [147]. However, little is known about their function. TTYH3 is a chloride ion channel said to be present on the plasma membrane of cells in excitable tissue such as that of the brain and heart [190]. However, there are no publications at present which suggest involvement in disease or cellular signalling. SIK3 has been identified in large scale human kinome and phosphoproteome experiments via mass spectrometry, however, there are no details regarding its role in signalling pathways [191, 192]. Although the extended STRING analysis from this project did not show an association between either TTYH3 or SIK3 with α-synuclein, pulldowns for α-synuclein interaction partners could be used to confirm this experimentally.

As well as COL2A1, four other proteins not identified by the examined proteomic studies (Table 8), showed significant fold changes in this project after incubation with α-synuclein fibrils, these were: RNA Polymerase-Associated Protein RTF1 Homolog (RTF1), alpha-mannosidase 2 (MAN2A1), coiled-coil domain-containing protein 9B (CCDC9B) and skin-specific protein 32 (XP32), (Table 4). RTF1 decreased significantly after 1-day incubation with α-synuclein fibrils. It is a component of the PAF1 complex which functions during transcription by RNA polymerase II. The PAF1 complex is implicated in regulation of development and maintenance of embryonic stem cell pluripotency [193]. STRING analysis did not show α-synuclein to be associated with RTF1, however, transcriptomics could be used to study whether exposure to α-

synuclein fibrils alters RTF1 gene expression as opposed to direct interaction. MAN2A1, CCDC9B and XP32 all increased significantly after 5-days incubation with α-synuclein fibrils. MAN2A1 localises to the Golgi and catalyses the final hydrolytic step in the maturation of complex N-glycans [194]. The function of XP32 and CCDC9B are not well understood with the only gene ontology term for CCDC9B being RNA binding (GO:0003723) and no data available for XP32.

6.2. Limitations and development of the model system

The SH-SY5Y GFP-α-synuclein cell line is a simple experimental system. The ability to overexpress GFP-α-synuclein allows for easy identification of α-synuclein cellular localisation and inclusion formation as well as easy observation of the cellular effects α-synuclein has on neuronal protein expression. However, because SH-SY5Y is a neuroblastoma derived cell line it may not fully replicate the full repertoire of neuronal responses to amyloid fibrils, therefore, the use of primary neurons would be beneficial to confirm the results of this project. Primary neurons from mice or neurons derived from human induced pluripotent stem cells (iPSCs) or embryonic stem cells (ESCs) may represent better model systems. It may also be suitable to observe the effects of α-synuclein fibrils in a model system that replicates the environment of the human brain. Glial cells make up a large portion of the cell population within the brain and they interact with neurons in a variety of processes such as the promotion of tissue repair and regulation of ion and neurotransmitter concentrations around synapses [195, 196]. There may be responses of neurons to α-synuclein fibril exposure in the context of brain tissue that occur in the early timepoints of LB formation due to their proximity with glial cells. These observations cannot be identified in isolated cell systems and could be crucial for further understanding the contribution of α-synuclein to the pathogenesis of LBs in synucleinopathies such as PD.

Further to the work in this project, transcriptomics could be used to observe changes in gene expression that occur due to exposure to α-synuclein fibrils. This would be useful as most of the proteins whose levels were significantly altered in this project have not been shown to associate with α-synuclein, therefore this could provide an answer for how their levels changed. This could occur via α-synuclein binding to the promoter regions of the genes expressing these proteins, as discussed earlier for the collagen proteins, or through interaction with transcription factors. Pulldown assays could be used alongside transcriptomics to identify α-synuclein interaction partners to explain how exposure to α-synuclein fibrils resulted in the proteomic changes observed in this project.

It would also be interesting to investigate whether α-synuclein fibril polymorphs have different effects on the SH-SY5Y GFP-α-synuclein cell line when compared to those studied herein, particularly whether the difference in structures between the polymorphs elicit different cellular responses. Also, the fibrils used for this project were produced *in vitro*, therefore, it would be beneficial to observe the effects of *ex vivo* fibrils from human brain to test whether they replicate the cellular effects shown in this work.

7. Conclusion

By performing viability and seeding assays it has been shown that the SH-SY5Y GFP-α-synuclein cell line is a suitable experimental model to study the cellular effect of amyloid fibrils. α-synuclein fibrils are not toxic to this cell line and they can successfully seed intracellular GFP-α-synuclein in this model. Proteomics has identified several proteins from this experimental model that may play roles in the early stages of degeneration of neurons in synucleinopathies. Some of the proteins whose levels were significantly altered after exposure to α-synuclein fibrils have been identified in other proteomic studies focussed on α-synuclein interactions, α-synuclein fibril uptake, PD models and LB formation. Understanding the role that these proteins play during typical cellular function and under pathological conditions will help provide new insights into the early stages of cellular dysfunction that result in the formation of LBs and the progression of synucleinopathies such as PD.

8. Methods

All reagents used were from Sigma unless otherwise stated.

8.1. Preparation of fibril samples

Fibrils for this project were prepared and provided by Michael Davies of the Hewitt research group. 500 μM recombinant monomeric α-synuclein was incubated for 3 days in PBS at 42°C with the addition of 5% Alexa Fluor 594-labelled monomer and constantly agitated by a magnetic stirrer bar (1500 rpm). The resultant fibrils averaged 50nm in length [197].

8.2. Cell culture

The SH-SY5Y GFP-α-synuclein cell line was derived from the SH-SY5Y neuroblastoma cell line (ATCC) which has been stability transfected with GFP-α-synuclein. These cells

were cultured in Dulbecco's modified Eagle medium supplemented with 10% fetal bovine serum, 5% Penicillin-Streptomycin, 5% GlutaMAX (Thermo Scientific) at 37°C in 5% CO_2.

8.3. Cell viability assays

For all viability assays, SH-SY5Y GFP-α-synuclein cells were plated out at 40,000 cells per well in 96-well CytoOne plates (Star Lab) and incubated for 24 hr at 37°C in 5% CO_2. The medium was replaced, and the cells were incubated for a further 24 hr in the presence or absence of Alexa Fluor 594-labelled α-synuclein fibrils (1 μM final monomer equivalent concentration) or equivalent volume of PBS, at 37°C and in 5% CO_2. Prior to the viability assays, lysis buffer provided in the Pierce LDH Cytotoxicity assay kit (Thermo Scientific) was added to a portion of untreated cells, these cells served as a background reading against which sample cells were compared. All viability assays were conducted in triplicate with three replicates for each treatment. Results of each viability assay were normalised against control cells incubated with PBS and presented as means for each treatment (mean ± 1 S.E.M). GraphPad Prism 9 was used for comparison of treatments using Welch's ANOVA or Kruskal Wallis, followed by Dunnett's T3 multiple comparison or Dunn's multiple comparison tests respectively with differences considered significant at $p<0.05$ (GraphPad Prism version 9.0.1 for Windows, GraphPad Software, San Diego, California USA, www.graphpad.com).

All viability assays were carried out with triplicate samples and three independent experimental repeats. Results were normalized using the signal for untreated cells incubated with PBS as 100% viability.

8.3.1. Adenosine Triphosphate (ATP) assay

The ATP assay was conducted in accordance with the protocol outlined in the ATPlite assay kit (PerkinElmer). Briefly, after incubation with fibrils, mammalian cell lysis solution was added to the cells for 5 minutes followed by ATP substrate solution for 5 minutes, both these incubation stages occurred at room temperature on an orbital shaker at 700 rpm. Cells were dark adapted for 10 minutes at room temperature. The luminescence of each sample was then measured on an OPTIMA plate reader (BMG Labtech).

8.3.2. *Lactate Dehydrogenase (LDH) assay*

The LDH assay was conducted in accordance with the protocol outlined in the Pierce LDH Cytotoxicity assay kit (Thermo Scientific). Briefly, after incubation with fibrils, reaction mixture was added to media from each cell sample and incubated for 30 minutes at room temperature. Stop solution was added and the absorbance of each sample was read at 485/620 nm on an OPTIMA plate reader (BMG Labtech).

8.3.3. *3-(4,5-Dimethylthiazol-2-yl)-2,5-Diphenyltetrazolium Bromide (MTT) assay*

After incubation with fibrils, the medium was replaced, and cells were incubated for 3 hr with MTT (5 mg/mL). The medium was discarded, and the resulting formazan crystals were resuspended in dimethyl sulfoxide (DMSO) and incubated at 37°C, in 5% CO_2 for 30 minutes. The absorbance was measured at 570 nm on an OPTIMA plate reader (BMG Labtech).

8.4. Analysis of fibril uptake

Cells were plated out at 100,000 cells/mL in 6-well CytoOne plates (Star Lab) and incubated for 24 hr at 37°C in 5% CO_2. Media was replaced and cells were incubated in the presence or absence of Alexa Fluor 594-labelled α-synuclein fibrils (1 µM monomer equivalent concentration in PBS) or equivalent volume of PBS, for 24 hr and 5 days. After incubation, cells were subjected to live cell imaging. Cell media was replaced with imaging media (Dulbecco's modified Eagle medium; phenol red free, supplemented with 10% (v/v) fetal bovine serum, 5% (v/v) Penicillin-Streptomycin, 5% (v/v) GlutaMAX (Thermo Scientific)). LysoTracker Deep Red (0.05 µM, Thermo Scientific) and Hoechst (5µg/mL) were added to cells 30 minutes prior to imaging. Cells were imaged using the Zeiss LSM700 confocal microscope with a 40X objective and analysed using ZEN software. Images were arranged and analysed using ImageJ [198].

8.5. Analysis of seeding of GFP-α-synuclein aggregation

Cells were plated out at 100,000 cells/mL in 6-well CytoOne plates (Star Lab) and incubated for 24 hr at 37°C in 5% CO_2. Media was replaced and cells were incubated in the presence or absence of Alexa Fluor 594-labelled α-synuclein fibrils (1µM monomer equivalent concentration in PBS) or equivalent volume of PBS, for 5 days. Cells were permeabilized with 0.2% saponin and fixed with 4% formaldehyde. LysoTracker Deep Red (0.05 µM, Thermo Scientific) and Hoechst (5 µg/mL) were

added to cells 30 minutes before imaging. Cells were imaged using the Zeiss LSM700 confocal microscope with a 40X objective and analysed using ZEN software. Images were arranged and analysed using ImageJ [198].

8.6. Cell lysate preparation from cells incubated with α-synuclein fibrils for proteomic analysis

Cells were plated out at 100,000 cells/mL in 6-well CytoOne plates (Star Lab) and incubated for 24 hr at 37°C in 5% CO_2. Media was replaced and cells were incubated in the presence or absence of Alexa Fluor 594-labelled α-synuclein fibrils (1 µM monomer equivalent concentration in PBS) or equivalent volume of PBS, for 24 hr and 5 days. There were three wells for each condition (0, 1 and 5-day incubation with fibrils). Cells were incubated for a total of 5 days with fibrils added at 1 or 5 days prior to collection. After incubation, media was removed, cells were washed with PBS and scraped from the plates, there was $1x10^6$ cells/mL at the point of collection. Cells were spun down in PBS at 300 rcf in a bench top centrifuge for 5 minutes. Supernatant was discarded and lysis buffer (1% Triton X-100 in PBS with protease inhibitors (Pierce protease inhibitor mini tablets EDTA-free, Thermo Scientific)), was added to each cell sample. Cell lysates were spun down at 2000 rcf in a bench top centrifuge for 5 minutes and the supernatant was retained. Samples were then frozen at -18°C until use.

8.7. Assay of Protein concentration in cell lysates

A BCA (Bicinchoninic acid) assay was conducted to quantify the protein concentration in each cell lysate sample. The principle of this assay is that proteins can reduce Cu^{2+} to Cu^{+} resulting in a colour change from light blue to purple that is proportional to the protein concentration of the solution [199]. Using the Pierce BCA Protein Assay kit (Thermo Scientific), samples were incubated with the assay solution for 45 minutes at 37°C. Absorbance of each sample was measured at 562 nm on a NanoDrop 2000 Spectrophotometer. The absorbances were compared to those of a standard curve to obtain the concentration for each sample analysed. For each timepoint, samples with a protein concentration of 2 mg/mL or higher were selected for further analysis.

8.7.1. SDS-PAGE of cell lysates

Whole lysate samples (0.5 mg/mL) were added to SDS sample buffer (0.0625 M Tris pH 6.8, 2% (w/v) SDS, 10% (v/v) glycerol, 0.1 M DTT, 0.01% (w/v) bromophenol blue) and boiled for 5 minutes. 0.5 mg/mL of protein from samples of each timepoint were

then separated on a tris-tricine gel (30% (w/v) acrylamide: 0.8% (w/v) bis-acrylamide) for 30 minutes at 60V followed by 90 minutes at 120V. The gel was then stained in PageBlue Protein Staining Solution (Thermo Scientific) at room temperature overnight on a rocker and then imaged using a Bio Rad ChemiDoc XRS+ gel imager.

8.8. Proteomic analysis

Proteomic analysis was conducted by Dr Kate Heesom and her team at the University of Bristol Proteomics Facility, as outlined below in the description provided by Dr Heesom.

8.8.1. TMT Labelling, and High pH reversed-phase chromatography

Aliquots of 50 µg of each sample were digested with trypsin (2.5 µg trypsin per 100 µg protein; 37°C, overnight), labelled with Tandem Mass Tag (TMT) 10plex reagents according to the manufacturer's protocol (Thermo Scientific) and the labelled samples pooled.

The pooled sample was desalted using a SepPak cartridge according to the manufacturer's instructions (Waters, USA). Eluate from the SepPak cartridge was evaporated to dryness and resuspended in buffer A (20 mM ammonium hydroxide, pH 10) prior to fractionation by high pH reversed-phase chromatography using an Ultimate 3000 liquid chromatography system (Thermo Scientific). In brief, the sample was loaded onto an XBridge BEH C18 Column (130Å, 3.5 µm, 2.1 mm X 150 mm, Waters, UK) in buffer A and peptides eluted with an increasing gradient of buffer B (20 mM Ammonium Hydroxide in acetonitrile, pH 10) from 0-95% over 60 minutes. The resulting fractions (15 in total) were evaporated to dryness and resuspended in 1% formic acid prior to analysis by nano-LC MSMS using an Orbitrap Fusion Lumos mass spectrometer (Thermo Scientific).

8.8.2. Nano-LC Mass Spectrometry

High pH RP fractions were further fractionated using an Ultimate 3000 nano-LC system in line with an Orbitrap Fusion Lumos mass spectrometer (Thermo Scientific). In brief, peptides in 1% (v/v) formic acid were injected onto an Acclaim PepMap C18 nano-trap column (Thermo Scientific). After washing with 0.5% (v/v) acetonitrile 0.1% (v/v) formic acid peptides were resolved on a 250 mm × 75 µm Acclaim PepMap C18 reverse phase analytical column (Thermo Scientific) over a 150 min organic gradient, using 7 gradient segments (1-6% solvent B over 1 min, 6-15% B over 58 min, 15-32% B over

58 min, 32-40% B over 5 min, 40-90% B over 1 min, held at 90% B for 6 min and then reduced to 1% B over 1min) with a flow rate of 300 nL/min. Solvent A was 0.1% formic acid and Solvent B was aqueous 80% acetonitrile in 0.1% formic acid. Peptides were ionized by nano-electrospray ionization at 2.0kV using a stainless-steel emitter with an internal diameter of 30 µm (Thermo Scientific) and a capillary temperature of 300°C.

All spectra were acquired using an Orbitrap Fusion Lumos mass spectrometer controlled by Xcalibur 3.0 software (Thermo Scientific) and operated in data-dependent acquisition mode using an SPS-MS3 workflow. FTMS1 spectra were collected at a resolution of 120,000, with an automatic gain control (AGC) target of 200,000 and a max injection time of 50 ms. Precursors were filtered with an intensity threshold of 5000, according to charge state (to include charge states 2-7) and with monoisotopic peak determination set to Peptide. Previously interrogated precursors were excluded using a dynamic window (60s +/-10 ppm). The MS2 precursors were isolated with a quadrupole isolation window of 0.7 m/z. ITMS2 spectra were collected with an AGC target of 10,000, max injection time of 70 ms and CID collision energy of 35%.

For FTMS3 analysis, the Orbitrap was operated at 50,000 resolution with an AGC target of 50,000 and a max injection time of 105 ms. Precursors were fragmented by high energy collision dissociation (HCD) at a normalised collision energy of 60% to ensure maximal TMT reporter ion yield. Synchronous Precursor Selection (SPS) was enabled to include up to 10 MS2 fragment ions in the FTMS3 scan.

8.8.3. Data Analysis

The raw data files were processed and quantified using Proteome Discoverer software v2.1 (Thermo Scientific) and searched against the UniProt Human database (downloaded August 2020: 167789 entries) using the SEQUEST algorithm. Peptide precursor mass tolerance was set at 10 ppm, and MS/MS tolerance was set at 0.6 Da. Search criteria included oxidation of methionine (+15.995 Da), acetylation of the protein N-terminus (+42.011 Da) and Methionine loss plus acetylation of the protein N-terminus (-89.03 Da) as variable modifications and carbamidomethylation of cysteine (+57.021 Da) and the addition of the TMT mass tag (+229.163 Da) to peptide N-termini and lysine as fixed modifications. Searches were performed with full tryptic digestion and a maximum of 2 missed cleavages were allowed. The reverse database search option was enabled and all data was filtered to satisfy false discovery rate (FDR) of 5%.

8.9. Identification of proteins with altered levels in whole cell lysates

Proteins were filtered out if; they were identified as contaminants (serum, keratin, not of human origin), they had less than two unique peptides or they had a fold change up or down of less than 1.5. Significant hits were determined by paired t-tests performed on the normalised data sets that showed a fold change up or down of 1.5, with *p*-values <0.05, using GraphPad Prism 9 (GraphPad Prism version 9.0.1 for Windows, GraphPad Software, San Diego, California USA, www.graphpad.com).

8.10. Gene ontology and pathway analysis

Statistical overrepresentation tests for the proteins that presented significant fold changes were conducted using the PANTHER Gene Ontology (GO) to apply a Fisher's exact test with false discovery rate correction using *H. sapiens* as the reference species [159-161]. Molecular function, biological process and cellular component GO terms were examined for enrichment. Enrichment of pathways was also conducted through application of the same test using PANTHER GO.

8.11. STRING protein association networks

An interactome was constructed using STRING for the proteins with significant fold changes [165]. This was also expanded to include proteins from the STRING database that are associated with the list of significant proteins. The interactome was constructed using default settings, the confidence score was set to medium (0.4) with network edges showing the confidence of an interaction.

9. References

1. Pringsheim, T., et al., *The Prevalence of Parkinson's Disease: A Systematic Review and Meta-analysis.* Movement Disorders, 2014. **29**(13): p. 1583-1590.
2. Dickson, D.W., *Parkinson's Disease and Parkinsonism: Neuropathology.* Cold Spring Harbor Perspectives in Medicine, 2012. **2**(8).
3. Jankovic, J., *Parkinson's disease: clinical features and diagnosis.* Journal of Neurology Neurosurgery and Psychiatry, 2008. **79**(4): p. 368-376.
4. Hornykiewicz, O., *The discovery of dopaMine deficiency in the parkinsonian brain.* Journal of Neural Transmission-Supplement, 2006(70): p. 9-15.
5. *Treatment Parkinson's Disease*. 2019 30 April 2019 [cited 2020 20 June]; Available from: https://www.nhs.uk/conditions/parkinsons-disease/treatment/.
6. Mandel, S.A., et al., *Biomarkers for prediction and targeted prevention of Alzheimer's and Parkinson's diseases: evaluation of drug clinical efficacy.* The EPMA journal, 2010. **1**(2): p. 273-92.
7. Lewy, F.H., *Paralysis agitans. I.* Pathologische Anatomie. Handbuch der Neurologie, 1912.
8. Spillantini, M.G., et al., *alpha-synuclein in Lewy bodies.* Nature, 1997. **388**(6645): p. 839-840.

9. Watanabe, I., E. Vachal, and T. Tomita, *DENSE CORE VESICLES AROUND LEWY BODY IN INCIDENTAL PARKINSONS-DISEASE - ELECTRON-MICROSCOPIC STUDY.* Acta Neuropathologica, 1977. **39**(2): p. 173-175.
10. Lashuel, H.A., *Do Lewy bodies contain alpha-synuclein fibrils? and Does it matter? A brief history and critical analysis of recent reports.* Neurobiology of disease, 2020. **141**: p. 104876-104876.
11. Schrag, A., et al., *Health-related quality of life in multiple system atrophy.* Movement Disorders, 2006. **21**(6): p. 809-815.
12. Peng, C., et al., *Cellular milieu imparts distinct pathological alpha-synuclein strains in alpha-synucleinopathies.* Nature, 2018. **557**(7706): p. 558-+.
13. Mehra, S., S. Sahay, and S.K. Maji, *alpha-Synuclein misfolding and aggregation: Implications in Parkinson's disease pathogenesis.* Biochimica Et Biophysica Acta-Proteins and Proteomics, 2019. **1867**(10): p. 890-908.
14. Miller, D.W., et al., *Absence of alpha-synuclein mRNA expression in normal and multiple system atrophy oligodendroglia.* Journal of Neural Transmission, 2005. **112**(12): p. 1613-1624.
15. Martin, L.J., et al., *Parkinson's disease alpha-synuclein transgenic mice develop neuronal mitochondrial degeneration and cell death.* Journal of Neuroscience, 2006. **26**(1): p. 41-50.
16. Candelise, N., et al., *Seeding variability of different alpha synuclein strains in synucleinopathies.* Annals of Neurology, 2019. **85**(5): p. 691-703.
17. Uchikado, H., et al., *Alzheimer disease with amygdala Lewy bodies: A distinct form of alpha-synucleinopathy.* Journal of Neuropathology and Experimental Neurology, 2006. **65**(7): p. 685-697.
18. Klein, C. and A. Westenberger, *Genetics of Parkinson's Disease.* Cold Spring Harbor Perspectives in Medicine, 2012. **2**(1).
19. Meade, R.M., D.P. Fairlie, and J.M. Mason, *Alpha-synuclein structure and Parkinson's disease - lessons and emerging principles.* Molecular Neurodegeneration, 2019. **14**: p. 14.
20. Clayton, D.F. and J.M. George, *The synucleins: a family of proteins involved in synaptic function, plasticity, neurodegeneration and disease.* Trends in Neurosciences, 1998. **21**(6): p. 249-254.
21. Davidson, W.S., et al., *Stabilization of alpha-synuclein secondary structure upon binding to synthetic membranes.* Journal of Biological Chemistry, 1998. **273**(16): p. 9443-9449.
22. Waxman, E.A., J.R. Mazzulli, and B.I. Giasson, *Characterization of Hydrophobic Residue Requirements for alpha-Synuclein Fibrillization.* Biochemistry, 2009. **48**(40): p. 9427-9436.
23. Sato, H., T. Kato, and S. Arawaka, *The role of Ser129 phosphorylation of alpha-synuclein in neurodegeneration of Parkinson's disease: a review of in vivo models.* Reviews in the Neurosciences, 2013. **24**(2): p. 115-123.
24. Hoyer, W., et al., *Impact of the acidic C-terminal region comprising amino acids 109-140 on alpha-synuclein aggregation in vitro.* Biochemistry, 2004. **43**(51): p. 16233-16242.
25. George, J.M., et al., *CHARACTERIZATION OF A NOVEL PROTEIN REGULATED DURING THE CRITICAL PERIOD FOR SONG LEARNING IN THE ZEBRA FINCH.* Neuron, 1995. **15**(2): p. 361-372.
26. Bendor, J.T., T.P. Logan, and R.H. Edwards, *The Function of alpha-Synuclein.* Neuron, 2013. **79**(6): p. 1044-1066.
27. Sutton, R.B., et al., *Crystal structure of a SNARE complex involved in synaptic exocytosis at 2.4 angstrom resolution.* Nature, 1998. **395**(6700): p. 347-353.
28. Burkhardt, P., et al., *Munc18a controls SNARE assembly through its interaction with the syntaxin N-peptid.* Embo Journal, 2008. **27**(7): p. 923-933.

29. Hammond, C., O. El Far, and M. Seagar, *Neurotransmitter release*, in *Cellular and Molecular Neurophysiology*. 2015, Academic Press. p. 145-169.
30. Burre, J., et al., *alpha-Synuclein Promotes SNARE-Complex Assembly in Vivo and in Vitro.* Science, 2010. **329**(5999): p. 1663-1667.
31. Hawk, B.J.D., R. Khounlo, and Y.-K. Shin, *Alpha-Synuclein Continues to Enhance SNARE-Dependent Vesicle Docking at Exorbitant Concentrations.* Frontiers in Neuroscience, 2019. **13**.
32. Ben Gedalya, T., et al., *alpha-Synuclein and Polyunsaturated Fatty Acids Promote Clathrin-Mediated Endocytosis and Synaptic Vesicle Recycling.* Traffic, 2009. **10**(2): p. 218-234.
33. Ellis, C.E., et al., *Mitochondrial lipid abnormality and electron transport chain impairment in mice lacking alpha-synuclein.* Molecular and Cellular Biology, 2005. **25**(22): p. 10190-10201.
34. Golovko, M.Y., et al., *alpha-Synuclein gene deletion decreases brain palmitate uptake and alters the palmitate metabolism in the absence of alpha-synuclein palmitate binding.* Biochemistry, 2005. **44**(23): p. 8251-8259.
35. Golovko, M.Y., et al., *alpha-Synuclein gene ablation increases docosahexaenoic acid incorporation and turnover in brain phospholipids.* Journal of Neurochemistry, 2007. **101**(1): p. 201-211.
36. Lee, H.-J., et al., *Impairment of microtubule-dependent trafficking by overexpression of alpha-synuclein.* European Journal of Neuroscience, 2006. **24**(11): p. 3153-3162.
37. Chen, R.H.C., et al., *alpha-Synuclein Membrane Association Is Regulated by the Rab3a Recycling Machinery and Presynaptic Activity.* Journal of Biological Chemistry, 2013. **288**(11): p. 7438-7449.
38. Wood, S.J., et al., *alpha-synuclein fibrillogenesis is nucleation-dependent - Implications for the pathogenesis of Parkinson's disease.* Journal of Biological Chemistry, 1999. **274**(28): p. 19509-19512.
39. Chiti, F. and C.M. Dobson, *Protein Misfolding, Amyloid Formation, and Human Disease: A Summary of Progress Over the Last Decade.* Annual Review of Biochemistry, Vol 86, 2017. **86**: p. 27-68.
40. MD, T., C. G, and N. AJ, *Solid-state NMR structure of a pathogenic fibril of full-length human alpha synuclein.* Nature Structural and Molecular Biology, 2016. **23**: p. 11.
41. Guerrero-Ferreira, R., et al., *Cryo-EM structure of alpha-synuclein fibrils.* Elife, 2018. **7**.
42. Li, Y., et al., *Amyloid fibril structure of alpha-synuclein determined by cryoelectron microscopy.* Cell Research, 2018. **28**(9): p. 897-903.
43. Sahay, S., et al., *Familial Parkinson Disease-associated Mutations Alter the Site-specific Microenvironment and Dynamics of alpha-Synuclein.* Journal of Biological Chemistry, 2015. **290**(12): p. 7804-7822.
44. Zarranz, J.J., et al., *The new mutation, E46K, of alpha-synuclein causes Parkinson and Lewy body dementia.* Annals of Neurology, 2004. **55**(2): p. 164-173.
45. Guerrero-Ferreira, R., et al., *Two new polymorphic structures of human full-length alpha-synuclein fibrils solved by cryo-electron microscopy.* Elife, 2019. **8**.
46. Lassen, L.B., et al., *Protein Partners of alpha-Synuclein in Health and Disease.* Brain Pathology, 2016. **26**(3): p. 389-397.
47. Karpowicz, R.J., Jr., J.Q. Trojanowski, and V.M.Y. Lee, *Transmission of alpha-synuclein seeds in neurodegenerative disease: recent developments.* Laboratory Investigation, 2019. **99**(7): p. 971-981.
48. Karpowicz, R.J., Jr., et al., *Selective imaging of internalized proteopathic alpha-synuclein seeds in primary neurons reveals mechanistic insight into transmission of synucleinopathies.* Journal of Biological Chemistry, 2017. **292**(32): p. 13482-13497.
49. Cremades, N., et al., *Direct Observation of the Interconversion of Normal and Toxic Forms of alpha-Synuclein.* Cell, 2012. **149**(5): p. 1048-1059.

50. Winner, B., et al., *In vivo demonstration that alpha-synuclein oligomers are toxic.* Proceedings of the National Academy of Sciences of the United States of America, 2011. **108**(10): p. 4194-4199.
51. Braak, H., et al., *Staging of brain pathology related to sporadic Parkinson's disease.* Neurobiology of Aging, 2003. **24**(2): p. 197-211.
52. Henderson, M.X., J.Q. Trojanowski, and V.M.Y. Lee, *alpha-Synuclein pathology in Parkinson's disease and related alpha-synucleinopathies.* Neuroscience letters, 2019. **709**: p. 134316-134316.
53. Visanji, N.P., et al., *The prion hypothesis in Parkinson's disease: Braak to the future.* Acta neuropathologica communications, 2013. **1**: p. 2-2.
54. Wolfe, M.S., *The Molecular and Cellular Basis of Neurodegenerative Diseases: Underlying Mechanisms*. 2018. 1-560.
55. Van Den Berge, N., et al., *Evidence for bidirectional and trans-synaptic parasympathetic and sympathetic propagation of alpha-synuclein in rats.* Acta neuropathologica, 2019. **138**(4): p. 535-550.
56. Walsh, D.M. and D.J. Selkoe, *A critical appraisal of the pathogenic protein spread hypothesis of neurodegeneration.* Nature Reviews Neuroscience, 2016. **17**(4): p. 251-260.
57. Irwin, D.J., et al., *Evaluation of Potential Infectivity of Alzheimer and Parkinson Disease Proteins in Recipients of Cadaver-Derived Human Growth Hormone.* Jama Neurology, 2013. **70**(4): p. 462-468.
58. Kordower, J.H., et al., *Lewy body-like pathology in long-term embryonic nigral transplants in Parkinson's disease.* Nature Medicine, 2008. **14**(5): p. 504-506.
59. Li, J.-Y., et al., *Lewy bodies in grafted neurons in subjects with Parkinson's disease suggest host-to-graft disease propagation.* Nature Medicine, 2008. **14**(5): p. 501-503.
60. Desplats, P., et al., *Inclusion formation and neuronal cell death through neuron-to-neuron transmission of alpha-synuclein.* Proceedings of the National Academy of Sciences of the United States of America, 2009. **106**(31): p. 13010-13015.
61. Luk, K.C., et al., *Pathological alpha-Synuclein Transmission Initiates Parkinson-like Neurodegeneration in Nontransgenic Mice.* Science, 2012. **338**(6109): p. 949-953.
62. Rey, N.L., et al., *Widespread transneuronal propagation of alpha-synucleinopathy triggered in olfactory bulb mimics prodromal Parkinson's disease.* Journal of Experimental Medicine, 2016. **213**(9): p. 1759-1778.
63. Volpicelli-Daley, L.A., et al., *Exogenous alpha-Synuclein Fibrils Induce Lewy Body Pathology Leading to Synaptic Dysfunction and Neuron Death.* Neuron, 2011. **72**(1): p. 57-71.
64. Masuda-Suzukake, M., et al., *Pathological alpha-synuclein propagates through neural networks.* Acta Neuropathologica Communications, 2014. **2**.
65. El-Agnaf, O.M.A., et al., *alpha-synuclein implicated in Parkinson's disease is present in extracellular biological fluids, including human plasma.* Faseb Journal, 2003. **17**(11): p. 1945-+.
66. Xu, Y., et al., *DNAJC5 facilitates USP19-dependent unconventional secretion of misfolded cytosolic proteins.* Cell Discovery, 2018. **4**.
67. Emmanouilidou, E., et al., *Cell-Produced alpha-Synuclein Is Secreted in a Calcium-Dependent Manner by Exosomes and Impacts Neuronal Survival.* Journal of Neuroscience, 2010. **30**(20): p. 6838-6851.
68. Paillusson, S., et al., *Activity-dependent secretion of alpha-synuclein by enteric neurons.* Journal of Neurochemistry, 2013. **125**(4): p. 512-517.
69. Abounit, S., et al., *Tunneling nanotubes spread fibrillar alpha-synuclein by intercellular trafficking of lysosomes.* Embo Journal, 2016. **35**(19): p. 2120-2138.
70. Jiang, P., et al., *Impaired endo-lysosomal membrane integrity accelerates the seeding progression of alpha-synuclein aggregates.* Scientific Reports, 2017. **7**.

71. Coutinho, M.F. and S. Alves, *From rare to common and back again: 60 years of lysosomal dysfunction.* Molecular Genetics and Metabolism, 2016. **117**(2): p. 53-65.
72. Saftig, P. and J. Klumperman, *Lysosome biogenesis and lysosomal membrane proteins: trafficking meets function.* Nature Reviews Molecular Cell Biology, 2009. **10**(9): p. 623-635.
73. Moors, T., et al., *Lysosomal Dysfunction and alpha-Synuclein Aggregation in Parkinson's Disease: Diagnostic Links.* Movement Disorders, 2016. **31**(6): p. 791-801.
74. Sacino, A.N., et al., *Proteolysis of alpha-synuclein fibrils in the lysosomal pathway limits induction of inclusion pathology.* Journal of Neurochemistry, 2017. **140**(4): p. 662-678.
75. Parenti, G., G. Andria, and A. Ballabio, *Lysosomal Storage Diseases: From Pathophysiology to Therapy.* Annual Review of Medicine, Vol 66, 2015. **66**: p. 471-486.
76. Boustany, R.M.N., *Lysosomal storage diseases-the horizon expands.* Nature Reviews Neurology, 2013. **9**(10): p. 583-598.
77. Grabowski, G.A., *Lysosomal storage disease 1 - Phenotype, diagnosis, and treatment of Gaucher's disease.* Lancet, 2008. **372**(9645): p. 1263-1271.
78. Sidransky, E. and G. Lopez, *The link between the GBA gene and parkinsonism.* Lancet Neurology, 2012. **11**(11): p. 986-998.
79. Sidransky, E., et al., *Multicenter Analysis of Glucocerebrosidase Mutations in Parkinson's Disease.* New England Journal of Medicine, 2009. **361**(17): p. 1651-1661.
80. Nichols, N., et al., *EIF4G1 mutations do not cause Parkinson's disease.* Neurobiology of Aging, 2015. **36**(8).
81. Cleeter, M.W.J., et al., *Glucocerebrosidase inhibition causes mitochondrial dysfunction and free radical damage.* Neurochemistry International, 2013. **62**(1): p. 1-7.
82. Mazzulli, J.R., et al., *Gaucher Disease Glucocerebrosidase and alpha-Synuclein Form a Bidirectional Pathogenic Loop in Synucleinopathies.* Cell, 2011. **146**(1): p. 37-52.
83. Du, T.T., et al., *GBA deficiency promotes SNCA/alpha-synuclein accumulation through autophagic inhibition by inactivated PPP2A.* Autophagy, 2015. **11**(10): p. 1803-1820.
84. Magalhaes, J., et al., *Autophagic lysosome reformation dysfunction in glucocerebrosidase deficient cells: relevance to Parkinson disease.* Human Molecular Genetics, 2016. **25**(16): p. 3432-3445.
85. Yap, T.L., et al., *Structural Features of Membrane-bound Glucocerebrosidase and alpha-Synuclein Probed by Neutron Reflectometry and Fluorescence Spectroscopy.* Journal of Biological Chemistry, 2015. **290**(2): p. 744-754.
86. Klionsky, D.J., *The molecular machinery of autophagy: unanswered questions.* Journal of Cell Science, 2005. **118**(1): p. 7-18.
87. Majeski, A.E. and J.F. Dice, *Mechanisms of chaperone-mediated autophagy.* International Journal of Biochemistry & Cell Biology, 2004. **36**(12): p. 2435-2444.
88. Cuervo, A.M., et al., *Impaired degradation of mutant alpha-synuclein by chaperone-mediated autophagy.* Science, 2004. **305**(5688): p. 1292-1295.
89. Murphy, K.E., et al., *Lysosomal-associated membrane protein 2 isoforms are differentially affected in early Parkinson's disease.* Movement Disorders, 2015. **30**(12): p. 1639-1647.
90. Dehay, B., et al., *Pathogenic Lysosomal Depletion in Parkinson's Disease.* Journal of Neuroscience, 2010. **30**(37): p. 12535-12544.
91. Fussi, N., et al., *Exosomal secretion of alpha-synuclein as protective mechanism after upstream blockage of macroautophagy.* Cell Death & Disease, 2018. **9**.
92. Zhang, S., et al., *Intercellular transfer of pathogenic alpha-synuclein by extracellular vesicles is induced by the lipid peroxidation product 4-hydroxynonenal.* Neurobiology of Aging, 2018. **61**: p. 52-65.
93. Xilouri, M., et al., *Impairment of chaperone-mediated autophagy induces dopaminergic neurodegeneration in rats.* Autophagy, 2016. **12**(11): p. 2230-2247.

94. Alvarez-Erviti, L., et al., *Influence of microRNA deregulation on chaperone-mediated autophagy and alpha-synuclein pathology in Parkinson's disease.* Cell Death & Disease, 2013. **4**.
95. Martinez-Vicente, M., et al., *Dopamine-modified alpha-synuclein blocks chaperone-mediated autophagy.* Journal of Clinical Investigation, 2008. **118**(2): p. 777-788.
96. Vogiatzi, T., et al., *Wild type alpha-synuclein is degraded by chaperone-mediated autophagy and macroautophagy in neuronal cells.* Journal of Biological Chemistry, 2008. **283**(35): p. 23542-23556.
97. Arotcarena, M.-L., M. Teil, and B. Dehay, *Autophagy in Synucleinopathy: The Overwhelmed and Defective Machinery.* Cells, 2019. **8**(6).
98. Winslow, A.R., et al., *alpha-Synuclein impairs macroautophagy: implications for Parkinson's disease.* Journal of Cell Biology, 2010. **190**(6): p. 1023-1037.
99. Hoffmann, A.-C., et al., *Extracellular aggregated alpha synuclein primarily triggers lysosomal dysfunction in neural cells prevented by trehalose.* Scientific Reports, 2019. **9**.
100. Xilouri, M., et al., *Abberant alpha-Synuclein Confers Toxicity to Neurons in Part through Inhibition of Chaperone-Mediated Autophagy.* Plos One, 2009. **4**(5).
101. Yang, Q., et al., *Regulation of Neuronal Survival Factor MEF2D by Chaperone-Mediated Autophagy.* Science, 2009. **323**(5910): p. 124-127.
102. Schapira, A.H.V., et al., *MITOCHONDRIAL COMPLEX I DEFICIENCY IN PARKINSONS-DISEASE.* Lancet, 1989. **1**(8649): p. 1269-1269.
103. Nakamura, K., *alpha-Synuclein and Mitochondria: Partners in Crime?* Neurotherapeutics, 2013. **10**(3): p. 391-399.
104. Devi, L., et al., *Mitochondrial import and accumulation of alpha-synuclein impair complex I in human dopaminergic neuronal cultures and Parkinson disease brain.* Journal of Biological Chemistry, 2008. **283**(14): p. 9089-9100.
105. Bender, A., et al., *TOM40 Mediates Mitochondrial Dysfunction Induced by alpha-Synuclein Accumulation in Parkinson's Disease.* Plos One, 2013. **8**(4).
106. Betzer, C., et al., *Identification of Synaptosomal Proteins Binding to Monomeric and Oligomeric alpha-Synuclein.* Plos One, 2015. **10**(2).
107. Yokota, T., et al., *Down regulation of DJ-1 enhances cell death by oxidative stress, ER stress, and proteasome inhibition.* Biochemical and Biophysical Research Communications, 2003. **312**(4): p. 1342-1348.
108. Kilarski, L.L., et al., *Systematic Review and UK-Based Study of PARK2 (parkin), PINK1, PARK7 (DJ-1) and LRRK2 in early-onset Parkinson's disease.* Movement Disorders, 2012. **27**(12): p. 1522-1529.
109. Ariga, H., et al., *Neuroprotective Function of DJ-1 in Parkinson's Disease.* Oxidative Medicine and Cellular Longevity, 2013. **2013**.
110. Miller, D.W., et al., *L166P mutant DJ-1, causative for recessive Parkinson's disease, is degraded through the ubiquitin-proteasome system.* Journal of Biological Chemistry, 2003. **278**(38): p. 36588-36595.
111. Jin, J.H., et al., *Identification of novel proteins associated with both alpha-synuclein and DJ-1.* Molecular & Cellular Proteomics, 2007. **6**(5): p. 845-859.
112. Burbulla, L.F., et al., *Mitochondrial proteolytic stress induced by loss of mortalin function is rescued by Parkin and PINK1.* Cell Death & Disease, 2014. **5**.
113. Jin, J., et al., *Proteomic identification of a stress protein, mortalin/mthsp70/GRP75 - Relevance to Parkinson disease.* Molecular & Cellular Proteomics, 2006. **5**(7): p. 1193-1204.
114. Nakamura, K., et al., *Direct Membrane Association Drives Mitochondrial Fission by the Parkinson Disease-associated Protein alpha-Synuclein.* Journal of Biological Chemistry, 2011. **286**(23): p. 20710-20726.

115. Choubey, V., et al., *Mutant A53T alpha-Synuclein Induces Neuronal Death by Increasing Mitochondrial Autophagy.* Journal of Biological Chemistry, 2011. **286**(12): p. 10814-10824.
116. Bellucci, A., et al., *Induction of the unfolded protein response by alpha-synuclein in experimental models of Parkinson's disease.* Journal of Neurochemistry, 2011. **116**(4): p. 588-605.
117. Baek, J.H., et al., *Unfolded protein response is activated in Lewy body dementias.* Neuropathology and Applied Neurobiology, 2016. **42**(4): p. 352-365.
118. Lill, C.M., *Genetics of Parkinson's disease.* Molecular and Cellular Probes, 2016. **30**(6): p. 386-396.
119. Martin, E.R., et al., *Association of single-nucleotide polymorphisms of the tau gene with late-onset Parkinson disease.* Jama-Journal of the American Medical Association, 2001. **286**(18): p. 2245-2250.
120. Colom-Cadena, M., et al., *Confluence of alpha-Synuclein, Tau, and beta-Amyloid Pathologies in Dementia With Lewy Bodies.* Journal of Neuropathology and Experimental Neurology, 2013. **72**(12): p. 1203-1212.
121. Giasson, B.I., et al., *Initiation and synergistic fibrillization of tau and alpha-synuclein.* Science, 2003. **300**(5619): p. 636-640.
122. Millecamps, S. and J.P. Julien, *Axonal transport deficits and neurodegenerative diseases.* Nature Reviews Neuroscience, 2013. **14**(3): p. 161-176.
123. Buyukkoroglu, G., et al., *Techniques for Protein Analysis.* Omics Technologies and Bio-Engineering: Towards Improving Quality of Life, Vol 1: Emerging Fields, Animal and Medical Biotechnologies, 2018: p. 317-351.
124. Patterson, S.D. and R. Aebersold, *MASS-SPECTROMETRIC APPROACHES FOR THE IDENTIFICATION OF GEL-SEPARATED PROTEINS.* Electrophoresis, 1995. **16**(10): p. 1791-1814.
125. Lane, C.S., *Mass spectrometry-based proteomics in the life sciences.* Cellular and Molecular Life Sciences, 2005. **62**(7-8): p. 848-869.
126. Wright, P.C., et al., *A review of current proteomics technologies with a survey on their widespread use in reproductive biology investigations.* Theriogenology, 2012. **77**(4): p. 738-765.
127. Ong, S.E. and M. Mann, *Mass spectrometry-based proteomics turns quantitative.* Nature Chemical Biology, 2005. **1**(5): p. 252-262.
128. Shukla, A.K. and J.H. Futrell, *Tandem mass spectrometry: dissociation of ions by collisional activation.* Journal of Mass Spectrometry, 2000. **35**(9): p. 1069-1090.
129. Cottrell, J.S., *Protein identification using MS/MS data.* Journal of Proteomics, 2011. **74**(10): p. 1842-1851.
130. Mann, M. and M. Wilm, *ERROR TOLERANT IDENTIFICATION OF PEPTIDES IN SEQUENCE DATABASES BY PEPTIDE SEQUENCE TAGS.* Analytical Chemistry, 1994. **66**(24): p. 4390-4399.
131. Zhang, L. and J.E. Elias, *Relative Protein Quantification Using Tandem Mass Tag Mass Spectrometry.* Proteomics: Methods and Protocols, 2017. **1550**: p. 185-198.
132. Thompson, A., et al., *Tandem mass tags: A novel quantification strategy for comparative analysis of complex protein mixtures by MS/MS (vol 75, pg 1895, 2003).* Analytical Chemistry, 2006. **78**(12): p. 4235-4235.
133. Chen, X., et al., *Quantitative proteomics using SILAC: Principles, applications, and developments.* Proteomics, 2015. **15**(18): p. 3175-3192.
134. McFarland, M.A., et al., *Proteomics Analysis Identifies Phosphorylation-dependent alpha-Synuclein Protein Interactions.* Molecular & Cellular Proteomics, 2008. **7**(11): p. 2123-2137.
135. Pickrell, A.M. and R.J. Youle, *The Roles of PINK1, Parkin, and Mitochondrial Fidelity in Parkinson's Disease.* Neuron, 2015. **85**(2): p. 257-273.

136. Dixit, A., et al., *Minocycline, levodopa and MnTMPyP induced changes in the mitochondrial proteome profile of MPTP and maneb and paraquat mice models of Parkinson's disease.* Biochimica Et Biophysica Acta-Molecular Basis of Disease, 2013. **1832**(8): p. 1227-1240.
137. Zhang, Y., et al., *The Effect of Alpha-Synuclein Overexpression on the Process of Cellular Energy Metabolism in Transgenic Mouse Model*. 2013 Icme International Conference on Complex Medical Engineering. 2013. 244-248.
138. Stokes, A.H., T.G. Hastings, and K.E. Vrana, *Cytotoxic and genotoxic potential of dopamine.* Journal of Neuroscience Research, 1999. **55**(6): p. 659-665.
139. Alberio, T., et al., *Proteomic analysis of dopamine and alpha-synuclein interplay in a cellular model of Parkinson's disease pathogenesis.* Febs Journal, 2010. **277**(23): p. 4909-4919.
140. Chan, C.S., T.S. Gertler, and D.J. Surmeier, *Calcium homeostasis, selective vulnerability and Parkinson's disease.* Trends in Neurosciences, 2009. **32**(5): p. 249-256.
141. Mor, D.E., M.J. Daniels, and H. Ischiropoulos, *The usual suspects, dopamine and alpha-synuclein, conspire to cause neurodegeneration.* Movement Disorders, 2019. **34**(2): p. 167-179.
142. Mor, D.E., et al., *Dopamine induces soluble alpha-synuclein oligomers and nigrostriatal degeneration.* Nature Neuroscience, 2017. **20**(11): p. 1560-+.
143. Cao, P., et al., *Alpha-Synuclein Disrupted Dopamine Homeostasis Leads to Dopaminergic Neuron Degeneration in Caenorhabditis elegans.* Plos One, 2010. **5**(2).
144. Liu, J., et al., *Identification of proteins involved in microglial endocytosis of alpha-synuclein.* Journal of Proteome Research, 2007. **6**(9): p. 3614-3627.
145. Henderson, M.X., et al., *Unbiased Proteomics of Early Lewy Body Formation Model Implicates Active Microtubule Affinity-Regulating Kinases (MARKs) in Synucleinopathies.* Journal of Neuroscience, 2017. **37**(24): p. 5870-5884.
146. Drewes, G., et al., *MARK, a novel family of protein kinases that phosphorylate microtubule-associated proteins and trigger microtubule disruption.* Cell, 1997. **89**(2): p. 297-308.
147. Mahul-Mellier, A.-L., et al., *The process of Lewy body formation, rather than simply alpha-synuclein fibrillization, is one of the major drivers of neurodegeneration.* Proceedings of the National Academy of Sciences of the United States of America, 2020. **117**(9): p. 4971-4982.
148. Wakabayashi, K., et al., *The Lewy Body in Parkinson's Disease and Related Neurodegenerative Disorders.* Molecular Neurobiology, 2013. **47**(2): p. 495-508.
149. Volpicelli-Daley, L.A., K.C. Luk, and V.M.Y. Lee, *Addition of exogenous alpha-synuclein preformed fibrils to primary neuronal cultures to seed recruitment of endogenous alpha-synuclein to Lewy body and Lewy neurite-like aggregates.* Nature Protocols, 2014. **9**(9): p. 2135-2146.
150. Braidy, N., et al., *Alpha-Synuclein Transmission and Mitochondrial Toxicity in Primary Human Foetal Enteric Neurons In Vitro.* Neurotoxicity Research, 2014. **25**(2): p. 170-182.
151. Hansen, C., et al., *A novel alpha-synuclein-GFP mouse model displays progressive motor impairment, olfactory dysfunction and accumulation of alpha-synuclein-GFP.* Neurobiology of Disease, 2013. **56**: p. 145-156.
152. *ATPlite Luminescence ATP Detection Assay System*. 2015 23/01/2021]; Available from: https://www.perkinelmer.com/uk/lab-solutions/resources/docs/MAN-ATPlite.pdf.
153. Coleman, M.L., et al., *Membrane blebbing during apoptosis results from caspase-mediated activation of ROCK I.* Nature Cell Biology, 2001. **3**(4): p. 339-345.
154. *Pierce LDH Cytotoxicity Assay Kit*. 2014 23/01/2021]; 7]. Available from: https://assets.thermofisher.com/TFS-Assets/LSG/manuals/MAN0011851_Pierce_LDH_Cytotoxicity_Asy_UG.pdf.

155. *Protocol Guide: MTT Assay for Cell Viability and Proliferation*. 23/01/2021]; Available from: https://www.sigmaaldrich.com/technical-documents/protocols/biology/roche/cell-proliferation-kit-i-mtt.html.
156. Apetri, M.M., et al., *Direct Observation of alpha-Synuclein Amyloid Aggregates in Endocytic Vesicles of Neuroblastoma Cells.* Plos One, 2016. **11**(4).
157. *LysoTracker and LysoSensor Probes*. 2013 23/01/2021]; 2:[Available from: https://www.thermofisher.com/document-connect/document-connect.html?url=https%3A%2F%2Fassets.thermofisher.com%2FTFS-Assets%2FLSG%2Fmanuals%2Fmp07525.pdf&title=THlzb1RyYWNrZXIgYW5kIEx5c29TZW5zb3IgUHJvYmVz.
158. Barretina, J., et al., *The Cancer Cell Line Encyclopedia enables predictive modelling of anticancer drug sensitivity.* Nature, 2012. **483**(7391): p. 603-607.
159. Mi, H., et al., *PANTHER version 16: a revised family classification, tree-based classification tool, enhancer regions and extensive API.* Nucleic acids research, 2021. **49**(D1): p. D394-D403.
160. Ashburner, M., et al., *Gene Ontology: tool for the unification of biology.* Nature Genetics, 2000. **25**(1): p. 25-29.
161. Carbon, S., et al., *The Gene Ontology resource: enriching a GOld mine.* Nucleic Acids Research, 2021. **49**(D1): p. D325-D334.
162. Jassal, B., et al., *The reactome pathway knowledgebase.* Nucleic Acids Research, 2020. **48**(D1): p. D498-D503.
163. Chen, S.Y. and H.C. Chen, *Direct interaction of focal adhesion kinase (FAK) with Met is required for FAK to promote hepatocyte growth factor-induced cell invasion.* Molecular and Cellular Biology, 2006. **26**(13): p. 5155-5167.
164. Parise, L.V., *Integrin alpha(llb)beta(3) signaling in platelet adhesion and aggregation.* Current Opinion in Cell Biology, 1999. **11**(5): p. 597-601.
165. Szklarczyk, D., et al., *STRING v11: protein-protein association networks with increased coverage, supporting functional discovery in genome-wide experimental datasets.* Nucleic Acids Research, 2019. **47**(D1): p. D607-D613.
166. Leverenz, J.B., et al., *Proteomic identification of novel proteins in cortical Lewy bodies.* Brain Pathology, 2007. **17**(2): p. 139-145.
167. Beviglia, L. and R.H. Kramer, *HGF induces FAK activation and integrin-mediated adhesion in MTLn3 breast carcinoma cells.* International Journal of Cancer, 1999. **83**(5): p. 640-649.
168. Lee, S., et al., *PTK2/FAK regulates UPS impairment via SQSTM1/p62 phosphorylation in TARDBP/TDP-43 proteinopathies.* Autophagy, 2020. **16**(8): p. 1396-1412.
169. Meriggioli, M.N. and J.H. Kordower, *TDP-43 Proteinopathy: Aggregation and Propagation in the Pathogenesis of Amyotrophic Lateral Sclerosis.* Movement Disorders, 2016. **31**(8): p. 1139-1139.
170. James, B.D., et al., *TDP-43 stage, mixed pathologies, and clinical Alzheimer's-type dementia.* Brain, 2016. **139**: p. 2983-2993.
171. Weidner, K.M., M. Sachs, and W. Birchmeier, *THE MET RECEPTOR TYROSINE KINASE TRANSDUCES MOTILITY, PROLIFERATION, AND MORPHOGENIC SIGNALS OF SCATTER FACTOR HEPATOCYTE GROWTH-FACTOR IN EPITHELIAL-CELLS.* Journal of Cell Biology, 1993. **121**(1): p. 145-154.
172. Barat-Houari, M., et al., *Mutation Update for COL2A1 Gene Variants Associated with Type II Collagenopathies.* Human Mutation, 2016. **37**(1): p. 7-15.
173. Carter, E.M. and C.L. Raggio, *Genetic and orthopedic aspects of collagen disorders.* Current Opinion in Pediatrics, 2009. **21**(1): p. 46-54.
174. Paiva, I., et al., *Alpha-synuclein deregulates the expression of COL4A2 and impairs ER-Golgi function.* Neurobiology of Disease, 2018. **119**: p. 121-135.
175. Neo, S.H. and B.L. Tang, *Collagen 1 signaling at the central nervous system injury site and astrogliosis.* Neural Regeneration Research, 2017. **12**(10): p. 1600-1601.

176. Hara, M., et al., *Interaction of reactive astrocytes with type I collagen induces astrocytic scar formation through the integrin-N-cadherin pathway after spinal cord injury.* Nature Medicine, 2017. **23**(7): p. 818-+.
177. Bodakuntla, S., et al., *Microtubule-Asssociated Proteins: Structuring the Cytoskeleton.* Trends in Cell Biology, 2019. **29**(10): p. 804-819.
178. Baas, P.W., et al., *Stability Properties of Neuronal Microtubules.* Cytoskeleton, 2016. **73**(9): p. 442-460.
179. Dehmelt, L. and S. Halpain, *The MAP2/Tau family of microtubule-associated proteins.* Genome Biology, 2005. **6**(1).
180. Ebneth, A., et al., *Overexpression of tau protein inhibits kinesin-dependent trafficking of vesicles, mitochondria, and endoplasmic reticulum: Implications for Alzheimer's disease.* Journal of Cell Biology, 1998. **143**(3): p. 777-794.
181. Gumy, L.F., et al., *MAP2 Defines a Pre-axonal Filtering Zone to Regulate KIF1-versus KIF5-Dependent Cargo Transport in Sensory Neurons.* Neuron, 2017. **94**(2): p. 347-+.
182. Semenova, I., et al., *Regulation of microtubule-based transport by MAP4.* Molecular Biology of the Cell, 2014. **25**(20): p. 3119-3132.
183. Mogessie, B., et al., *A novel isoform of MAP4 organises the paraxial microtubule array required for muscle cell differentiation.* Elife, 2015. **4**.
184. McNally, K.P., D. Buster, and F.J. McNally, *Katanin-mediated microtubule severing can be regulated by multiple mechanisms.* Cell Motility and the Cytoskeleton, 2002. **53**(4): p. 337-349.
185. Qiang, L., et al., *Tau protects microtubules in the axon from severing by katanin.* Journal of Neuroscience, 2006. **26**(12): p. 3120-3129.
186. Lei, P., et al., *Tau deficiency induces parkinsonism with dementia by impairing APP-mediated iron export.* Nature Medicine, 2012. **18**(2): p. 291-295.
187. Zhang, J. and X.P. Dong, *Dysfunction of microtubule-associated proteins of MAP2/tau family in prion disease.* Prion, 2012. **6**(4): p. 334-338.
188. Bodaleo, F.J., et al., *Microtubule-associated protein 1B (MAP1B)-deficient neurons show structural presynaptic deficiencies in vitro and altered presynaptic physiology.* Scientific Reports, 2016. **6**.
189. Liu, Y., J.W. Lee, and S.L. Ackerman, *Mutations in the Microtubule-Associated Protein 1A (Map1a) Gene Cause Purkinje Cell Degeneration.* Journal of Neuroscience, 2015. **35**(11): p. 4587-4598.
190. Suzuki, M. and A. Mizuno, *A novel human Cl- channel family related to Drosophila flightless locus.* Journal of Biological Chemistry, 2004. **279**(21): p. 22461-22468.
191. Oppermann, F.S., et al., *Large-scale Proteomics Analysis of the Human Kinome.* Molecular & Cellular Proteomics, 2009. **8**(7): p. 1751-1764.
192. Rigbolt, K.T.G., et al., *System-Wide Temporal Characterization of the Proteome and Phosphoproteome of Human Embryonic Stem Cell Differentiation.* Science Signaling, 2011. **4**(164).
193. Ding, L., et al., *A Genome-Scale RNAi Screen for Oct4 Modulators Defines a Role of the Paf1 Complex for Embryonic Stem Cell Identity.* Cell Stem Cell, 2009. **4**(5): p. 403-415.
194. Misago, M., et al., *MOLECULAR-CLONING AND EXPRESSION OF CDNAS ENCODING HUMAN ALPHA-MANNOSIDASE-II AND A PREVIOUSLY UNRECOGNIZED ALPHA-MANNOSIDASE-IIX ISOZYME.* Proceedings of the National Academy of Sciences of the United States of America, 1995. **92**(25): p. 11766-11770.
195. Kreutzberg, G.W., *Microglia: A sensor for pathological events in the CNS.* Trends in Neurosciences, 1996. **19**(8): p. 312-318.
196. Bak, L.K., A. Schousboe, and H.S. Waagepetersen, *The glutamate/GABA-glutamine cycle: aspects of transport, neurotransmitter homeostasis and ammonia transfer.* Journal of Neurochemistry, 2006. **98**(3): p. 641-653.
197. Pinotsi, D., et al., *Direct Observation of Heterogeneous Amyloid Fibril Growth Kinetics via Two-Color Super-Resolution Microscopy.* Nano Letters, 2014. **14**(1): p. 339-345.

198. Rueden, C.T., et al., *ImageJ2: ImageJ for the next generation of scientific image data.* Bmc Bioinformatics, 2017. **18**.
199. *Chemistry of Protein Assays*. 01/02/2021]; Available from: https://www.thermofisher.com/uk/en/home/life-science/protein-biology/protein-biology-learning-center/protein-biology-resource-library/pierce-protein-methods/chemistry-protein-assays.html.